

**LATE QUATERNARY PALAEOENVIRONMENT  
AND  
EVOLUTION OF NAL REGION,  
GUJARAT, INDIA**

**Thesis submitted to**  
*The Maharaja Sayajirao University of Baroda*

**for the degree of  
DOCTOR OF PHILOSOPHY  
IN  
GEOLOGY**

**by**  
**Sushma Prasad**

*September 1996*

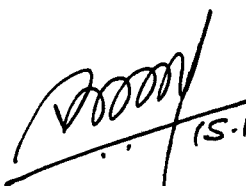
**Earth science Division  
Physical Research Laboratory  
Navrangpura, Ahmedabad 380009  
Gujarat, INDIA.**

## CERTIFICATE

I hereby declare that the work presented here in this thesis is original and has not formed the basis for the award of any Degree or Diploma by any University or Institution.

Sushma Prasad  
(Candidate)

Certified by:



(S.K. GUPTA)

Dr. S.K. Gupta

(Guide)

Physical Research Laboratory

Ahmedabad 380 009, India.

Dr. L.S. Chamyal

(Co-Guide)

M.S. University of Baroda

Vadodara 390 002, India.

Head, Dept. of Geology  
M.S. University of Baroda  
Vadodara 390 002, India.

# **CONTENTS**

Table of contents	(i)
List of figures	(v)
List of tables	(x)
Acknowledgements	(xi)
Abstract	(xiii)

## **CHAPTER 1 INTRODUCTION**

1.1 Study area	1
1.2 Climate	3
1.3 Flora and fauna	3
1.4 Geology	4
1.5 Tectonics	4
1.6 Motivation and scope	7
1.7 Objectives	8
1.8 Approach	8
1.8.1 Evolution of Nal region	8
1.8.2 Palaeoenvironmental studies	9

## **CHAPTER 2 GEOLOGICAL AND GEOMORPHOLOGICAL STUDIES**

2.1 Background information	11
2.1.1 Quaternary sediments of central and north Gujarat	13
2.1.2 Quaternary sediments of Saurashtra	15
2.1.3 Quaternary sediments of the Ranns of Kachchh	17
2.1.4 Quaternary sediments of the Nal depression	18

2.2	Present study	18
2.2.1	Remote sensing studies	19
2.2.1.1	Methodology	19
2.2.1.2	Results	23
2.2.1.3	Discussion	28
2.2.2	Subsurface lithological correlation	33
2.2.2.1	Methodology	33
2.2.2.2	Results and discussion	33
2.2.3	Studies on Nal Sarovar core	38
2.2.3.1	Lithological description	38
2.2.3.2	Sedimentological and mineralogical studies	41

## **CHAPTER 3 PALAEOCLIMATIC STUDIES**

3.1	Background information	53
3.1.1	Dating of young sediments	53
3.1.2	Sources of palaeoclimatic information	56
3.1.3	Palaeoclimatic studies in north-west India	56
3.2	Present study	58
3.2.1	Basic principles	58
3.2.2	Results and discussion	61

## **CHAPTER 4 LUMINESCENCE DATING STUDIES**

4.1	Thermal and optically stimulated luminescence	76
4.1.1	Age equation	76
4.1.2	Luminescence dating of sediments	79
4.1.3	Factors affecting the luminescence signal	83
4.1.4	Factors affecting the dose rate	87

4.2	Present study	88
4.2.1	Results	88
4.2.1.1	Salient features of results	92
4.2.1.2	Tests for anomalous fading and disequilibrium	94
4.2.2	Discussion	97
 <b><u>CHAPTER 5</u> SUMMARY, SYNTHESIS AND FUTURE PERSPECTIVES</b>		
5.1	Summary	102
5.1.1	Remote sensing and field studies	102
5.1.2	Sub surface lithological studies	102
5.1.3	Core studies	103
5.2	Synthesis	103
5.2.1	Geomorphic evolution of Nal region	104
5.2.2	Palaeoclimate of Nal region during past 7ka	108
5.3	Future perspectives	110
<b><u>Appendix A</u> Sampling Procedures</b>		112
<b><u>Appendix B</u> Experimental Procedures For Sedimentological And Mineralogical Analyses</b>		120
B.1	Textural analysis	120
B.2	Heavy mineral separation	120
B.3	X-Ray diffraction	120
<b><u>Appendix C</u> Experimental Procedures For Radiocarbon Dating</b>		126
C.1	Sample pre-treatment	125
C.2	Preparation of sample for counting	125

C.3	Measurement of activity	126
C.4	Age determination	127
<b><u>Appendix D</u></b>	<b>Experimental Procedures For <math>\delta^{13}\text{C}</math> And C/N Analyses</b>	<b>128</b>
D.1	Calibration of the assembly line	128
D.2	Sample pre-treatment and gas extraction	131
D.3	Mass spectrometric measurements	133
<b><u>Appendix E</u></b>	<b>Experimental Procedures For Luminescence Dating</b>	<b>135</b>
E.1	Sample collection	135
E.2	Laboratory procedures for determination of ED	135
E.3	Laboratory procedure for measurement of dose rate	140
E.4	Water Content Estimation	141
E.5	Data Analysis	142
<b>REFERENCES</b>		<b>143</b>

## **LIST OF FIGURES**

### **CHAPTER 1 INTRODUCTION**

- Fig. 1.1** Map of India and satellite imagery of Gujarat showing the location of Nal Sarovar and surrounding regions. 2
- Fig. 1.2** Geological map of Nal and surrounding regions. 5
- Fig. 1.3** Tectonic map of Nal and surrounding regions (Modified after Chandra and Chaudhary, 1969). 6

### **CHAPTER 2 GEOLOGICAL AND GEOMORPHOLOGICAL STUDIES**

- Fig. 2.1** The sub-divisions of Quaternary sediments of Gujarat. 12
- Fig. 2.2** Composite Quaternary sediment profiles of river basins of Gujarat. (A) Narmada, (B) Mahi, (C) Sabarmati. (Redrawn from Chamyal and Merh, 1992). 14
- Fig. 2.3** Satellite imagery and interpretation showing deranged drainage pattern in older mud flats south of Nal Sarovar. 20
- Fig. 2.4** Satellite imagery and interpretation showing the location of palaeochannels (dashed lines), dunes (dots) and alluvial plains north of Nal Sarovar. 21
- Fig. 2.5** Satellite imagery and interpretation showing inland deltas, zone of terminating streams and older mud flats, south of Nal Sarovar. 22
- Fig. 2.6** A composite map showing the present day drainage pattern and location of palaeochannels in and around Nal region. 24
- Plate 1** Photograph of a small stream formed by silting of older channel. 26
- Plate 2** Photograph of cross bedding observed in inland delta region. 26

<b>Fig. 2.7</b>	A composite map showing deranged drainage pattern and zone of terminating streams below 20m contour in the Nal region. Above 40m contour only the major rivers are shown.	27
<b>Fig. 2.8</b>	Geomorphological map of Nal region.	29
<b>Fig. 2.9</b>	Plots of eustatic sea level change (Redrawn from Gillespie and Molnar, 1995).	32
<b>Fig. 2.10</b>	Map showing the location of bore hole sites and transects taken. Also shown are eastern and western margins of Cambay Graben. The approximate boundaries of the Nal region are shown by dotted lines.	34
<b>Fig. 2.11</b>	Lithological variation along the transects shown in Fig. 2.10.	35
<b>Fig. 2.12</b>	Additional bore hole lithologs for sites shown in Fig. 2.10.	36
<b>Fig. 2.13</b>	Additional bore hole lithologs for sites shown in Fig. 2.10.	37
<b>Fig. 2.14</b>	Map showing the location of 54m long core and shallow trenches in Nal Sarovar.	39
<b>Fig. 2.15</b>	Lithology of the Nal Sarovar core.	40
<b>Fig. 2.16</b>	Lithology of shallow trenches showing the presence of shell layer in Nal Sarovar.	42
<b>Plate 3</b>	Field photograph of sediments from the shell layer, Horizon-1, taken during trenching.	43
<b>Fig. 2.17</b>	Variation of grain size with depth, Nal Sarovar core.	45
<b>Fig. 2.18</b>	Variation of total clay percentage and mineralogy with depth, Nal Sarovar core.	46
<b>Fig. 2.19</b>	E-W section along the Cambay Graben. (Drawn on basis of data given in Mathur et al, 1968).	51



## **CHAPTER 3 PALAEOCLIMATIC STUDIES**

- Fig. 3.1** The extent of fossil aeolian features and isohyet contours in north western India (modified version largely redrawn from Chawla et al, 1992). Sites mentioned in text are indicated. 54
- Fig. 3.2** Plot of radiocarbon dates vs depth, Nal Sarovar core. 63
- Fig. 3.3** Age variation of %C, %N, C/N,  $\delta^{13}\text{C}$ , and % sand in sediment samples from Nal Sarovar core. 67
- Fig. 3.4** Palaeoclimatic interpretation of C/N and  $\delta^{13}\text{C}$  variations in sediment samples from Nal Sarovar core. 69
- Fig. 3.5** A comparison of palaeoclimatic data from Didwana and Lunkaransar lakes in Rajasthan with Nal Sarovar. (a) Wasson et al, 1984; (b)&(c), Bryson and Swain, (1981). 72

## **CHAPTER 4 LUMINESCENCE DATING STUDIES**

- Fig. 4.1(a)** Explanation of the basic process of TL induction using the band theory of solids (after Aitken, 1985). (i) Irradiation by ionising radiation results in the production of free charges some of which get trapped at various defects in the crystal. (ii) Energy 'E' is required for the detrapping of the charges. (iii) Stimulation by heating (or optically) can cause detrapping of these charges some of which recombine radiatively with the opposite charge at a recombination centre 'L' and emit light called as TL or OSL depending on type of stimulation. 77
- Fig. 4.1(b)** Schematic portrayal of simple types of defects such as negative ion vacancy, interstitial defect and impurities in an ionic crystal (after Aitken, 1974). 77
- Fig. 4.2** Comparative study of bleaching of quartz and feldspar (after Godfrey-Smith et al, 1988) showing faster bleaching of OSL signal; for OSL, 1% of initial signal was reached for

quartz after 10 seconds of sun exposure whereas 9 min were required for a feldspar sample. For TL, exposure time of several hours was needed. Note reverse sensitivity of minerals to bleaching for OSL and TL. 80

**Fig. 4.3** Schematic of methods used in estimation of equivalent dose for sediments. X-axis refers to laboratory dose (after Wintle and Proszynska, 1983). 81

**Fig. 4.4** IRSL growth curve and age plateau for sample N-143. Also indicated are the mean values of ED and age. 90

**Fig. 4.5** IRSL growth curve and age plateau for sample N-168. Also indicated are the mean values of ED and age. 91

**Fig. 4.6** Variation of IRSL dates with depth in Nal Sarovar core. The open circles represent the anomalous dates (see text for discussion). The filled circles represent the dates used for interpolation. 93

**Fig. 4.7** (a) Glow curves, (b) growth curves and (c) age plateau, for partial bleach dating (10 min sun exposure) of sample N-127. 95

**Fig. 4.8** Result of anomalous fading test on a typical sample. The dashed lines show the TL of two aliquots immediately after irradiation of 44Gy. The continuous lines show the TL record of two other aliquots of the same sample similarly irradiated 3 months previously. 96

## **CHAPTER 5 SUMMARY, SYNTHESIS AND FUTURE PERSPECTIVES**

**Fig. 5.1** Schematic representation of the geography of the Nal and surrounding regions during the period (~125ka BP) of last major interglacial transgression (in Stage 1 of evolution of Nal region) 105

<b>Fig. 5.2</b> Schematic representation of the geography of the Nal and surrounding regions during the period (~18ka BP) of last glacial maximum (LGM) regression (in Stage 2 of evolution of Nal region)	106
--	-----

<b>Fig. 5.3</b> Schematic representation of the geography of the Nal and surrounding regions during the period (~5ka BP) of Holocene transgression (in Stage 3 of evolution of Nal region)	109
--	-----

**Appendix D    Experimental Procedures For  $\delta^{13}\text{C}$  And C/N Analyses**

<b>Fig. D.1</b> Assembly line for extraction of Carbon dioxide and Nitrogen.	129
--	-----

<b>Fig. D.2</b> Calibration curve for determination of nitrogen.	130
--	-----

<b>Fig. D.3</b> Calibration curve for determination of carbon dioxide.	132
--	-----

## **LIST OF TABLES**

### **CHAPTER 3 PALAEOCLIMATIC STUDIES**

<b>Table 3.1</b>	Major palaeoclimatic data sources and their characteristics. (Compiled from Bradley, 1985; Matsumoto, 1991).	57
<b>Table 3.2</b>	Radiocarbon dates for Horizon- 2 & 3, Nal Sarovar core.	61
<b>Table 3.3</b>	Radiocarbon dates for Horizon-1, Nal Sarovar core.	62
<b>Table 3.4</b>	Results of C, N and $\delta^{13}\text{C}$ analyses on present day samples from Nal Sarovar.	64
<b>Table 3.5</b>	Results of C, N, $\delta^{13}\text{C}$ and % sand analyses on samples from Nal Sarovar core.	65

### **CHAPTER 4 LUMINESCENCE DATING STUDIES**

<b>Table 4.1</b>	Results of luminescence and dosimetry measurements on samples from Nal Sarovar core.	89
<b>Table 4.2</b>	Estimation of U and Th on samples from Nal Sarovar core by $\gamma$ counting in different parts of decay chain. Also given are the estimates from $\alpha$ counting.	98
<b>Table 4.3</b>	Mean grain size of samples from sandy horizon that have been dated by luminescence method.	99

### **Appendix A    Sampling procedures**

<b>Table A.1</b>	Details of Nal Sarovar core samples.	114
------------------	--------------------------------------	-----

### **Appendix B    Experimental Procedures For Sedimentological And Mineralogical Analyses**

<b>Table B.1</b>	Results of grain size analyses on samples from Nal Sarovar core	122
<b>Table B.2</b>	Results of clay mineral analyses on samples from Nal Sarovar core	124

## **ACKNOWLEDGEMENTS**

I wish to thank my guide, Dr. S.K. Gupta for stimulating discussions, leading to selection of the present research problem. He has been very supportive and encouraging throughout the duration of my work. My grateful thanks are also due to Dr. L.S. Chamyal who agreed to be my co-guide and gave invaluable help at various stages of this work. His keen sense of humour, especially in times of stress, also taught me to keep problems in perspective.

Prof. S.S. Merh is especially thanked for his generous help, useful discussions and encouragement during the course of this work. His comments on draft of this thesis have helped considerably in improving it.

The 54m long Nal Sarovar core was raised by the staff of the Directorate of Geology and Mining, Govt. of Gujarat. I would like to thank the Director and the highly efficient staff, for their co-operation. Thanks are also due to the Forest Dept., Govt. of Gujarat for giving permission to drill in the protected Nal Sarovar sanctuary.

The remote sensing work was carried out at GERI Baroda, Geology Dept., M.S. University of Baroda and CEPT, Ahmedabad. The staff at all these institutes are acknowledged for their help. Dr. Anjana Vyas and Ms. Sheetal from CEPT are especially thanked for their co-operation. The bore hole data was collected from GWRDC, CGWB, GWSSB, Ahmedabad. The help of all these agencies and their staff is acknowledged. Dr. S.D. Nayak, Remote Sensing Division, Space Application Centre, Ahmedabad is thanked for useful discussions. Mr. R.L. Jain, GSI, Gandhinagar helped in the identification of shells found in Nal Sarovar core.

Prof. S. Krishnaswami, Prof. N. Bhandari, Dr. R.K. Pant, Dr. P. Sharma are acknowledged for their useful suggestions for improving this work. Dr. P. Sharma additionally made several suggestions for improving the draft of the thesis.

Dr. Sheela Kusumgar is acknowledged for help in radiocarbon dating, and computer facilities whenever needed. Prof. A.K. Singhvi is thanked for providing access to TL laboratory facilities, stimulating discussions and also

for checking the draft of the chapter on luminescence dating. Dr. M.M. Sarin is thanked for his prompt help in AAS analyses.

Dr. V.S. Kishan Kumar and Mr. Someshwar Rao are acknowledged for patiently teaching the basic concepts in TL dating. Mr. Navin Juyal is thanked for useful and interesting discussions. Mr. Anil Shukla is thanked for his help with gamma spectrometry analyses. Mr. D. Banerjee is acknowledged for use of programmes for dose rate calculation and error estimation.

The stable isotope work was made possible due to co-operation from staff of glass blowing section and liquid nitrogen plant. Mr. R.A. Jani is especially thanked for spending time to teach the operation of mass spectrometer. Mr. M.G. Yadava and Mr. N.B. Vaghela, radiocarbon lab, provided generous and timely help in times of crisis. Mr. M.H. Patel made life and work interesting with his help.

My officemates and colleagues Mr. R.D. Deshpande and Dr. Kailash Pandarinath, provided considerable help during field trips. Dr. Pandarinath additionally carried out grain size and mineralogical analyses. Both these friends are thanked.

Mr. D.R. Ranpura, photography section and Mr. S.C. Bhavsar, drafting section, are acknowledged for their help.

This work was partly supported by the Department of Science and Technology (grant number EST/44/014/90).

Finally, I take this opportunity to thank my family and some of my closest friends, Rashmi, Pauline and Shikha for being there whenever I needed them.

## **ABSTRACT**

The Nal region is a low lying tract, linking the Gulf of Kachchh through the Little Rann to the Gulf of Khambhat. Lying in the middle of this depression (22°48'N, 72°E) is a large (~120km<sup>2</sup>) shallow (average depth 2m, +14m msl) lake, Nal Sarovar. This region lies within the palaeo-Thar Desert margin and is a potential site for palaeoclimatic investigations. On the basis of its location and elevation, it has earlier been surmised by many workers that Nal Sarovar represents the remnant of a sea link that existed between the two gulfs until recently (~2ka BP). Owing to its low elevation, proximity to the Gulfs of Kachchh and Khambhat, and also to the tectonically active Cambay Graben, it is likely that both eustatic sea level changes and tectonism have played a role in the evolution of Nal region. It was, therefore, essential to reconstruct the evolutionary history of this region to provide a framework for any palaeoclimatic investigations.

This study was, therefore, carried out with the dual objectives of understanding the evolution of Nal region, in terms of an interplay of regional tectonism and eustatic sea level changes, and to decipher its Holocene palaeoclimatic history. This study represents the first major attempt in this direction and is based on the application of a variety of techniques that included: (i) remote sensing studies, (ii) subsurface lithological correlation, (iii) sedimentological and mineralogical characterisation of sediments, (iv) isotopic and C/N ratio studies, (v) radiocarbon, and (vi) luminescence dating. Detailed laboratory investigations were carried out on a 54m long core raised from the bed of Nal Sarovar.

Based on the results of various investigations, a three stage model for the evolution of the entire Nal region, during Late Quaternary, has been developed. In STAGE 1 of evolution, spanning the marine isotope stage 5 (127-73ka), a shallow sea linked the Gulf of Kachchh with the Gulf of Khambhat. Fine grained sediments from south and/or west were being deposited in the Nal region. This study also indicated that the sea

connection between the Gulf of Kachchh and Gulf of Khambhat broke up around the beginning of marine isotope stage 4 due to regression of the sea. Subsequently, only a land link remained. In STAGE 2 (73-7ka) of evolution, fluvial sediments from east were episodically being deposited in the Nal region in response to the westward migration of the depositional front of the eastern rivers. This was probably caused by a combination of regression of the sea, leading to lowering of base level and/or tectonic uplift in the region of Cambay Graben. In STAGE 3, as a result of the combined influence of westward advance of the sedimentation front, tectonism and post-glacial sea level rise, Nal Sarovar came to within a few metres of its present elevation at about 7ka when it became a closed basin.

Palaeoclimate reconstruction for the last ~7ka was attempted using  $\delta^{13}\text{C}$  and C/N ratios of organic matter from sediments deposited during STAGE 3 of evolution. This is the first high resolution palaeoclimatic study from the palaeo-Thar margin. The observed variations in  $\delta^{13}\text{C}$  and C/N indicate that the period from ~6.6-6ka was generally drier than present with the exception of a short wet phase around 6.2ka. From 6-4.8ka the rainfall was lower than present but possibly more evenly distributed as a result of a slight increase in winter rainfall. From 4.8-3ka the climate was wetter than present. The trend towards aridity began around 3ka and present day conditions set in ~2ka BP. This picture is somewhat different from the one deciphered by earlier workers from Rajasthan lakes for the period 6.5-4.8ka when, in opposition to the wetter climate in Rajasthan, the climate here was drier. From 4.8ka to present however the climatic changes in this region are similar to those in Rajasthan. Also, a general agreement between periods of glacier expansion in Eurasia and drier periods in Nal Sarovar is observed. This suggests that the palaeoclimatic record from Nal is a regional feature.



# **CHAPTER 1**

## **INTRODUCTION**

The Quaternary sediments of Gujarat preserve a record of a complex interplay of eustatic, climatic and tectonic changes through geological time. It is only in the past few decades that a concerted attempt has been made to decipher their evolutionary history through a study of various exposed sections. This, however, has resulted in leaving low lying areas, that lack exposed sections, remaining unstudied or receiving only cursory attention. The aim of the present work is to decipher the evolutionary history, of the low lying Nal region, through a multidisciplinary study of sub-surface Quaternary sediments.

### **1.1 Study area**

The Nal region is a low lying tract (average elevation  $\sim +15\text{m msl}$ ) which links the Gulf of Kachchh through the Little Rann to the Gulf of Khambhat (also known as the Gulf of Cambay) (Fig 1.1). The region lies between the Saurashtra highlands, to the west, and the Gujarat alluvial plains to the east. There are no major rivers draining into the region today. However, the region gets flooded during the summer monsoon months of June to September by the surface runoff from the surrounding districts of Ahmedabad and Surendranagar. In the following summer, the accumulated water dries up leaving behind a white salt crust covering large areas in the Nal region. Lying almost in the centre ( $22^{\circ}48'$ ,  $72^{\circ}\text{E}$ ) of this depression is a large ( $\sim 120$  sq km) shallow (average depth

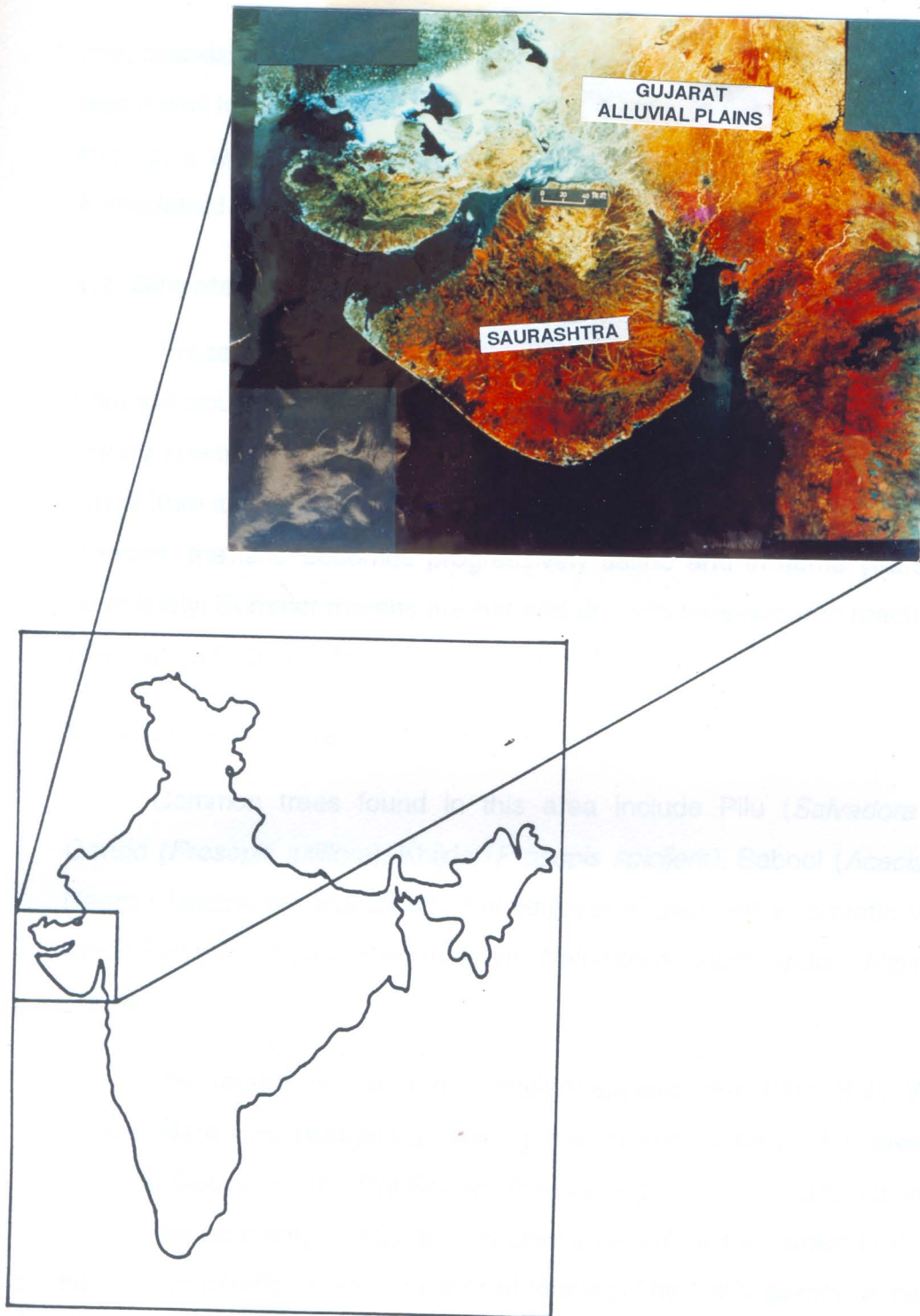


Fig. 1.1 Map of India and satellite imagery of Gujarat showing the location of Nal Sarovar and surrounding regions.

2m), brackish water lake, Nal Sarovar, (Sarovar in Hindi meaning lake) which is also a well known bird sanctuary of India. The entire region is easily accessible through a well laid network of roads. There are convenient bus services from Ahmedabad for reaching Nal Sarovar.

## 1.2 Climate

Presently, the region receives about 500mm of annual rainfall, mainly from the south-west monsoon in the months of July, August and September. During these months the lake is fresh and relatively deep. Winter temperatures range from a maximum of 22°C during daytime to 8°C at night. With the onset of summer, the lake becomes progressively saline and in some years dries up completely. Summer months are hot and dry with temperatures reaching a high of about 45°C during daytime and a low of 30°C during nights.

## 1.3 Flora and fauna

Common trees found in this area include Pilu (*Salvadora persica*), Gando (*Prosopis juliflora*), Khijdo (*Prosopis spicijera*), Babool (*Acacia nilotica*), Neem (*Azadirachta indica*) etc. Nal Sarovar is also rich in aquatic vegetation which includes *Typha*, *Potamogeton*, *Nelumbium*, *Aponogeton*, *Najas*, *Chara*, *Nitella*.

The region harbours mammalian species like Blue Bull, Wild Ass, Jackal, Hare and Hedgehog. Among the snakes found in this area are the common Cobra and the Rat Snake. The Nal region is especially rich in bird life. In fact, the economy of this area is chiefly based on the varied bird life found here which attracts a large number of tourists. The Nal supports some 250 bird species including Brahmini Maina, Ringed Plover, Cormorants, Koel, Oriole and Pelicans to name a few. In addition several species of migratory birds e.g. Flamingos visit the lake every year.

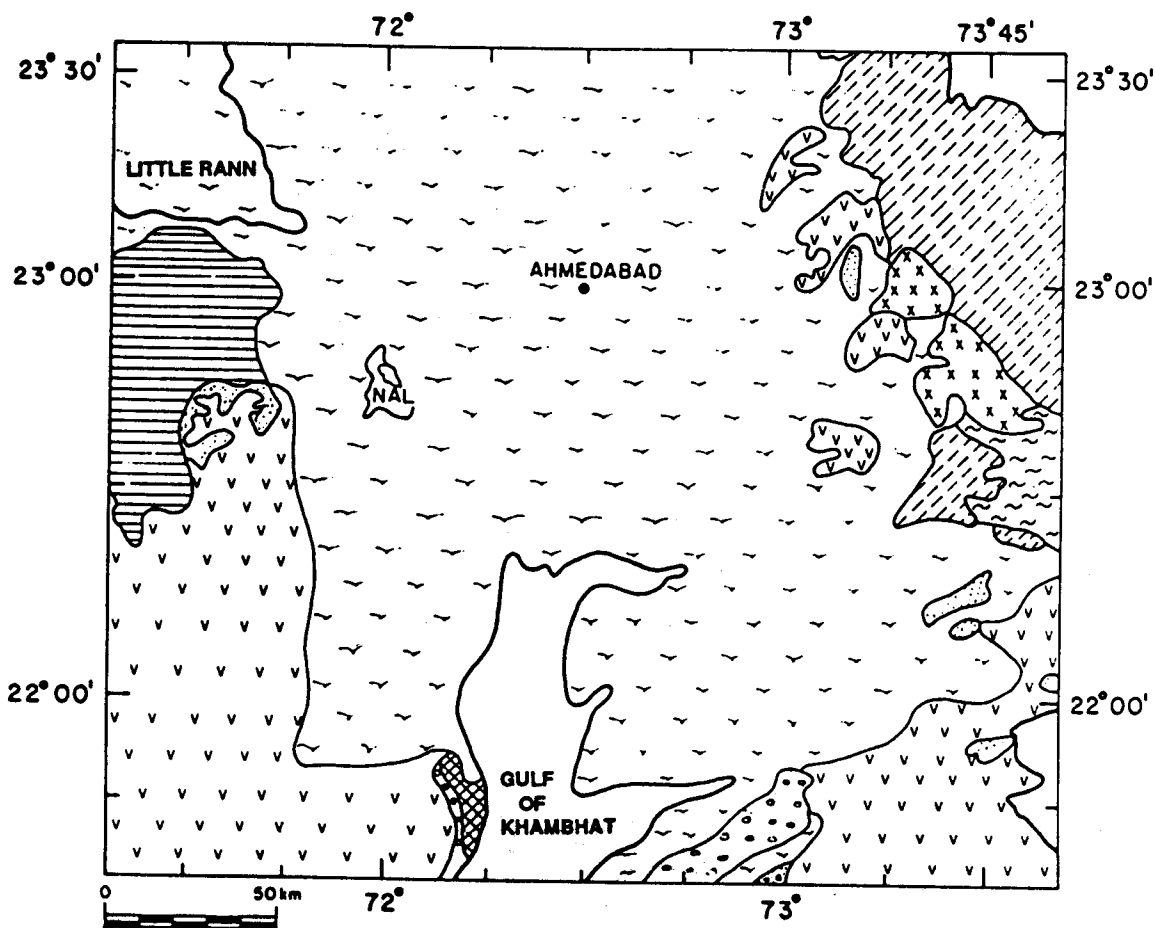
## 1.4 Geology

Nal depression, which constitutes the study area, is bounded by the Saurashtra basalts on the west and by the Juro-Cretaceous sandstones in the north-west. Alluvial plains are found to the east and north-east. To the extreme north-east are present the igneous and metamorphic rocks of the Aravallis comprising granites, dolerites, garnetiferous mica schist, hornblende schist and phyllites. Fig. 1.2 shows the geological map of the Nal and surrounding regions. The salt plains of Kachchh (the Little and the Great Ranns of Kachchh) are present in the northern vicinity of the Nal Sarovar while the mud flats are found towards the southern extremity.

## 1.5 Tectonics

The Nal study area is bounded by the following major faults (Fig 1.3):

- a) Approximately 30km to the east of Nal region lies the western boundary of Cambay Graben (WCBF), where the Deccan trap rocks have been downthrown by nearly 2000m.
- b) There is a fault (AA') to the west of Nal region which manifests itself as a prominent lithological boundary, trending N-S, beginning west of Nal Sarovar in the north and ending near the town of Palitana in the south. This is a contact between the Deccan volcanics in the west and alluvium in the east.
- c) Another important fault (A'B') extends from near Bhavnagar in the east to Damnagar in the west and trends roughly E-W. This fault marks the boundary between an enormous thickness of the alluvium to the north and the Deccan Basalts to the south. This suggests that the fault block to the north may have been downthrown as there is no trace of basalts on the surface, the entire region being occupied by the alluvium in the north. However, basalts have been encountered at depths varying from 200-600m by Oil and Natural Gas Corporation (ONGC) during the course of drilling (Biswas, 1987).
- d) Sridhar (1995), inferred a rotational fault (CC') passing through Nal Sarovar.



Source: Ground Water Dept., Gujarat.

# **LEGEND**

	Quaternary Deposits		Deccan Traps
	Eocene Kirthar-Laki beds		Aravalli System
	Upper Cretaceous Sandstone		Gaj-Nari Series
	Jura Cretaceous Sandstone		Archean Gneisses
	Laterite		Archean Granites

Fig. 1.2 Geological map of Nal and surrounding regions.

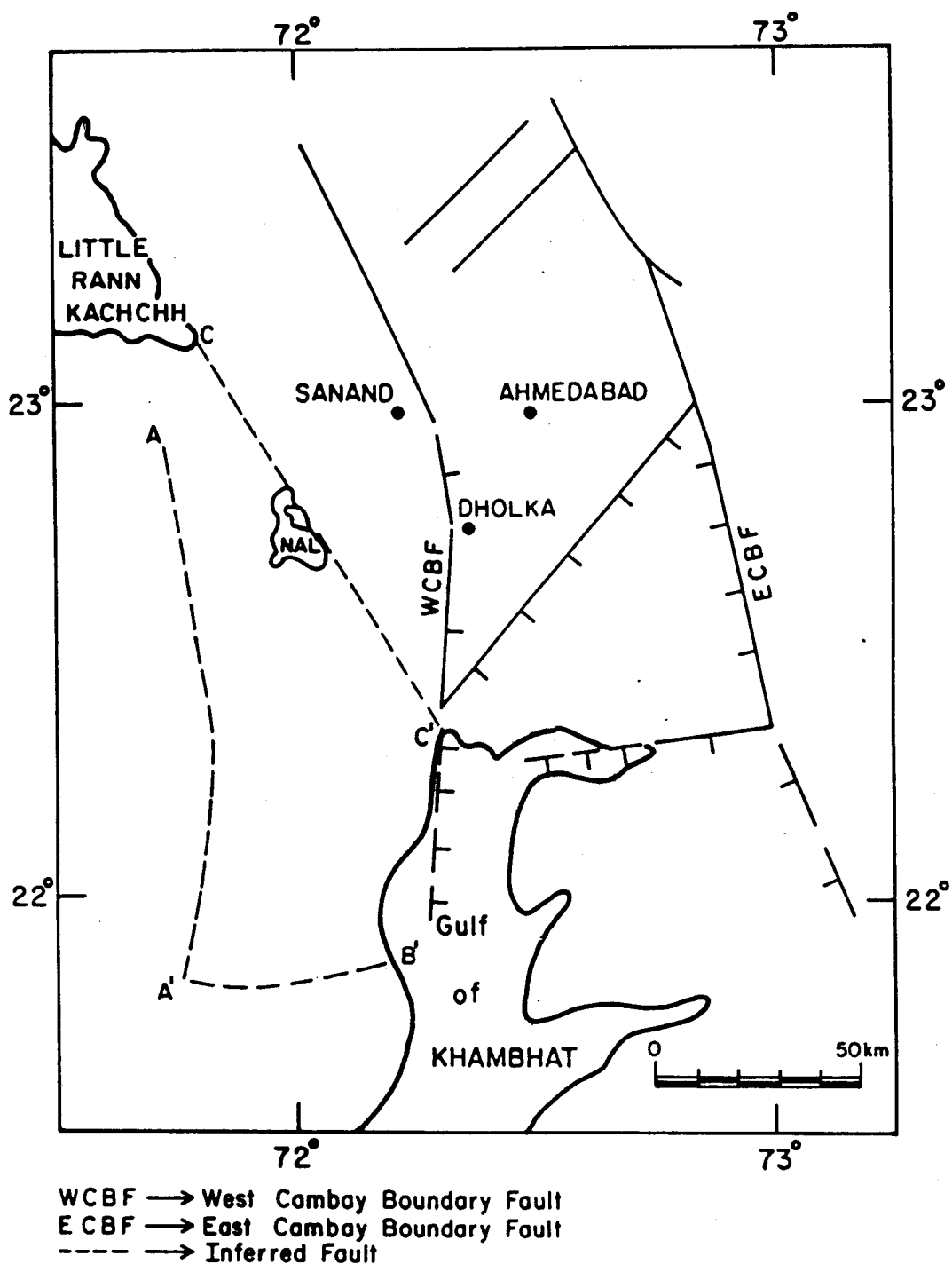


Fig. 1.3 Tectonic map of Nal and surrounding regions.

(Modified after Chandra and Chaudhary, 1969).

## 1.6 Motivation and scope

Being located within the palaeo-Thar Desert margin (Goudie et al, 1973), the entire Nal region is a potential site for palaeoclimatic investigations. However, little is known about the evolution of this region. Based on its location in a low lying area, it had been surmised by earlier workers that the Nal lake is a remnant of a sea which linked the Little Rann of Kachchh and Gulf of Khambhat. This link was believed to have been progressively filled due to fluvial input from N-NE and west (Sukeshwala, 1948; Allchin et al, 1978). This proposed sea link was thought to have existed till ~2 ka and is believed to have been present at the time of the Holocene transgression (Merh, 1992). However, some questions remain:

1. Why does this topographic low not coincide with the Cambay Graben, located to the east of Nal, where the Deccan traps have been downthrown by more than 2000 m?
2. Based on radiocarbon dating, the elevation of Nal Sarovar was estimated to have been ~+10m, at the time of Holocene optimum (Gupta, 1973). Therefore, considering the magnitude of Holocene eustatic sea level rise on the west coast of India, variously quoted at +2 to +6m (Gupta, 1976), ~+3m (Pant and Juyal, 1993; Hashimi et al, 1995), and the absence of any reported evidence of uplift for the region, a sea link at the time of Holocene transgression seems unlikely.
3. In view of the fact that the global sea level was ~+7m msl during the last major interglacial (Ku et al, 1974; Cronin et al, 1981; Chappel and Shackleton, 1985; Pant and Juyal, 1993) and the low lying topography of the area, the existence of a sea link at some time during pre - Holocene cannot be ruled out. In such a case, if and when did the sea link exist?
4. The Nal region lies in close proximity to the Cambay Graben where evidences of Quaternary tectonism in the form of entrenched streams, cliffy sections and fault controlled drainage pattern have been

observed (Sridhar et al, 1994). What role was played by eustasy and regional tectonism in the evolution of Nal region?

The motivation for this work has therefore been to find answers to the questions posed above and to supplement the meagre palaeoclimatic data that is available from this semi arid region bordering the Thar Desert.

## **1.7 Objectives**

The objectives of the thesis are two fold:

1. To decipher the evolutionary history of the Nal region in terms of eustasy and tectonism.
2. To reconstruct the Holocene palaeoclimatic history of the region.

## **1.8 Approach**

### ***1.8.1 Evolution of Nal region***

The study is based on the interpretation of remote sensing data and subsurface lithological correlation of bore hole data from regions around Nal Sarovar. In this connection, following studies were carried out.

1. Identification and mapping of drainage pattern and palaeochannels using toposheets and IRS FCC 1A imagery (1:250,000 and 1:50,000 scale) for studying past drainage patterns. This was necessary to identify the probable source of sediments in this region as also to study the changes in drainage pattern. The channels were identified on the imageries on the basis of colour, tone and linearity. Both pre- and post-monsoon imageries were studied and compared with the toposheets to identify the defunct channels.
2. Geomorphological features such as palaeo-deltas and mud flats which are indicative of sea level changes were also delineated and mapped using IRS FCC 1A imagery.
3. There are no surface exposures of Quaternary sediments in the Nal region. Hence, bore hole lithologs were collected from Central Ground Water Board



(CGWB), Gujarat Water Resources Development Corporation (GWRDC) and Gujarat Water Supply and Sewerage Board (GWSSB), for thirty stations spread over the Gujarat alluvial plains and Nal region. Three transects, two in NE-SW and one in NS direction were drawn, to enable subsurface lithological correlation as well as to study facies variation.

### **1.8.2 Palaeoenvironmental studies**

The basic framework was provided by

1. Sedimentological studies to obtain information about the environment of transport and deposition of sediments.
2. Mineralogical studies using X-ray diffraction (XRD) and heavy mineral analysis for provenance identification.
3. Study of stable isotopic ( $\delta^{13}\text{C}$ ) and carbon/nitrogen (C/N) variations on organic matter for palaeoclimatic reconstruction.
4. Chronology, using radiocarbon and luminescence dating techniques, on the 54m long core raised from the bed of Nal Sarovar.

The results of these studies were synthesised with the available data on the eustatic sea level changes and a scenario for the evolution of entire Nal region was developed. Within the framework of this scenario, paleoclimatic reconstruction of the Holocene was planned.

The thesis is structured as follows:

In **Chapter 2** is discussed the methodology and results of geological and geomorphological studies.

In **Chapter 3** are discussed the results of radiocarbon dating, stable isotope ( $\delta^{13}\text{C}$ ) and C/N ratio analyses. Also discussed are the palaeoclimatic interpretation of these studies.

In **Chapter 4** are discussed the basic principles and results of luminescence dating of Nal core.

In **Chapter 5**, the results of various studies carried out are summarised and synthesised. A model for the evolution of Nal region is also presented.

Sampling procedures and experimental details of laboratory studies are discussed in the Appendixes.

In **Appendix A** the sampling procedures and details of Nal Sarovar core are presented.

In **Appendix B** the procedures employed in sedimentological and mineralogical studies are presented.

In **Appendix C** the details of procedures employed for radiocarbon dating are presented.

In **Appendix D** the procedures employed for stable isotope ( $\delta^{13}\text{C}$ ) and %C, %N measurements are presented.

In **Appendix E** the details of procedures employed for luminescence dating are presented.

## **CHAPTER 2**

### **GEOLOGICAL AND GEOMORPHOLOGICAL STUDIES**

The Nal area presently is a regional low and derives its sediment input both from the Saurashtra side and from the eastern alluvial plains. It, therefore, becomes important to know the Quaternary geological history of both the regions as they are likely to have influenced the sediment record of the Nal region. In this Chapter, the available information about the geology and tectonic history of the surrounding regions, is summarised. This provided a framework within which the results of present geologic and geomorphic investigations, also discussed in this chapter, were interpreted.

#### **2.1 Background information**

The Quaternary sediments of Gujarat show the presence of palaeo-strandlines, inland and elevated miliolites, fault controlled variable thickness of sediments, fault controlled drainage pattern and raised mud-flats indicating the active role of tectonism, both syn- and post-depositional, in the development of present day landscape. On the basis of geological history and sediment types, the Quaternary sediments of Gujarat can be sub-divided as (see Fig. 2.1):

1. Quaternary sediments of Central and North Gujarat.
2. Quaternary sediments of Saurashtra.
3. Quaternary sediments of Ranns of Kachchh.
4. Quaternary sediments of Nal depression.

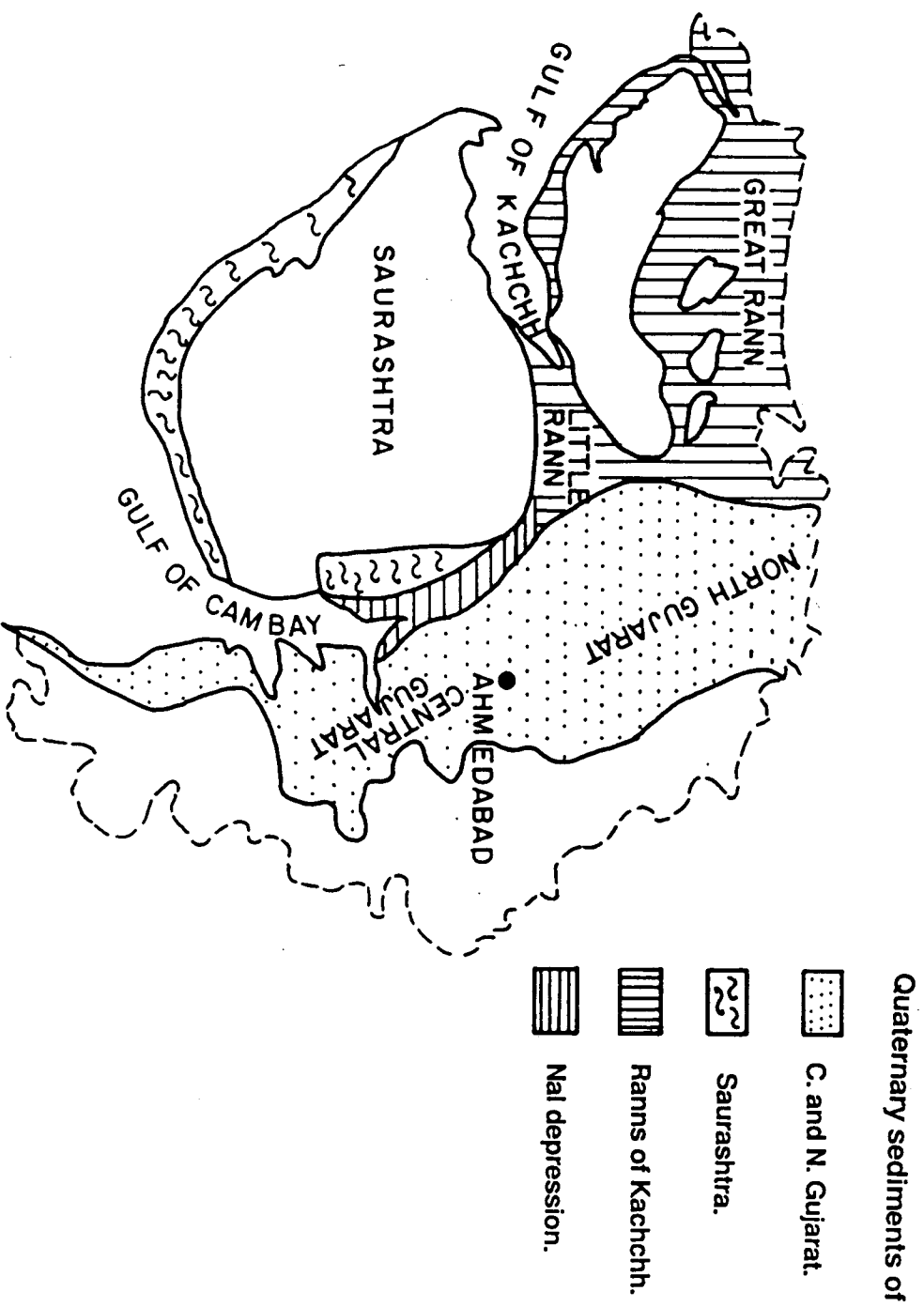


Fig. 2.1 The sub-divisions of Quaternary sediments of Gujarat.

The geographic distribution and available geological information for each of these units is discussed below.

### ***2.1.1 Quaternary sediments of central and north Gujarat***

The Quaternary sediments of Gujarat alluvial plains are bounded by the Aravalli range in the NE, by the Narmada geofracture in the south and on the northern side gradually merge with the recent aeolian deposits of the Thar Desert. To the west, these alluvial deposits gradually slope towards the Nal depression (Fig. 2.1). The major part of deposition has occurred within the Cambay and Narmada Grabens. These Quaternary sediments have been extensively studied and reported. A summary of these studies is presented below.

The Cambay basin is a graben bounded by two NS trending faults (Fig. 1.3) that developed at the close of the Cretaceous. Biswas, (1982, 1987) attributed this basin formation to the rifting of the western continental margin. During Tertiary, the sedimentation was dominantly marine. However, with the advent of the Quaternary, a change in sedimentation pattern occurred. The Lower Pleistocene deposits have been reported to comprise fluvio-marine/deltaic sediments indicating fluctuating shallow water marine and continental conditions (Chandra and Chaudhary, 1969). Later tectonic activity has exposed several sections along river courses which have been described by several workers (Foote, 1898; Sankalia, 1945; Zeuner, 1950; Sareen et al, 1992). The first major transgression during Quaternary took place only in Middle Pleistocene and is represented by the mottled clays having blue green colour in some sections. Chamyal and Merh (1992), have described the sequence in the Sabarmati basin (Fig. 2.2) in detail. The sequence comprises of the Hirpura Formation of late Middle to Middle Pleistocene age, consisting of mottled basal clay, consolidated gravels, pedogenised mud and cross stratified gravels. Overlying these are red soils developed over silty sands and pedogenised laminated muds of the Vijapur Formation which have been

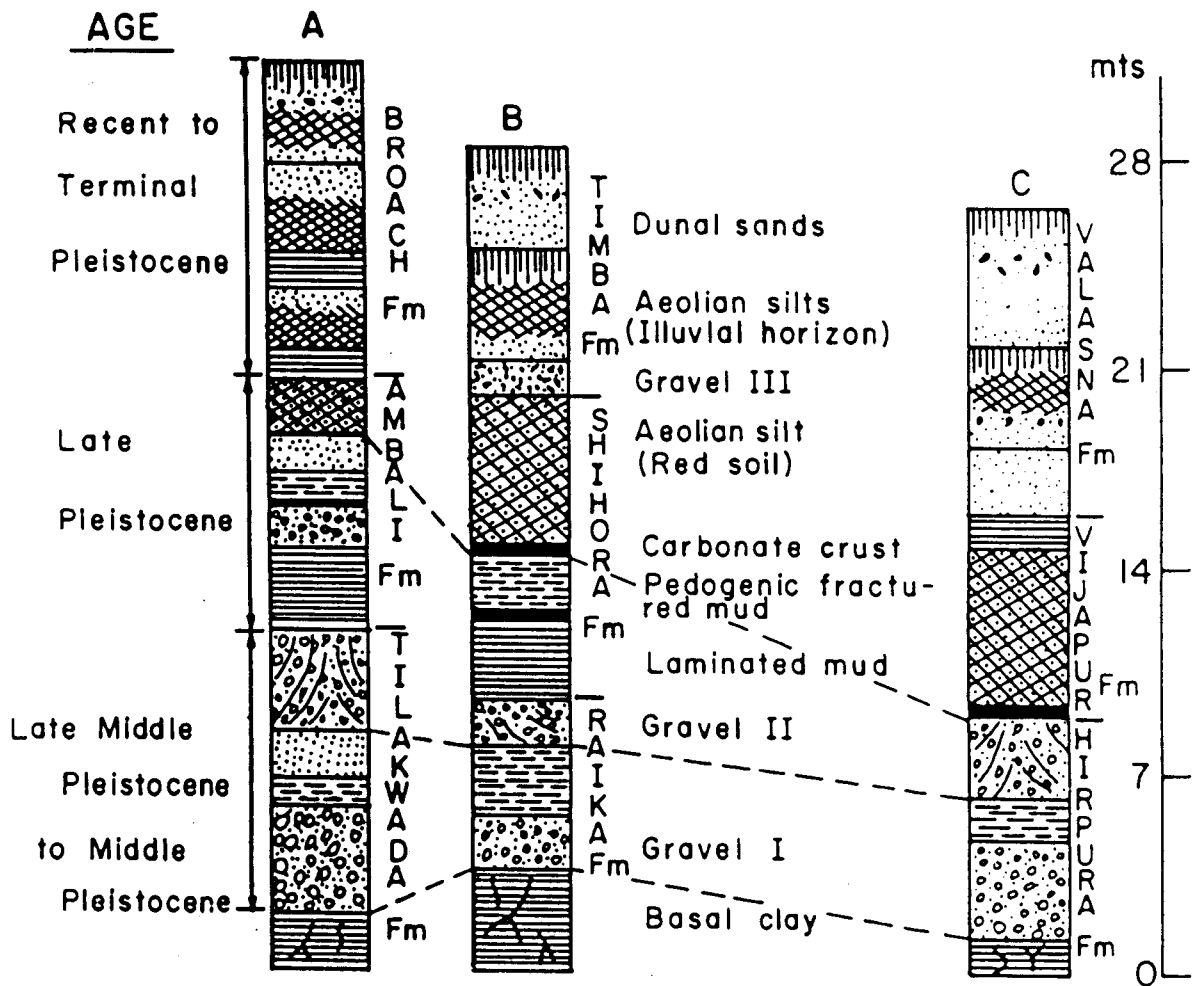


**Fig. 2.2** Composite Quaternary sediment profiles of river basins of Gujarat.

(A) Narmada (B) Mahi (C) Sabarmati.

(Redrawn from Chamyal and Merh, 1992)

assigned an age of Late Pleistocene. On top is the Valasna Formation comprising sands, aeolian sand and silts of Terminal Pleistocene to Recent age. Chamyal and Merh (1992), and Merh and Chamyal (1993), have attempted to provide an integrated picture of the exposed sequences in the various N. Gujarat rivers and correlate them with those of Mahi and Narmada to the south (Fig. 2.2). South of Narmada the alluvial deposits do not exceed 100m, between Narmada and Sabarmati the maximum thickness is 200m, while in north Gujarat it reaches upto 500m (Merh and Chamyal, 1993). The varying thickness of Quaternary sediments has been attributed to their deposition within a number of sub-basins of different sizes and depth which were formed due to the reactivation of the pre-existing Tertiary faults (Maurya et al, 1995). Such a huge thickness of sediments cannot be attributed to the action of present day rivers which are erosional. Sridhar et al (1994), have visualised the existence of a stronger fluvial system to explain the vast thickness of sediments accumulated in the graben. This 'super-fluvial' system was believed to have originated in the Aravallis and to flow south-west to drain into the Gulf of Kachchh. The disruption of the super-fluvial system, during middle to late Quaternary, appears to have been caused by differential uplifts within the graben (Ghosh, 1952; Sareen et al, 1993), eustatic changes in the base level and uplift of the Aravallis (Ahmad, 1986). The evidences of tectonism can be seen in the form of entrenched rivers, cliffy banks and fault controlled river courses.

Early Holocene coastal deposits, comprising raised mud flats are found between Mahi and Narmada rivers (Merh and Chamyal, 1993).

### ***2.1.2 Quaternary sediments of Saurashtra***

The Lower Pleistocene, on the Saurashtra coast, is represented by fluvial sands and conglomerates (Merh and Chamyal, 1993). After the advent of the mid-Pleistocene, which was marked by a major marine transgression, the Quaternary record in Saurashtra is better developed. The Lower Pleistocene deposits are overlain by deposits of miliolite formation. These are the most

striking Pleistocene deposits of Saurashtra. They are essentially consolidated biogenic beach sands and the constituent rocks dominantly made up of sand sized calcareous shell fragments and tests of foraminifers of family Miliolidae. The miliolites occupy the western and southern coastal fringes (Fig. 2.1) and also occur as discrete outliers in the inland areas (Barda, Alech hills, Chotila hill, foothills of Mt. Girnar). The occurrences of miliolites at different levels has resulted in a lively discussion with one side invoking a succession of high strandlines during Quaternary (see references in Merh, 1992) and the other side (Bhaskaran et al, 1989) proposing to explain the occurrence of miliolites at higher levels by invoking a tectonic upliftment of the order of 0.23 to 2.2 mm per year during the Late Quaternary. Both these theories are, however, not acceptable to most workers who point to the reported (Pascoe, 1964; Chapman, 1900; Wadia, 1953; Patel and Bhatt, 1995) abundance of typical aeolian features preserved in most of the inland occurrences. The coastal miliolites have been grouped into two distinct members - an underlying shelly limestone (unconsolidated beach rock) and overlying aeolian beach accumulations (Merh and Chamyal, 1993). The underlying member has occurrences at elevations of +25m msl and is encountered up to 15-20km inland. Beyond this the shelly limestone is absent and all miliolite occurrences comprise aeolian accumulations of miliolite resting over older rocks (Merh, 1995). On this basis, the maximum level of mid Pleistocene transgression is estimated to be about +25m msl. Uranium series dating has been used to suggest that miliolite formation over Saurashtra may have occurred in three age brackets ranging from  $170 \pm 30$ ,  $95 \pm 15$ , and  $60 \pm 10$  ka (Bhaskaran et al, 1989). These dates must however be treated with caution in view of the possibility of contamination of samples and the absence of field evidence for tectonism on the scale reported by these workers (Gupta, 1991).

On the eastern side of Saurashtra, a sharp contact of alluvium with the basalt is observed in the N-S direction extending from a little west of the Nal Sarovar (Fig. 1.2 and Fig. 2.1). This may represent a faulted boundary. The eastern portion is believed to have been under the sea until recent times (Sood, 1983). Further east of Saurashtra, the alluvium gradually slopes into the Nal



depression. The east-west trending Bhavnagar fault extending from Bhavnagar in the east to Damnagar in the west (A'B' in Fig. 1.3) marks the boundary between an enormous thickness of alluvium in the north and Deccan traps in the south. There is no trace of Deccan traps in the north. The basalt flows, to the south of Bhavnagar fault, dip to the north at  $30^{\circ}$  suggesting that the northern side may be the downthrown side (Sood, 1983).

The Holocene sediments of Saurashtra comprise the Chaya formation consisting of semi-consolidated to consolidated shell limestone, coral reefs and oyster beds and are found to be resting over Dwarka formation or over Miliolite (Merh, 1995). The youngest Holocene sediments consist of alluvium deposited by the Bhadar and other rivers of Saurashtra.

### ***2.1.3 Quaternary sediments of the Ranns of Kachchh***

The Ranns of Kachchh are marshy salt plains, north of Saurashtra. These lie just above normal high tide and stretch for nearly 300 km from east to west and nearly 150 km north to south. These are divided by the island of Kachchh into two areas: Great Rann in the north and the Little Rann in the south. The two Ranns get flooded during monsoon season due to sea water forced up by SW monsoon and river input from the east. It was surmised (Pascoe, 1964) that in the recent past the Ranns of Kachchh were a shallow gulf or an arm of the sea that was filled up during Holocene by the silt brought in by the streams draining the surrounding areas.

Gupta (1973, 1975) reported a three layer sequence, from the Little Rann, comprising of a layer of stiff bluish and black clay overlying a layer of gritty sandy clay. This sandy layer, in turn, was underlain by a layer of yellowish clay locally called 'Murund'. He also reported that, unlike the gradual transition from bluish black clay to sandy clay, the contact between sandy clay layer and underlying yellow 'Murund' was abrupt. On the basis of sedimentation rates of 2mm/yr, calculated from radiocarbon dates, Gupta (1973, 1976) concluded that even as late as 2ka BP, the Rann was about 4m deep and remained inundated throughout the year.

#### **2.1.4 Quaternary sediments of the Nal depression**

This region is a low lying area between the alluvial plains of the central Gujarat and the alluvial deposits of the eastern Saurashtra (Fig. 2.1). There are no exposed sections in this region and hence very little is known about this area. Owing to its low lying topography, it is believed to represent a filled up sea link, that previously existed between the Little Rann in the north and the Gulf of Khambhat in the south (Sukeshwala, 1948; Allchin et al, 1978; Merh and Chamyal, 1993). The link is believed to have existed till ~2ka BP (Merh, 1992) and remnants of this sea are thought to be represented by the Nal Sarovar. Gupta (1973), raised a shallow core from Nal Sarovar and indicated an age of 7ka, on the inorganic fraction, at 5m depth. Till date, no detailed study has been done in the Nal region.

#### **2.2 Present study**

The aim of present work is to understand the geologic evolution of the Nal region and to study its palaeoclimatic history. Therefore, a multi-pronged approach was used to decipher the sedimentary and geomorphic record of this region. Satellite imageries and toposheets have been used to study and map the geomorphology and drainage pattern. This, together with the existing bore hole data in the region, was synthesised with the available data on global eustatic sea level changes, to develop a hypothesis for the evolution of the Nal region. This hypothesis was subsequently tested by raising a core from Nal Sarovar, in the central part of Nal depression, and subjecting it to extensive sedimentological and chronometric investigations.

In the following, the details of the methodology adopted, results and their interpretation pertaining to the evolution of the Nal region are presented.

## **2.2.1 Remote sensing studies**

### **2.2.1.1 Methodology**

The objective of these studies was to construct drainage and geomorphological maps of the region and to identify palaeochannels. IRS FCC 1A imagery was used in combination with Survey of India toposheets.

The studies were carried out at the Gujarat Engineering Research Institute (GERI), Baroda; the M.S. University of Baroda; Centre for Environmental Planning and Technology (CEPT), Ahmedabad, and the Space Application Centre (SAC), Ahmedabad. A paper print of IRS FCC imagery (Row: 32 Path: 52, colour code: 2,3,4) on 1:250,000 scale obtained from National Remote sensing Agency (NRSA), Hyderabad was used. This imagery is covered in Survey of India Toposheets 46A, 46B, 41M and 41N on 1:250,000 scale. Both pre- and post- monsoon imageries were initially compared. It was found that in the pre-monsoon print the drainage pattern could be distinguished quite clearly on the basis of tonal changes and linearity of channels. This is because of diminished vegetation cover and the river courses being dry or having very little water. In the post-monsoon imagery, the drab dusty summer colours were replaced by a blaze of colours. It then became difficult to interpret the imagery. Hence, for drainage pattern analysis, pre-monsoon imagery was used. The drainage pattern was traced out from the toposheets and subsequently compared with the satellite imagery. This made possible the identification of palaeochannels. Some minor shifts in the river courses in the past 30yrs, especially in case of Sabarmati river were observed but are not of much interest to this study. The emphasis, of the present study, was on older abandoned channels which may have been responsible for bringing sediments to the Nal area and would give some clue about the tectonic evolution of the region. The same imagery was also used for the preparation of the geomorphological map of the region which showed the presence of features like stabilised dunes, raised mud flats and inland deltas. Fig. 2.3, 2.4 and 2.5

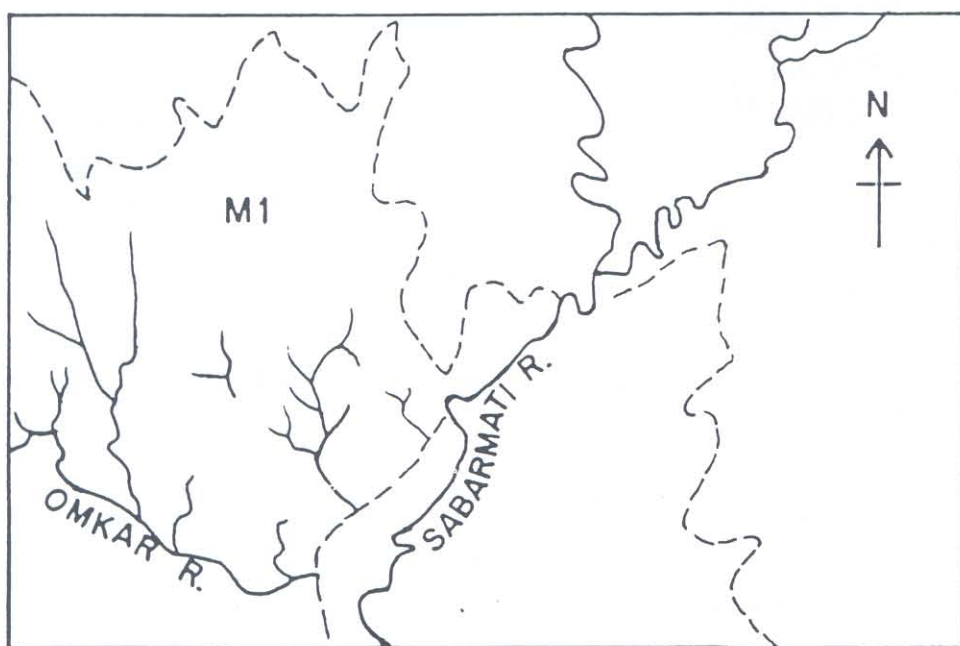
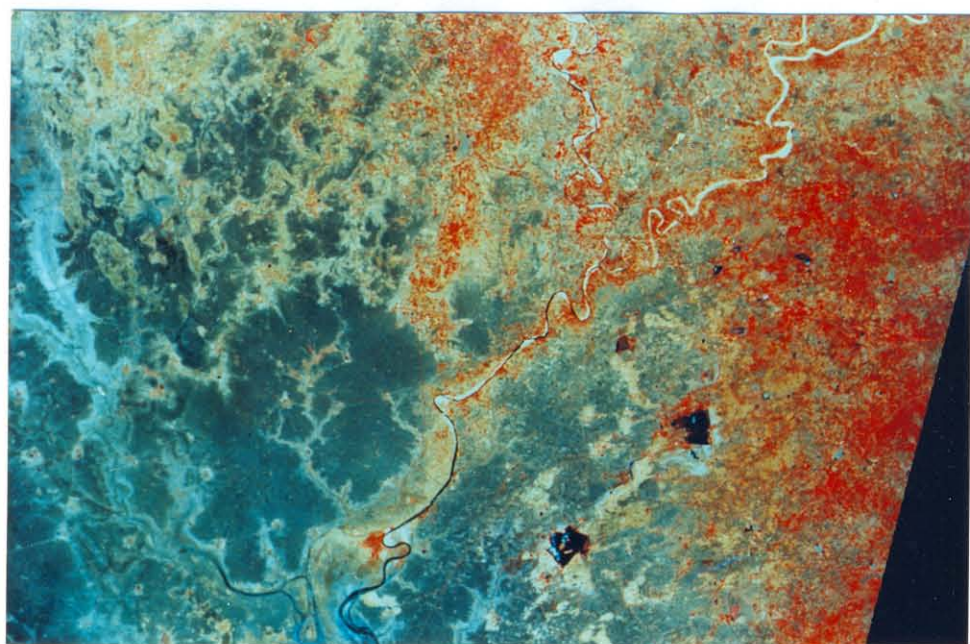


Fig. 2.3 Satellite imagery and interpretation showing deranged drainage pattern in older mud flats, south of Nal Sarovar.

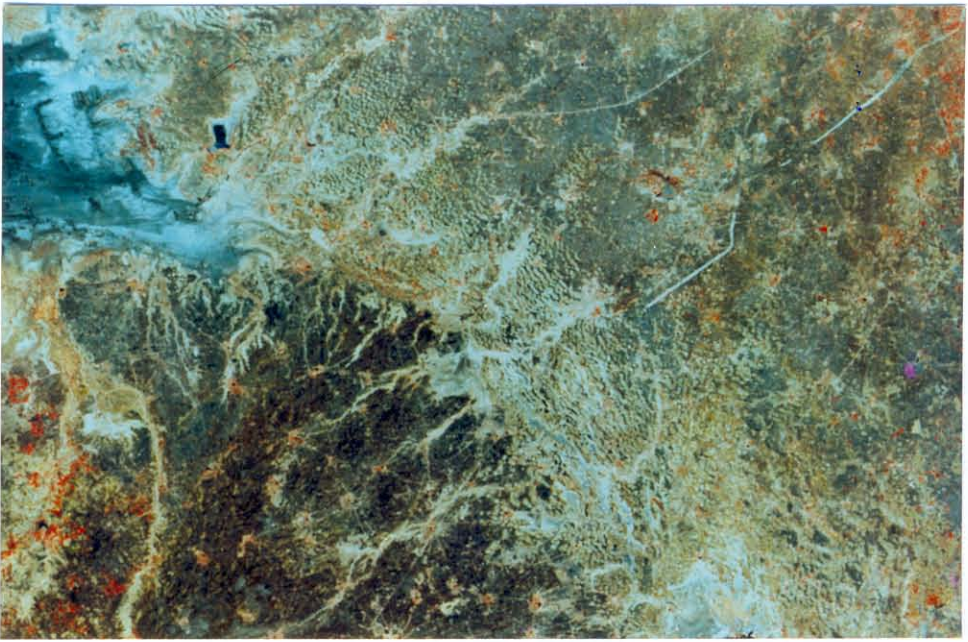


Fig. 2.4 Satellite imagery and interpretation showing the location of palaeochannels (dashed lines), dunes (dots) and alluvial plains, north of Narsar Sarovar.



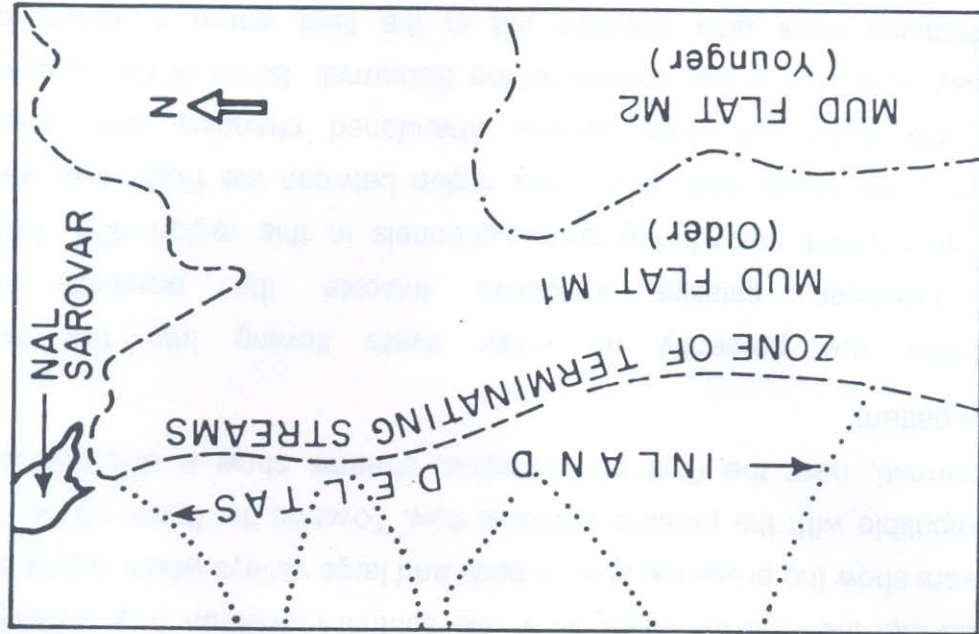
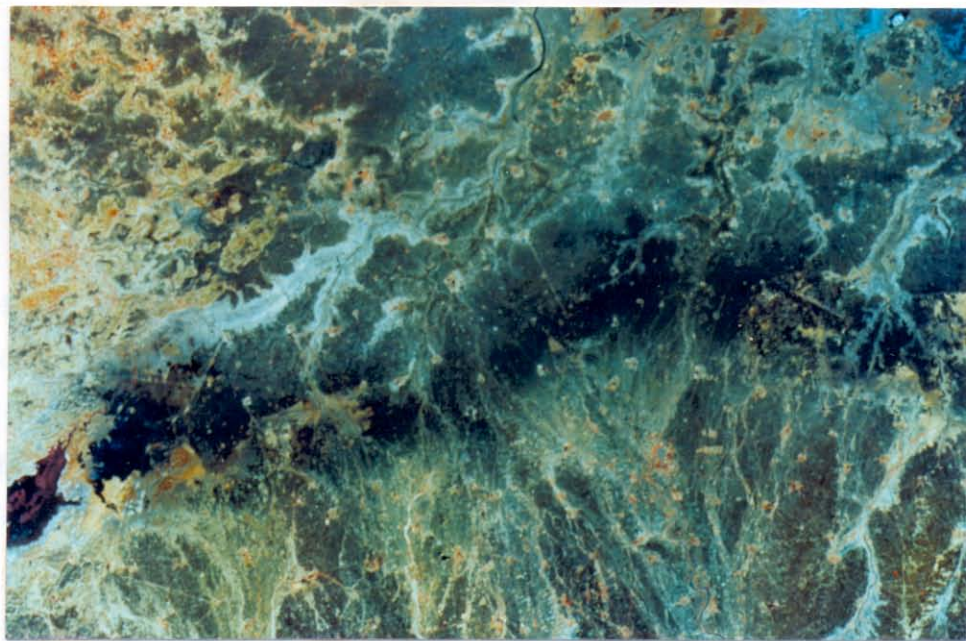


Fig. 2.5 Satellite imagery and interpretation showing inland deltas, zone of terminating streams and older mud flats, south of Nal Sarovar.

show some typical features observed in the satellite imagery. The presence of palaeochannels and other geomorphological features were confirmed by selected field checks during the Jan '96 field season.

In the 1:250,000 scale drainage map, several unusual features of drainage pattern on the Saurashtra side were observed, e.g. thinning down of the major rivers, abrupt termination of streams about 35-40 km inland, changes in stream direction etc. Hence, a more detailed study was justified and carried out in the region (71°30' to 72°30') in the immediate vicinity of Nal Sarovar. For this, Survey of India toposheets 46A/4, 46A/8, 46B/1, 46B/2, 46B/3, 46B/4, 46B/5, 46B/6, 46B/7, 46B/8, 41N/9, 41N/10, 41N/11, 41N/12, 41N/13, 41N/14, 41N/15, 41N/16, 41M/12, 41M/16, (on 1:50,000 scale), were used and a drainage map of larger scale was prepared.

#### 2.2.1.2 Results

##### **Drainage pattern studies**

On the eastern side, the major rivers of the region, Banas, Saraswati, and Rupen flow into the Little Rann/Gulf of Kachchh along the SW slope of the region, with the exception of the Sabarmati which cuts across the general slope and flows into the Gulf of Khambhat in the southern direction (Fig. 2.6). All these rivers show the presence of wide beds and large valleys which appear to be incompatible with the present seasonal flow. Towards the lower course of the Sabarmati, near the Gulf of Khambhat, streams show a disorganised drainage pattern.

There are presently no major rivers flowing into the Nal region. However, satellite imageries indicate the presence of several abandoned meandering palaeo-channels in this region (Fig. 2.6). Upstream of the Rodh river, and in the region between the Rodh river and present day Sabarmati river, several abandoned channels were seen which may represent former courses of the Sabarmati. Some of the mapped palaeochannels were also checked out in the field where a variety of related features were observed. At Phangdi, the pre-existing channels exist in patches as small seasonal streams (Plate 1) that

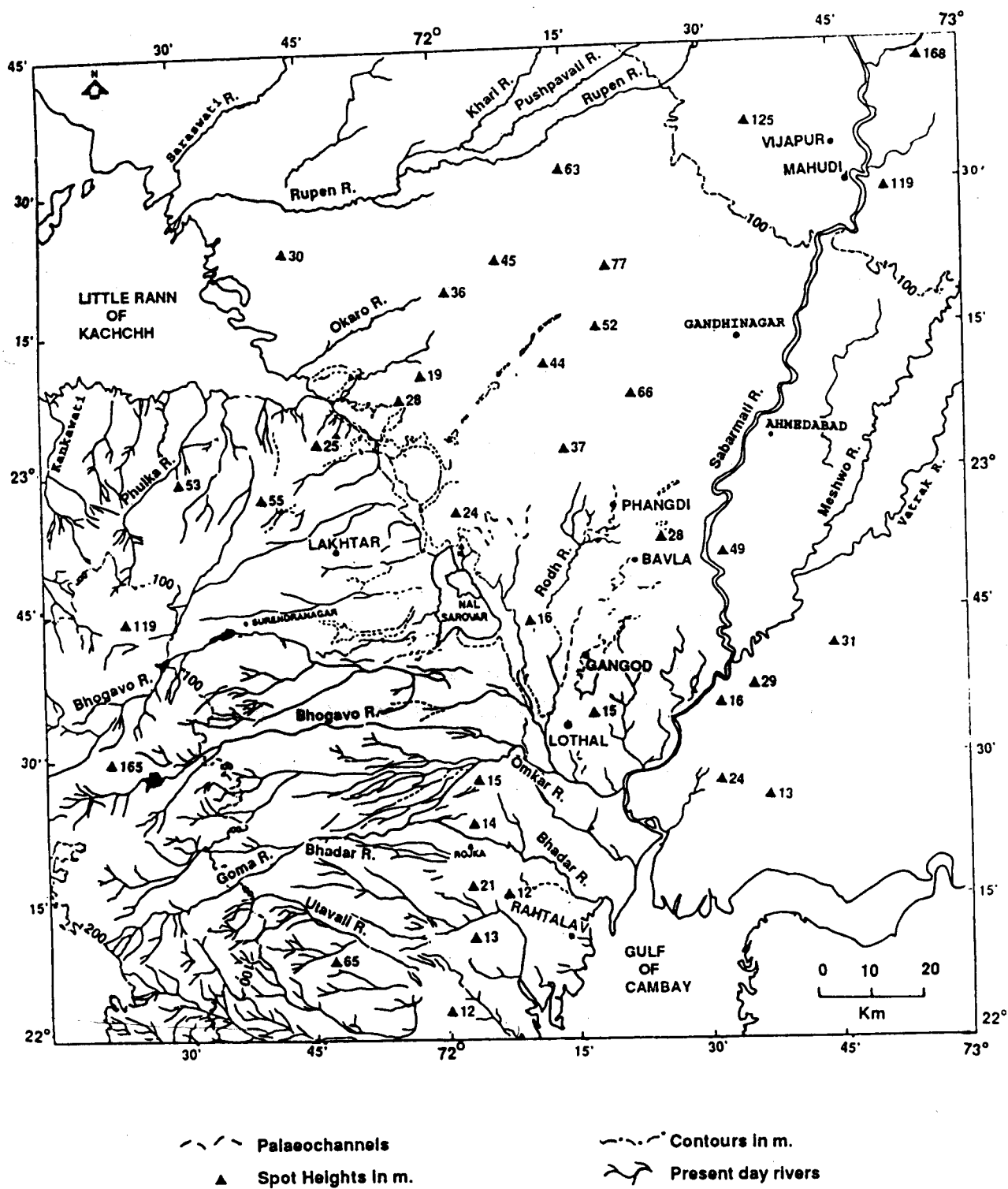


**Fig. 2.6** A composite map showing the present day drainage pattern and location of palaeochannels in and around Nal region.



terminate abruptly. Near Bavla, it was observed that the shallow wells in the vicinity of the palaeochannels had relatively fresher water as compared to the surrounding regions. On the other hand, at Gangod, it was found that the ponds along the former river courses lost the accumulated water soon after the monsoon season due to percolation through coarse sand bed. A trench in one such pond revealed the presence of fluvial sand at 1.5m depth. Thus, it appears that the presently barren area to the east of Nal had several channels flowing through it which may have been responsible for bringing sediments into this region.

On the western, Saurashtra side, the major rivers are Bhadar and Bhogava. These flow from the Saurashtra highlands eastwards to the south of Nal Sarovar. A significant feature observed is the presence of large valleys which have been identified on the basis of their tonal changes. In this region of Saurashtra, on the IRS FCC imagery, the channels exhibit a light photo tone. Also, below the 20m contour and to the south of Nal, a zone of abruptly terminating streams was observed (Fig. 2.5 and Fig. 2.7). Only the major rivers have managed to cut across this zone and continued their flow towards the sea. Further eastwards of this zone, towards the Gulf of Khambhat, several smaller streams showing deranged drainage pattern are observed (Fig. 2.3).

On the western, Saurashtra side, very few abandoned channels have been found. The older channels still exist even though the flow through them is now largely seasonal.

### **Geomorphological Studies**

On the Saurashtra side, fan shaped features were observed on the satellite imageries, which appear to coalesce in their lower part (Fig. 2.5). These may perhaps represent deltas now presently inland, or alluvial fans. To resolve this question a field study was carried out to confirm their origin. During field checks, in a section upstream of Bhogava river, east of Limbdi, occurrence of basalt dominated coarse sand, showing foreset beds was observed (Plate 2). Underlying these, in some of the wells dug in the river bed, clayey sediments, similar to Horizon- 3 which was deposited in marine environment in the Nal region were seen (see section 2.2.2 and 2.2.3). The occurrence of foreset deposits, underlying a layer of surface silt and sand and the occurrence of clayey sediments in the dugwells (possibly representing bottomset deposits) would suggest these fan shaped features to be deltas of the Gilbert type (see Reineck and Singh, 1980; pg. 322). It must however be emphasised here that



**Plate 1** Photograph of a small stream formed by silting of older channels



**Plate 2** Photograph of foreset beds observed in inland delta region.

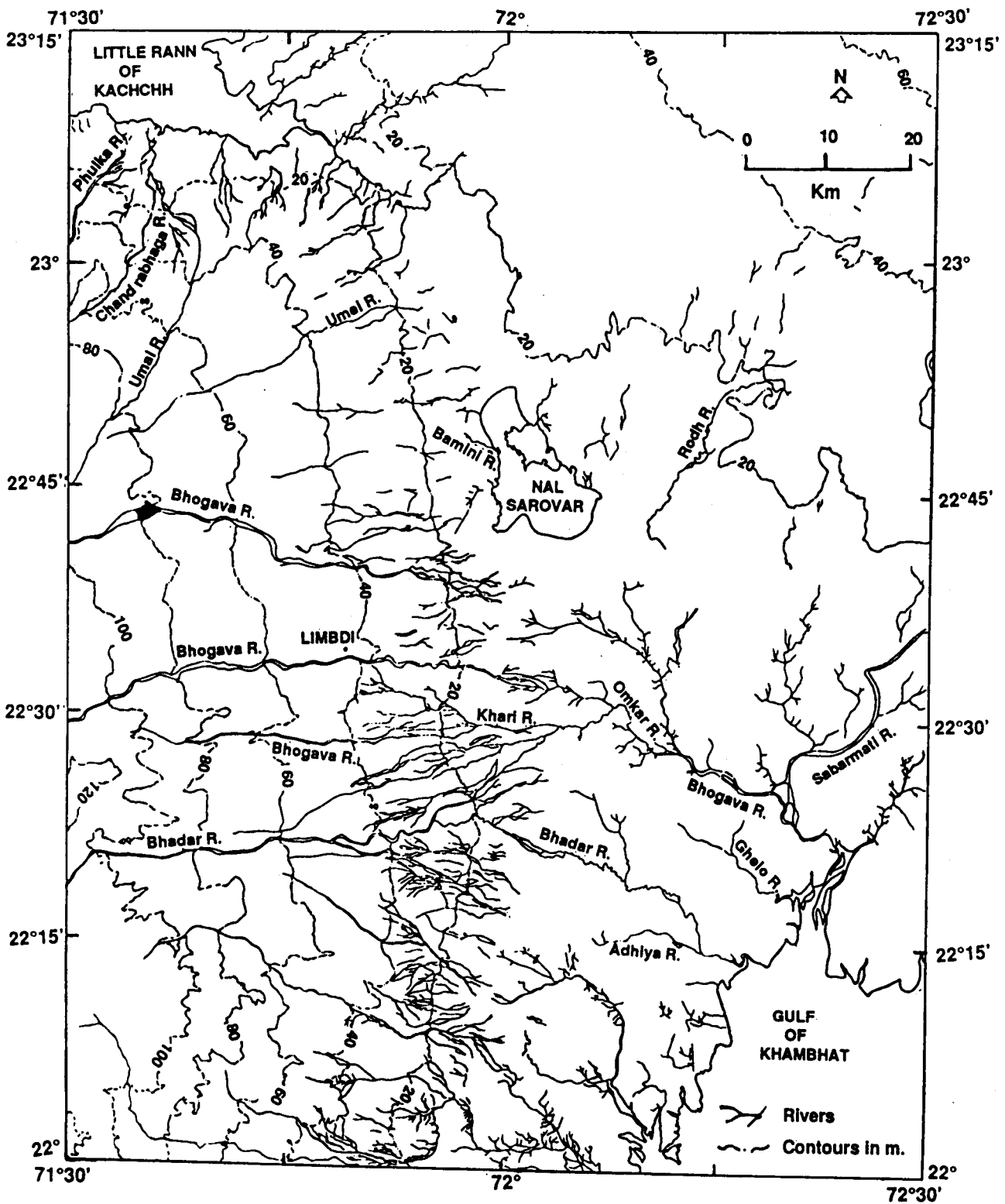


**Fig. 2.7** A composite map showing deranged drainage pattern and zone of terminating streams below 20m contour in the Nal region. Above 40m contour only the major rivers are shown.

the region does not have adequate exposures and this study can, at best, be indicative of a deltaic origin. Our surmise however, does tally with Sood (1983) who had also identified these features as deltas. Thus, on the Saurashtra side, both continental and marine evidences of sea level changes were found. The continental evidence includes inland deltas. The marine evidence includes mud flats at a lower elevation, to the east of the inland deltas and south of Nal, identified on the basis of tonal and colour changes (Fig. 2.5 and Fig. 2.8). The older one (M1), with a darker tone is at  $\sim +14\text{m}$  msl and was mapped on both the eastern and western side of the Gulf of Khambhat. The younger (M2), at a slightly lower elevation, had a lighter tone and is noticeable only on the western side. The region of mud flats showed the presence of deranged drainage pattern (Fig. 2.3 and Fig. 2.7). Present day mud flats were also mapped from the satellite imageries.

On the eastern side, however, no such evidence of sea level changes was observed and the entire region is covered by the alluvium. To the N-NE of Nal Sarovar, however, stabilised dunes which are indicative of past aridity in this region could be seen (Fig. 2.4 and Fig. 2.8).

#### 2.2.1.3 Discussion

Summarising, the features mapped in the Nal region represent three distinct depositional environments: marine, aeolian and fluvial. On the basis of satellite imagery and field studies, the area could be sub-divided into the following geomorphologic units (Fig. 2.8):

1. Inland deltas.
2. Older mud flats.
3. Alluvium.
4. Stabilised dunes.

In the following, significance of each of these features to the evolution of the Nal region is discussed.

**1. Inland deltas:** These are presently 30km inland, at an elevation  $>15\text{m}$  and the palaeo-strandline located at  $\sim +15\text{m}$  msl (Fig. 2.8). In this region several small streams are seen which terminate abruptly at the palaeo-strandline. According to Thornbury (1985), two conditions are necessary for the formation of deltas - the availability of sediments and sheltered conditions at the site of deposition. Deltas may not form at the mouths of streams which enter the sea where their mouths are so exposed to wave and current action that the

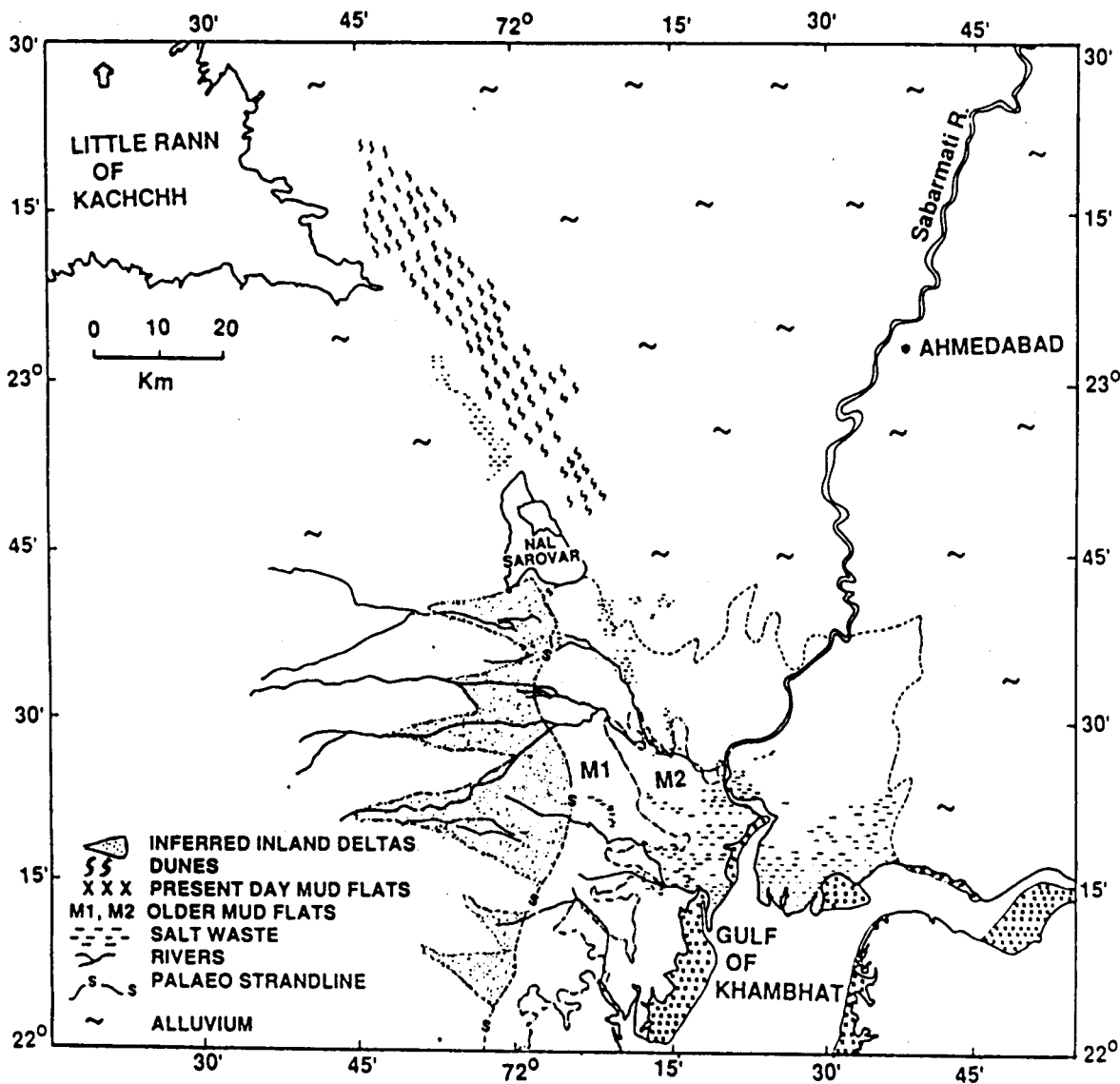


Fig. 2.8 Geomorphological map of Nal region.

sediments are removed as soon as they are deposited. The rivers to the west of the palaeo-strandline have large valleys which are incompatible with their present seasonal flow. It is likely that these were formed during a substantially wetter period in the past, when the rivers had higher erosional potential and larger load carrying capacity.

Field studies indicated limited river entrenchment of about 4m in the palaeo-delta region indicating that there has not been a significant uplift in this region subsequent to their formation. The two observations, namely, larger valleys and the absence of significant entrenchment suggest a higher stillstand of sea, at some time in the past, being responsible for the formation of these inland deltas.

**2. Older mud flats:** At a lower elevation to the east of inland deltas and south of Nal Sarovar, towards the Gulf of Khambhat, two sets of inland mud-flats (M1 and M2) have been identified between  $\sim +14\text{m}$  and  $\sim +10\text{m}$  msl. No significant entrenchment (maximum observed 2m) of rivers is observed in the mud flats indicating that, since their formation, there has not been any major uplift in this region. The region of mud flats also showed the presence of deranged drainage pattern. This drainage pattern is indicative of the recent development of drainage in a region (Thornbury, 1985). The present elevation of these older mud flats may not be taken as an indication of the extent of sea level rise since the region close to Gulf of Khambhat is subjected to tidal surges as high as 12m. In this region, present day mud flats are being formed at elevations upto +8m. So a sea level rise of even a few meters accompanied by tidal surges would be enough to form both the older mud flats.

**3. Dunes:** Stabilised dunes are present N-NE of Nal Sarovar. However, no exposed sections were found in the northern part. Patel and Desai (1988), have attributed the formation of these dunes to periods of stronger aeolian activity during periods of regression following the Flandrian sea level rise.

**4. Alluvium:** This is found to the east and north of Nal Sarovar. No surficial expression of Pleistocene sea level change was found. Rather, these

sediments show the influence of tectonism in the form of abandoned river channels, entrenched streams and fault controlled river courses. The general slope of the region is towards SW.

It is possible to explain the formation of these geomorphic features keeping in view the eustatic sea level changes (Fig. 2.9) and possible role of tectonism during the Late Quaternary. Presence of inland deltas and older mud flats was interpreted to indicate the evidence of at least two episodes of transgression in the Nal region. The evidence of topographical position and deranged drainage pattern pointed to the mud flats (M1 and M2) having been formed during the most recent, Holocene, transgression with M2 probably representing one of the stillstands of the sea during regression. This would imply that the inland deltas were formed during an earlier transgression of the sea. Available record of eustatic sea level changes indicated a high sea level of +7m during the last major interglacial transgression (isotope stage 5e, ~125ka) (Ku et al, 1974; Cronin et al, 1981; Chappel and Shackleton, 1986; Pant and Juyal, 1993) and for the Holocene, a range of 2-6m, (Gupta, 1976); or ~3m (Pant and Juyal, 1993; Hashimi et al, 1995) has been suggested. Since the palaeo-strandline is presently at +15m msl, assigning an age of isotope stage 5e (~125ka) to the inland deltas, would require only a small tectonic uplift subsequent to their formation. These would be consistent with the evidences of only two transgressions of the sea, in the Nal region, and field observations of limited river entrenchment, on the Saurashtra side, in the inland delta region. This is contrary to the view held by Bhaskaran et al (1989), who have indicated an uplift of >50m for the Saurashtra peninsula, in this region, during Late Quaternary on the basis of miliolite ages. In any case, at the time of formation of these palaeo-deltas, the entire Nal region would have been covered by a shallow sea.

According to Patel and Desai (1988), the sand dunes to the north and north-east of Nal Sarovar were formed during periods of stronger aeolian activity during regression, following the Flandrian sea level rise. However, TL data of Langhnaj, north of Ahmedabad, would suggest the dune building activity to have begun as early as ~20 ka (Wasson et al, 1983) with intervening periods of stabilisation.

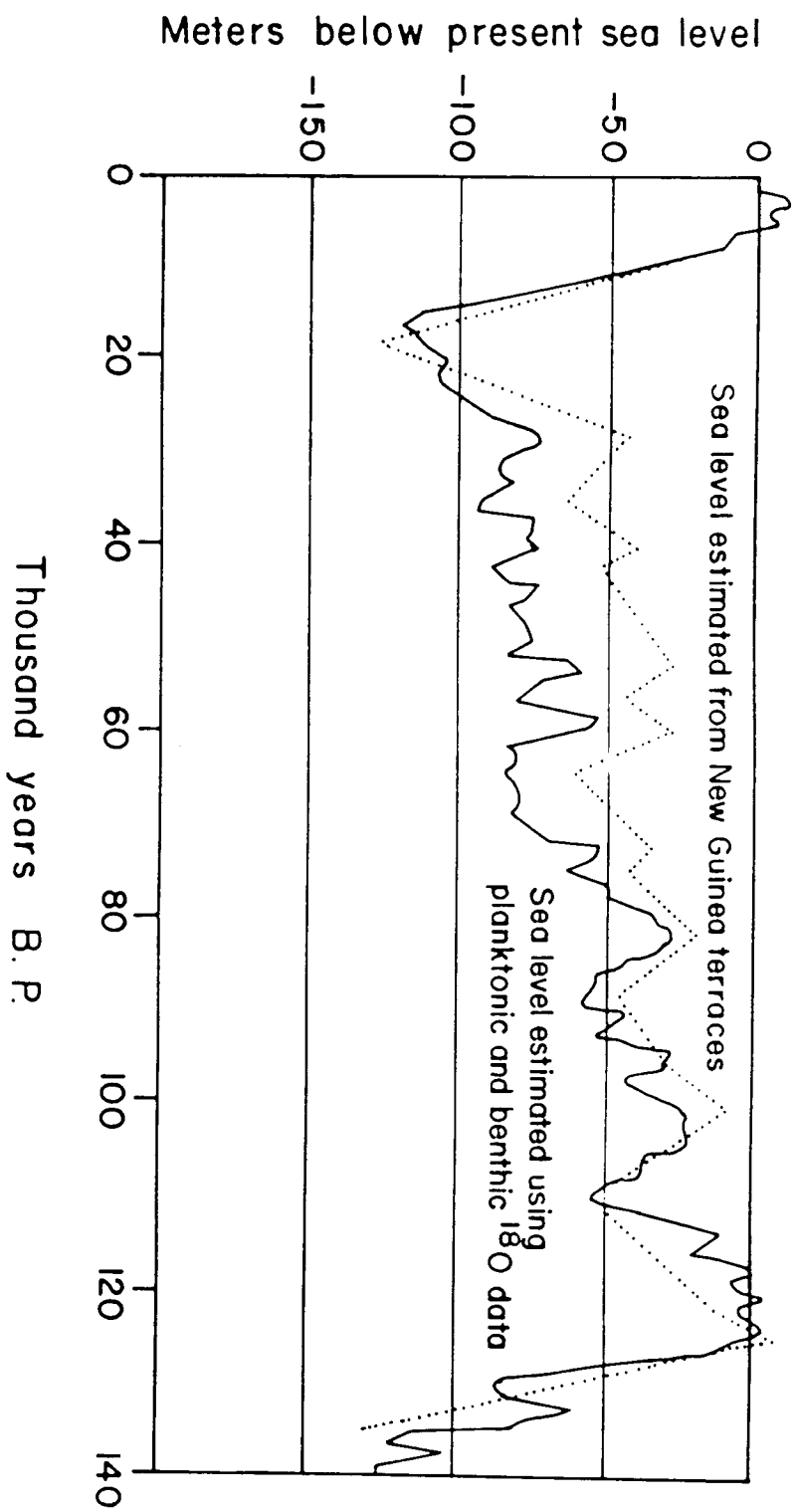


Fig. 2.9 Plots of eustatic sea level change (Redrawn from Gillespie and Molnar, 1995).



## **2.2.2 Subsurface lithological correlation**

In the absence of surface exposures, preliminary investigations into the geological evolution of the Nal region was attempted through the study of lithologs of bore holes (depth of sections 60-200m) drilled for ground water exploitation by the Central and State govt. agencies CGWB, GWRDC, GWSSB.

### **2.2.2.1 Methodology**

As a standard practice, the litholog is prepared in the field itself by the geologists present with the team. The appearance and texture of the sediment form the basis for preparation of the litholog. As such, no detailed description of sand size such as coarse, medium or fine were available for the present study. Instead only broad divisions like top mud (comprising dominantly silt), sand and clay/silty clay have been made for the purpose of lithological correlation. Location of bore holes analysed for this study are shown in Fig. 2.10. On the basis of well log data, three transects, two in NE-SW direction and one in N-S direction, (Fig. 2.11) were constructed. The lithologs of other bore wells, not included in transects are shown in Figures 2.12 and 2.13.

### **2.2.2.2 Results and Discussion**

The NE-SW transect (Fig. 2.11) indicated that, in the eastern side of Nal, the lithology is dominated by sand with intercalations of clay/silty clay. In the vicinity of Nal and in the N-S direction, extending from near the Little Rann in the north to Dholera in south, near the Gulf of Khambhat, a change in lithology to a layer of sand underlain by a thick (40-55m) sequence of clay/silty clay is seen (Fig. 2.11). This feature is also seen in the lithologs of Vekria (Fig. 2.12), Ranagadh and Phulwadi (Fig. 2.13) which also lie in the Nal region. This indicates a similarity in depositional environment in the entire low lying region, extending from near the Gulf of Khambhat to the Little Rann, in a narrow corridor about ~25 km wide as shown in Fig. 2.10. In the following, the expression Nal

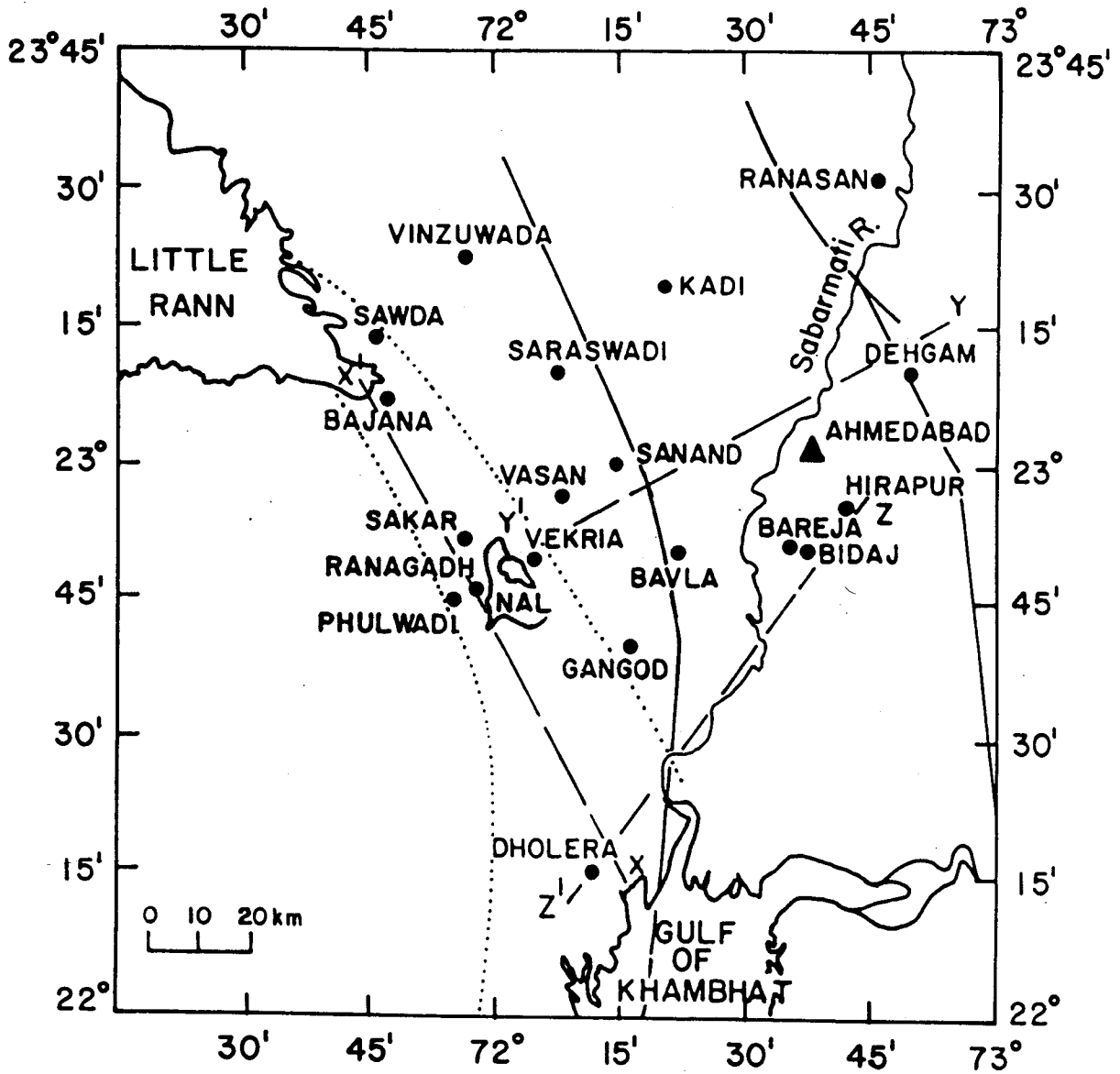


**Fig. 2.10** Map showing the location of bore hole sites and transects taken. Also shown are eastern and western margins of Cambay Graben. The approximate boundaries of the Nal region are shown by dotted lines.

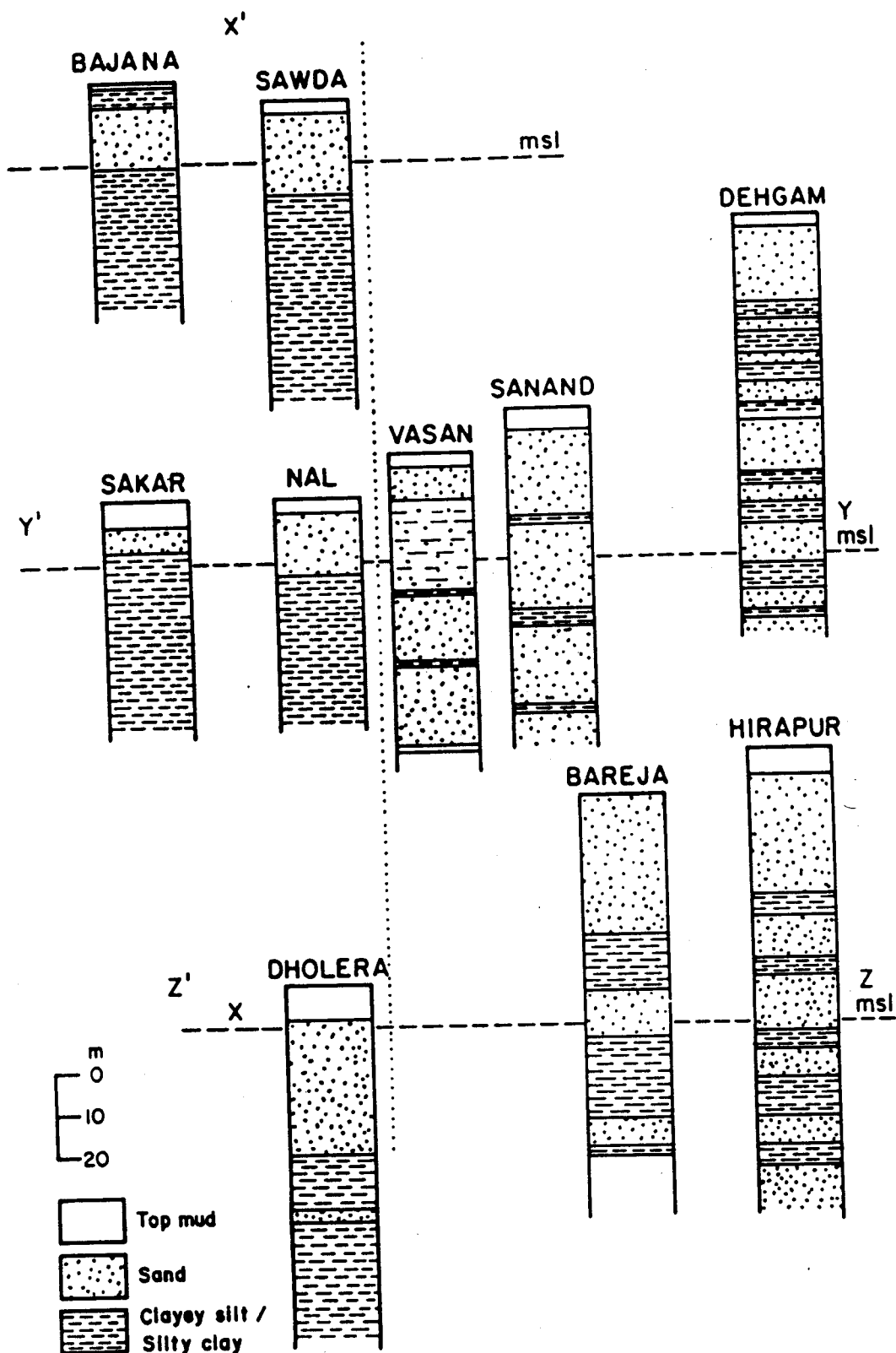
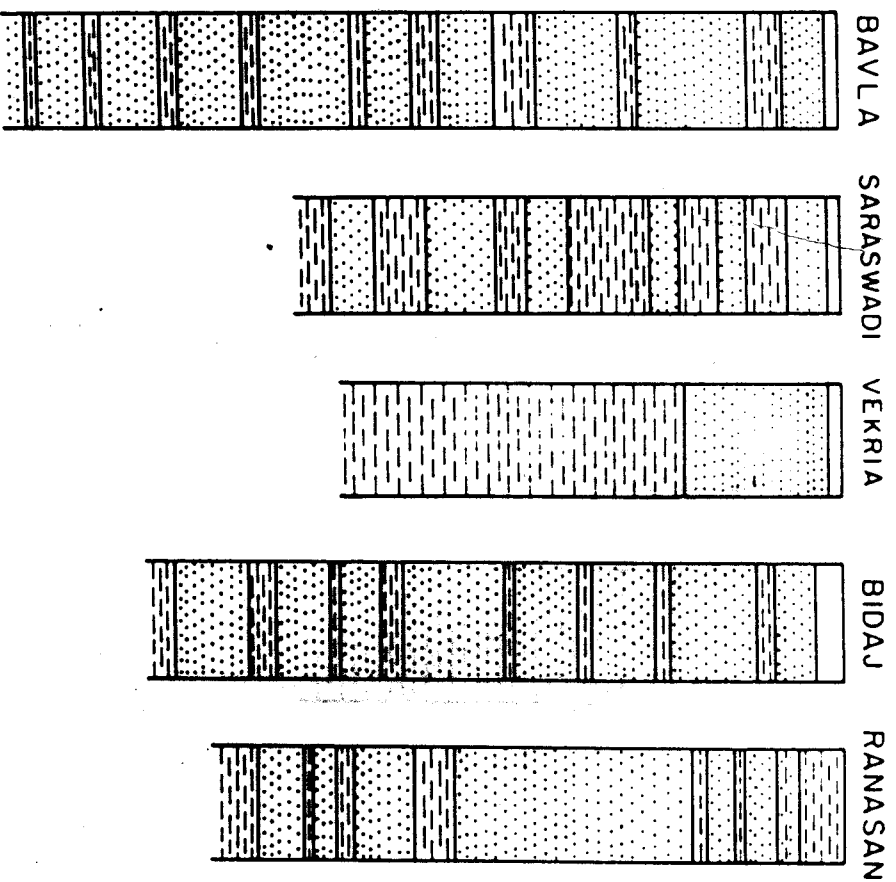


Fig. 2.11 Lithological variation along the transects shown in Fig. 2.10.



**Fig. 2.12 Additional bore hole lithologs for sites shown in Fig. 2.10.**  
 (Legend is given on next page)

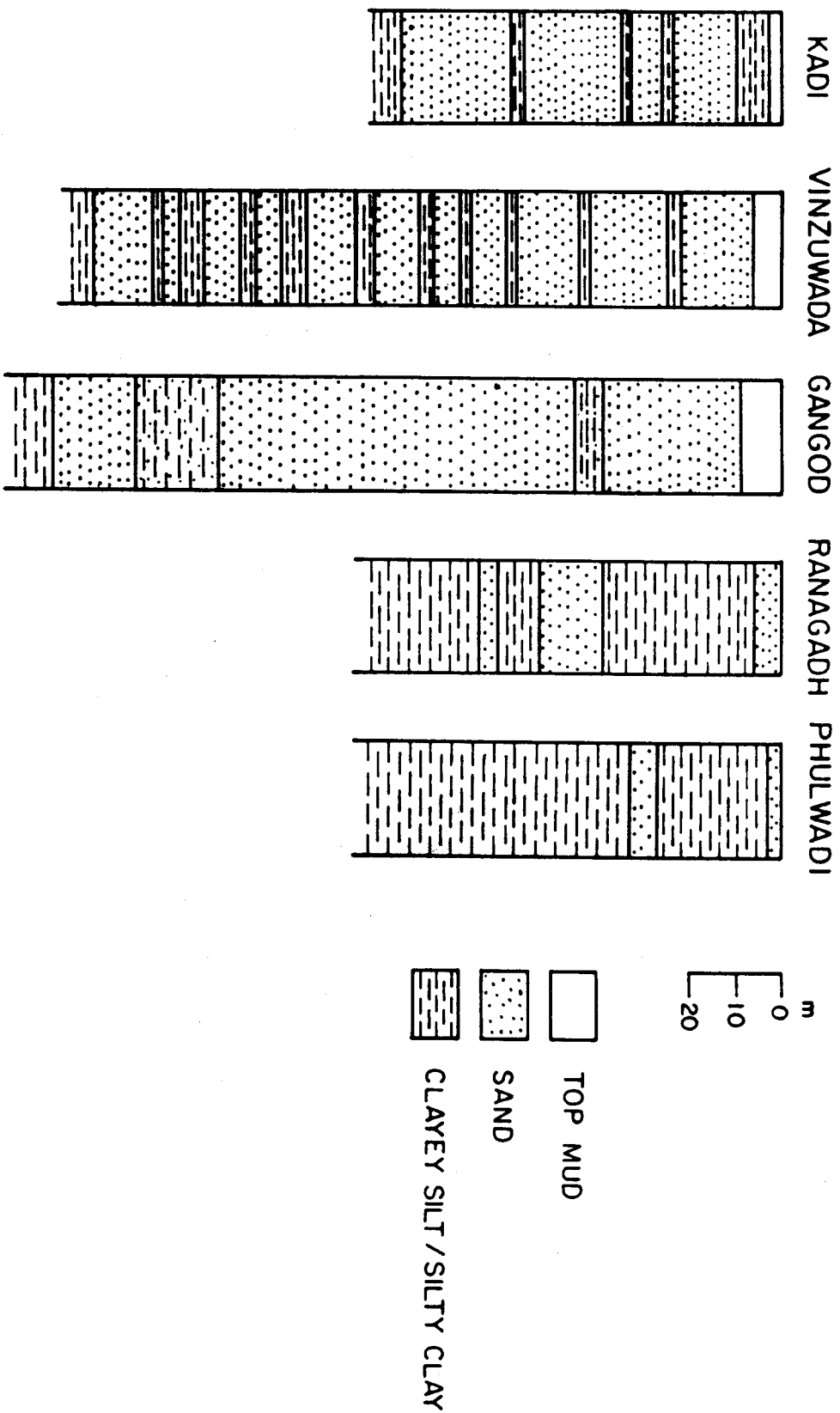


Fig. 2.13 Additional bore hole lithologs for other sites shown in Fig. 2.10.

region has been interchangeably used with Nal corridor because, as discussed subsequently, the region approximately bounded by the two dashed lines in Fig. 2.10 has had a similar geological evolution, distinct from both the eastern and western flanks.

### **2.2.3 Studies on Nal Sarovar core**

Based on the results of remote sensing and sub-surface lithological correlation studies, which indicated evidence of sea level changes and lithological similarity in a narrow corridor extending from Little Rann to near the Gulf of Khambhat, a core was raised from the Nal Sarovar (Fig. 2.14) which lies almost in the centre of the narrow corridor. The sampling procedures are discussed in Appendix A.

#### **2.2.3.1 Lithological description**

On the basis of field observations and laboratory studies (discussed in next section) the core raised from the Nal Sarovar bed was divided into three horizons (Fig. 2.15).

**1. Horizon-3 (54-18m):** This layer comprised of sticky, silty clay/clayey silt with occasional thin layers of fine sand. Occasional occurrences of coarse basalt fragments were seen. This layer also showed the presence of calcium carbonate nodules at various depths. Some of the carbonate nodules had a black coating in the hand specimen and were mistaken for basalt fragments, as subsequently indicated by acid treatment. The amount of organic matter is very low (<0.01%) and no fossils were observed in >63 $\mu$ m size fraction. The dominant clay mineral was identified as smectite. The contact between this horizon and overlying Horizon-2 was abrupt. The base of this layer was not reached in the core.

**2. Horizon-2: (18-3m):** This horizon is dominantly sandy and poorly cemented by secondary calcareous deposition. It also indicated a change in depositional environment. Sorting is moderate to poor and grain size is medium to coarse. Sand is dominated by quartz, heavy minerals are opaques, epidote, staurolite and garnet. Occasionally silty layers are present but since the focus here was on obtaining a regional picture, the dominant grain size (>50%) was

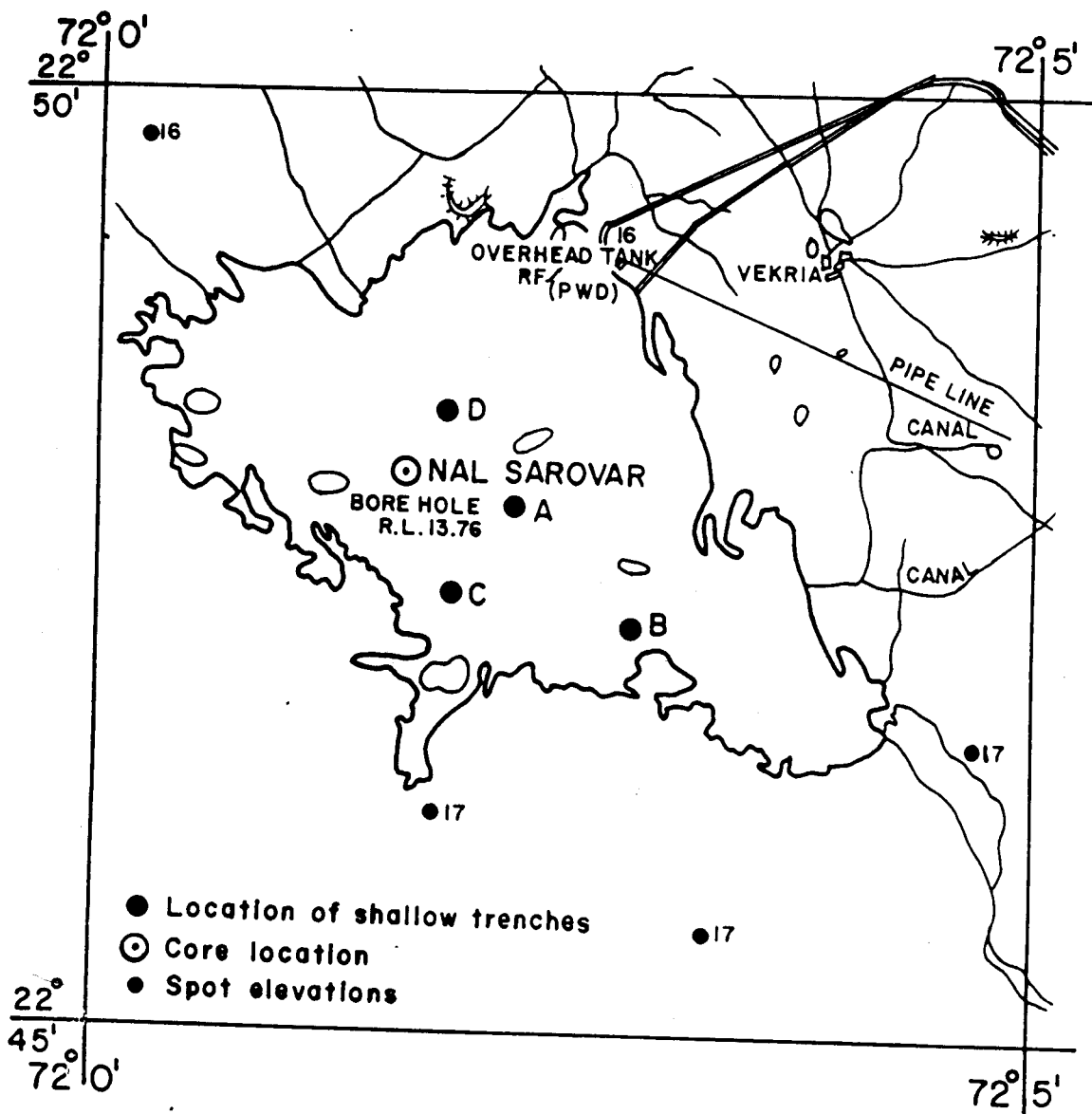


**Fig. 2.14** Map showing the location of 54m long core and shallow trenches in Nal Sarovar.

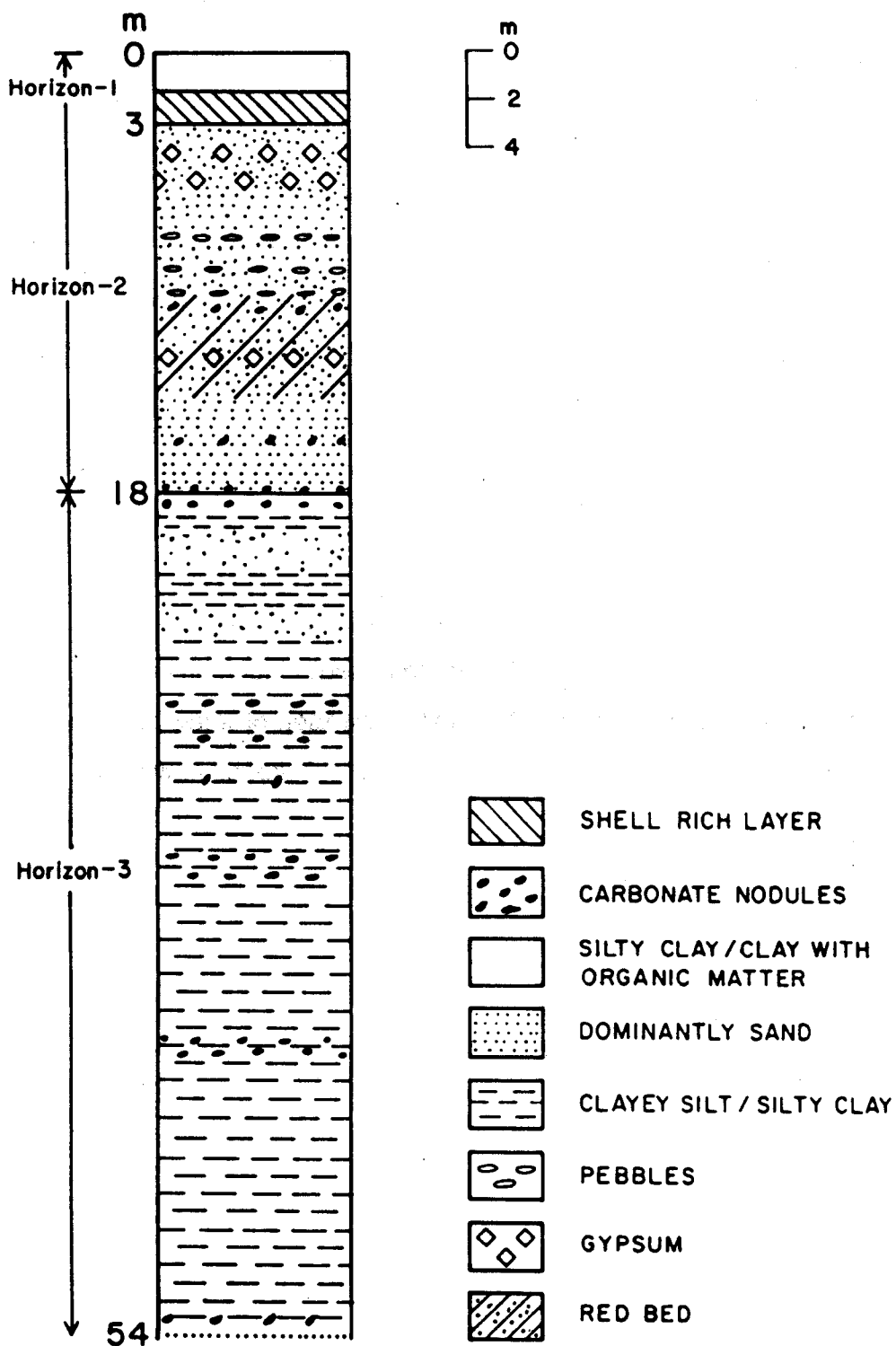


Fig. 2.15 Lithology of the Nal Sarovar core.



used for lithological correlation.

This horizon showed the presence of fine to coarse crystals of gypsum at 4m, 5m and 7m depth. The sand had a red coloration between 10-14m. Occasional basalt fragments were also found. No fossils were observed in the  $>63\mu$  size range. The amount of organic matter was low ( $<0.01\%$ ). The contact between this layer and the overlying Horizon-1 was gradational.

**3. Horizon-1: (3-0m):** This horizon comprised of silty clay/clay with organic matter ( $\sim 0.9\%$ ). The layer became slightly sandy towards the lower part. Dominant clay mineral identified was Illite. Midway through this horizon (1.6m) was found, a gastropod (Genus *Bittium*) rich layer with a few shells of land snails, which persisted till the bottom of Horizon-1. These shells were identified by Mr. R.L. Jain, Palaeontologist, Geological Survey of India, Gujarat Circle, Gandhinagar. According to Jain (pers. comm., 1996), the habitat of these shells is very shallow fresh water to near shore tidal flat or estuarine; further the small size of these shells was suggestive of death in young age due to emergence of dry conditions.

Four other trenches, dug subsequently, in the lake bed confirmed the presence of gastropod rich layer at varying depths throughout the lake bed (Fig. 2.16). A field photograph of this shell layer, showing the gastropod shells, taken during trenching operations, is shown in Plate 3.

#### 2.2.3.2. Sedimentological and mineralogical studies

##### Results and discussion

Classification of the core was done on the basis of dominant grain size coupled with field observations on core samples. For purpose of provenance identification, the mineralogy of the dominant grain size has been considered i.e. clay minerals in case of Horizon-1 and -3 and, heavy minerals in case of sandy Horizon-2. The laboratory procedures employed have been discussed in Appendix B. The results of grain size analysis and mineralogy are

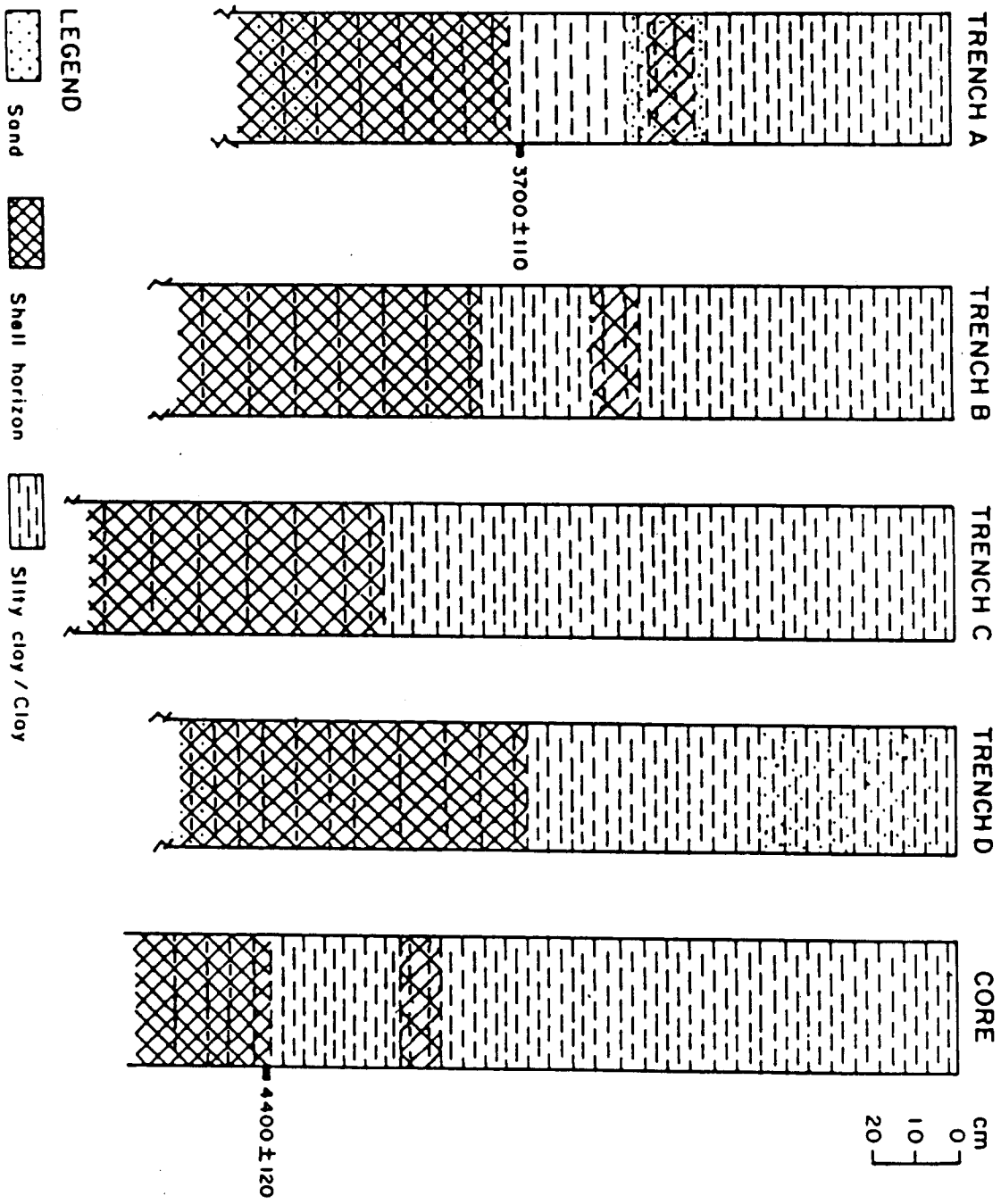


Fig. 2.16 Lithology of shallow trenches showing the presence of shell layer in Nal Sarovar.



**Plate 3.** Field photograph of sediments from the shell layer, Horizon-1, taken during trenching.

given in tabular form in Appendix B (Table B1 and B2) and shown graphically in Fig. 2.17 and Fig. 2.18 respectively.

**Horizon-3:** This comprised of silty clay/clayey silt with occasional sand layers. Core studies indicated that, mineralogically, the clay rich Horizon-3 was dominated (>70%) by smectite, indicative of its origin from the basaltic terrain. This was possibly derived from the basaltic rocks on the Saurashtra side or brought from the Gulf of Khambhat due to action of tidal currents. The latter possibility cannot be ruled out considering the RL of this horizon (-4 to -40m in the core). Mineralogically and sedimentologically, the sediments in the inner shelf near the Gulf of Khambhat are dominantly smectite and clayey/silty clay in nature (Rao, 1991; Rao and Rao, 1995), similar to the Horizon-3 of the core. Also, the clay mineral studies on sediments from near the mouths of Mahi and Narmada rivers show the dominance of smectite (Islam and Merh, 1988). There appears to be little or no contribution, to Horizon-3, from the Gulf of Kachchh side. This follows from the study of Rao and Rao (1995), which indicated that present day sediments off the Gulf of Kachchh, on the outer continental shelf, show the dominance of illite (63%) which was derived from the weathering of Himalayan rocks and transported by the Indus river. They also indicated that the inner shelf sediments show an increase in smectite (22% as compared to 9% in the outer shelf). Interestingly, a yellowish, clayey layer (RL -7m) comprising about 80-90% smectite, devoid of shells and with an abrupt contact with overlying gritty sandy clay layer, has also been reported from Little Rann of Kachchh (Gupta, 1975). This layer may be correlatable with Horizon-3 of the Nal core. In terms of lithology, the Horizon-3 of the core is similar to the lower silty clay horizon found in the bore hole lithologies in the Nal region.

Considering (i) the thickness of the silty clay horizon in the borehole sections (varying between 40-55 m) in the N-S transect throughout the Nal corridor; (ii) the RL of the bottom and top of this layer (-75 to +3m respectively); (iii) mineralogy (smectite dominated); (iv) geomorphological evidence of transgressive events; (v) the global eustatic sea level curve and (vi) the possibility of some post depositional tectonic uplift of the region, an age of 73-127 ka, corresponding to the entire isotope stage 5, maybe assigned for the deposition of the silty clay, Horizon-3. For most part during this interval, the

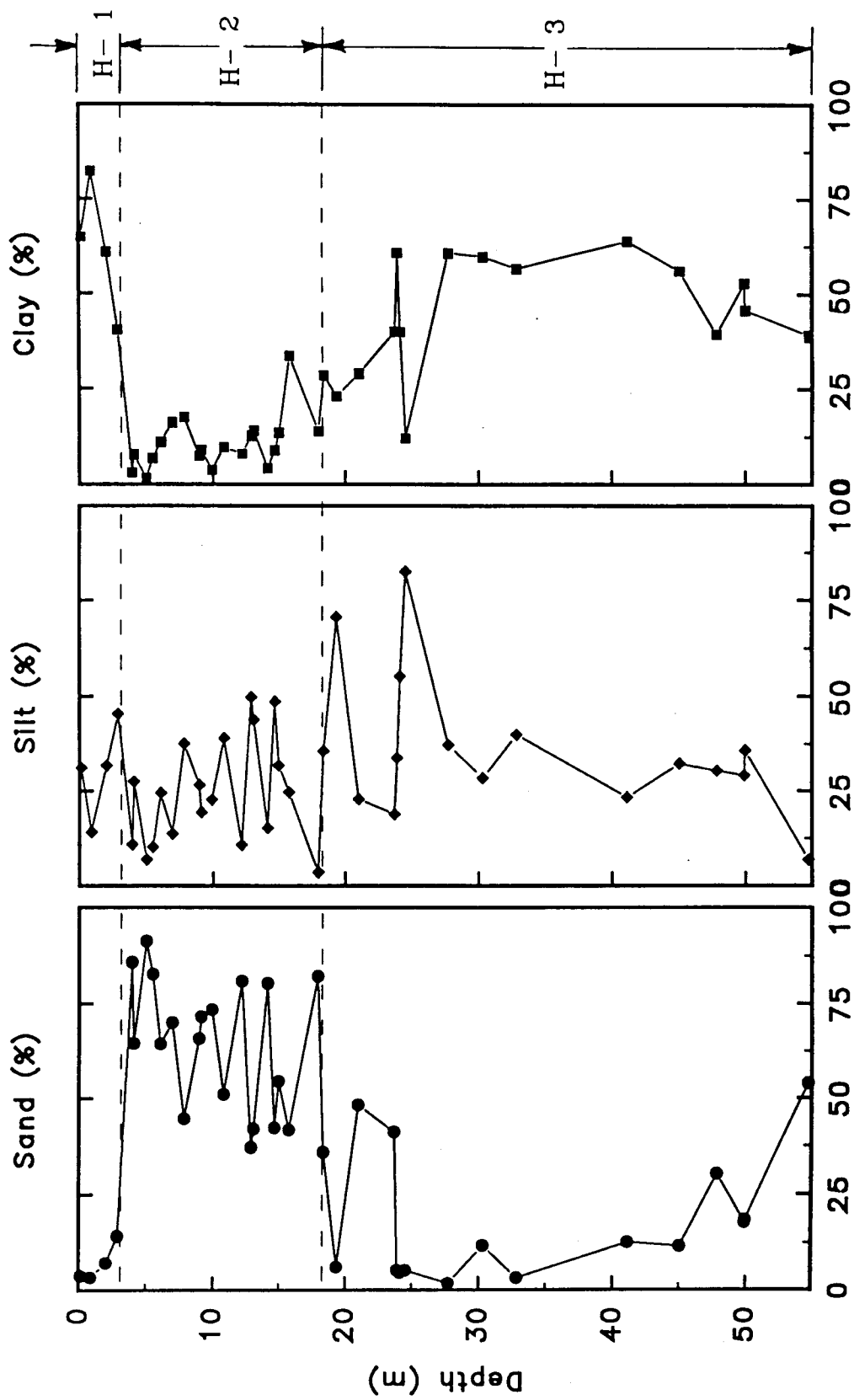


Fig. 2.17 Variation of grain size with depth, Nal Sarovar core.

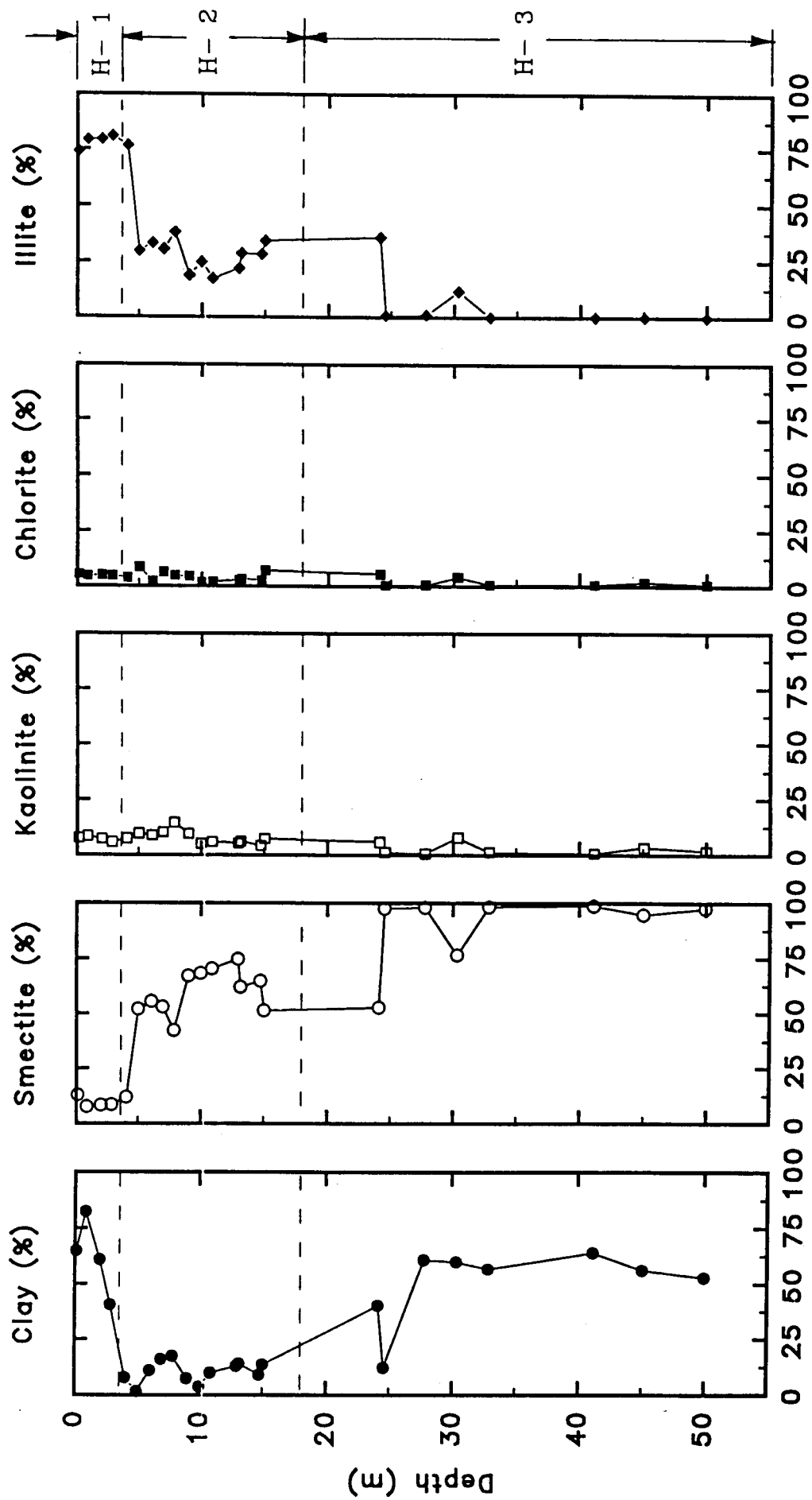


Fig. 2.18 Variation of total clay percentage and mineralogy with depth, Nal Sarovar core.

entire region would have been covered by a shallow sea. The absence of marine fauna ( $>63\mu$ ), in few of the samples checked is puzzling. However, the environment visualised here, for the most part, was a landlocked shallow sea with influx of water and sediments from both the land and the sea. It would have been subject to considerable salinity fluctuations induced by tidal changes, fresh water flux during monsoon months and high rates of evaporation during summer months. Very few species can survive under such stressed environments of wide salinity fluctuations (Raup and Stanley, 1985). An indication of this is also found in a study of present day distribution of planktonic foraminifera in the Arabian sea. Near the Gulf of Khambhat, very low concentrations of foraminifera ( $<700$  specimens in  $1000\text{m}^3$  of water) were found as compared to 7000-40,000 specimens (in  $1000\text{m}^3$  of water) further south. This has been attributed to arid climate around this region and resulting intense evaporation (Rao et al, 1991).

The extremely small contribution to sediments in Horizon-3, from the eastern rivers, is indicative that they were depositing their sediments in a sink farther to the east of the Nal region.

**Horizon-2:** This horizon comprised of sand with occasional silt rich layers. It is dominated by sand size grains of quartz, both angular and subrounded. Sorting was found to be moderate to poor and the mean grain size in the range  $0.8-1.5\Phi$ . The amount of clay was found to be very small, 3-15%. The dominant clay mineral was smectite with some amount of illite ( $\sim 25\%$ ). The Sabarmati river suspended particulate matter (SPM), collected during the flood of Sept. '94 showed the distribution, smectite: illite: (chlorite+kaolinite) as 30:42:28. Similar clay mineral distribution was found in sediment samples from an 8m deep soak pit in Ahmedabad, only  $\sim 5\text{Km}$  from the Sabarmati river (Deshpande, unpubl. data). This, together with the clay mineral data of Horizon-2, where a dominance of smectite was found, would suggest that the clay minerals in Horizon-2 had a mixed contribution from both the western, Saurashtra, and eastern side. But since clay minerals account for only 3-15% of sediment by weight, the heavy mineral analysis of the dominant sand fraction

was used to identify the provenance for Horizon-2. The heavy mineral assemblage consisted of opaques, epidote, staurolite and garnet, indicating that this material could have been derived from the igneous and/or metamorphic rocks from the east and north-east. This does not rule out redeposition of eroded sediments that had their primary source in metamorphic and/or igneous rocks of east and north-east. This is in contrast to Horizon-3 which indicated a dominant input from south and/or west.

The red beds were found in Horizon-2 (between 10-14m). Zeuner (1950), has stated that a rainfall of 20-40 inches with a long dry season would be responsible for the formation of red soils. Reddening may also take place under relatively humid conditions (Krynine, 1949; Kubeina, 1963; Folk, 1976), or it may occur under high temperature oxidising conditions with rapid decomposition of organic matter in semi-arid/arid environments. If a source of iron and oxidising conditions exist, red beds can form in both humid and arid tropics (Pye, 1983). In the present case, however, secondary calcareous accumulations suggest reddening under semi-arid regime and subaerial exposure. It is noteworthy that red beds have been reported from all over Gujarat and are used as a marker bed (Pant and Chamyal, 1990). The difference in elevation between the red beds reported in Sabarmati basin at Vijapur and the red beds in Nal core is ~100m. While the topographic component cannot be ruled out, it is interesting to note that the red beds in the Gujarat alluvial plains are presently exposed in cliffy sections ~40-50m high. These beds have been dated using luminescence technique in the Vijapur section of the Sabarmati river and indicate an age of  $58 \pm 5$  ka (Tandon et al, 1996). Occurrence of evaporite minerals like gypsum at 4m and 7m depth, in Horizon-2, is also indicative of an arid phase.

It is believed that the Sabarmati too used to flow westwards (Zeuner, 1950) into the Little Rann along the course of Rupen (Sridhar et al, 1994). Sareen et al (1993), believe the shift of Sabarmati to have occurred sometime during Late Quaternary as a result of fluvial readjustment in response to neotectonic reactivation in the region. There are several abandoned river channels to the east of Nal (mentioned earlier in Section 2.2.1.2 and Fig. 2.6) which have been identified, in this study, on the IRS FCC imagery. Possibly



these represent older courses of Sabarmati river as it shifted southwards. These may have been transporting sediments to this region in the past. The rivers became inactive either due to a changeover to a drier climate and/or due to tectonism which disrupted the drainage pattern. The abandoned river courses lie in the Cambay Graben which is known to have been tectonically active during the Late Quaternary (Ghosh, 1952; Sareen et al, 1993).

The presence of a thick (5-35 m) sandy horizon (RL +14m to -30m), in the bore well sections in the entire Little Rann to Gulf of Khambhat corridor, suggests that during its deposition the sea link no longer existed in this region. During this period of lowered sea level, high energy fluvial sediments were being deposited in this entire belt by the rivers which were extending their courses on the exposed Nal region. The coarser grain size, breaks in deposition as evidenced by red beds and evaporite minerals, indicate subaerial exposure and episodic deposition by a high energy agency.

The abrupt change in provenance - from south and/or west in Horizon-3 to one dominated by east and north-east in Horizon-2 is thought provoking. A regression of the sea should result in the rivers from both east and west sides extending their courses, through the Nal corridor, into the sea. This may be accompanied by advancement of depositional front into the Nal region from either side. That there is a dominance of eastern source is indicated by the heavy mineral data of Horizon-2. Sridhar et al (1994), have hypothesised the existence of a super-fluvial system which originated in east and north-east and was responsible for depositing the enormous thickness of sediments in north and central Gujarat; this super fluvial system was disrupted in Middle to Late Quaternary. If this super fluvial system existed during the deposition of Horizon-3, its depositional front then did not reach the Nal region as indicated earlier. Regression of the sea could have resulted in the westward migration of the depositional front as indicated above. Alternatively, it is possible that there was a tectonic uplift on the eastern margin of the Nal region subsequent to deposition of Horizon-3 which resulted in the reworking and deposition of

coarser sediments from the east, in the Nal region. In the absence of published subsurface data, on the thickness of Quaternary deposits from the eastern flank of the Nal corridor, it is difficult to confirm either of the two hypotheses discussed above. However, an E-W cross section constructed across Nal region (Fig. 2.19) indicates that the Cambay Graben lying to the east of Nal Sarovar was topographically the lowest elevation and had acted as a sediment sink at least until Miocene. Presently, this area has a surface elevation of +80 m to +100 m and the low elevation area has shifted to Nal Sarovar which is +13 m to +16 m msl. Evidences of Late Quaternary tectonism in the Cambay Graben have been reported (Ghosh, 1952; Sareen et al, 1993).

**Horizon-1:** This comprised of clay/silty clay. The dominant clay mineral was determined to be illite. Studies on clay minerals of Sabarmati river (SPM) and soak pit samples in Ahmedabad (Deshpande, unpublished data) indicate a dominance of illite. This suggests that sediments in Horizon-1 have been derived primarily from the eastern and north eastern side which comprises granitic and metamorphic rocks. Since, on the basis of textural and mineralogical characteristics, whole of Horizon-1 is similar to surface sediment, it is likely that there has not been a significant change in the provenance from today during the deposition of this horizon. At present there is no major stream draining into the Nal Sarovar. The deposits are reworked sediments derived by surface runoff draining into the Nal lake. The  $\delta^{13}\text{C}$  and C/N ratios of organic fraction of this Horizon-1, reported subsequently (Chapter 3), indicate that lacustrine conditions slowly began to set in and the area became a closed basin.

Thus, as a result of the combined influence of (i) westward advance of the sedimentation front; (ii) tectonism and; (iii) the post glacial sea level rise, the elevation of the Nal Sarovar came to within few metres of its present elevation at about 7ka when it became a closed basin. The present Nal Sarovar, therefore, originated as a result of westward advance of the sedimentation front until it could no longer advance due to the presence of high land of Saurashtra. At that time either due to sedimentation process alone or aided by tectonism the west flowing rivers shifted their courses and presently only the abandoned channels remain.

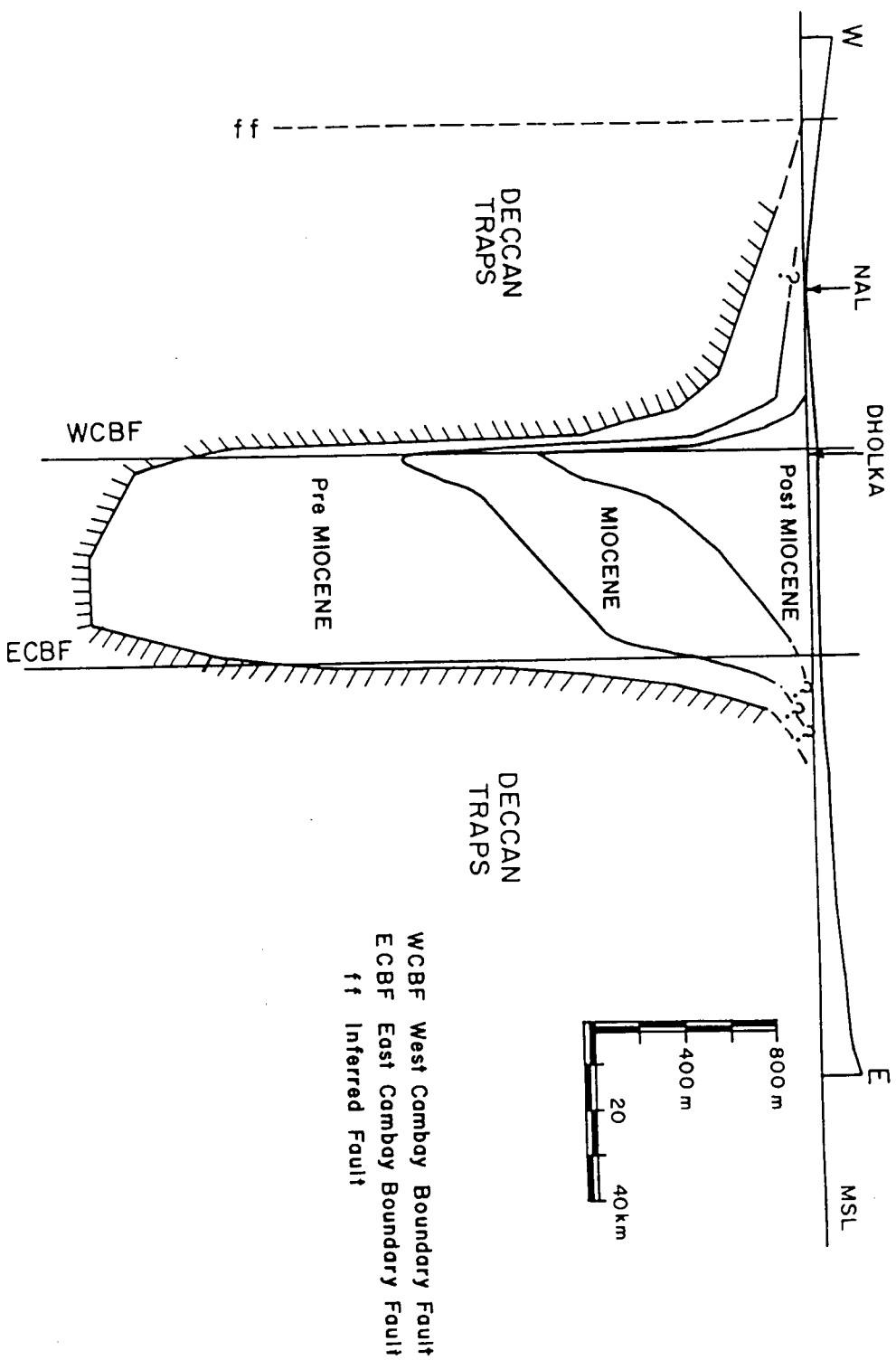


Fig. 2.19 E-W section along the Cambay Graben. (Drawn on basis of data given in Mathur et al, 1968).

## **CHAPTER 3**

### **PALAEOCLIMATIC STUDIES**

In the last few decades, a series of climate related disasters have focused attention on the importance of understanding and modelling of process of climate change, with a view to optimise land use and planning strategies. Since instrumental climatic records are available for only last 100-150 years, scientists are turning to proxy recorders of climate to calibrate their models. Studies on ocean cores have provided information about global climatic changes for the Quaternary period. However, these records have the twin constraints of coarse time resolution and inability to provide a regional/local picture - the latter is especially important because features like mountains, deserts etc. are known to locally influence the climate of an area. To an extent both these limitations can be overcome by using continental palaeoclimatic records from climatically sensitive regions. It is now being realised that the use of continental records in combination with oceanic data could provide a better understanding of the climatic system.

Instrumental records have indicated the sensitivity of Afro-Asian arid/semi-arid regions to small perturbations in the climatic system (Yan and Petit-Maire, 1994). For example, a wet episode was recorded from the 1920's until the 1960's in Sahel, India and northern China (Parthasarathy et al, 1986; Zhang, 1989) associated with a rapid warming over the northern hemisphere during the 1920's (Jones et al, 1986; Gossens and Berger, 1987). In contrast, shortly following a significant cooling over the northern hemisphere (Yan, Z. et al, 1990), a sharp dry phase was recorded since the 1960's in the northern Sahel (Demaree and Nicholis, 1990), the Arabian peninsula (Winstanley, 1976), India, the Tibetan plateau and northern China. This has led to a renewed interest in studying the palaeoclimate in these regions.

To date, paleoclimatic studies from the Indian subcontinent have been fragmentary, being confined to certain areas like Ladakh (Bhattacharya, 1989) and Kashmir in the north (Agrawal and Gupta, 1988; Agrawal et al, 1989; Krishnamurthy et al, 1986), Rajasthan lakes in the west (Singh et al, 1972; Bryson and Swain, 1981; Wasson et al, 1984; Singh et al, 1990; Chawla et al, 1992) and Nilgiris in the south (Sukumar et al, 1993; Caratini et al, 1994). The semi-arid regions of Gujarat, show evidence of past climatic variability in the form of stabilised dunes indicating a westwards spatial shift (Fig 3.1), of the order of 300km, of the 250mm isohyet (Goudie et al, 1973). However, paleoclimatic changes, with firm chronological control, in this arid/semi-arid zone, have not yet been adequately studied or documented. It is in this context that the present study becomes important.

### **3.1 Background information**

This section is divided into three subsections. The first part deals with methods available for dating of young sediments. The second part discusses the sources of palaeoclimatic information. The third part summarises the palaeoclimatic studies from north-west India as the Nal region is closest to it and forms part of the Palaeo-Thar (Goudie et al, 1973).

#### ***3.1.1 Dating of young sediments***

Accurate dating control is essential to put the palaeoclimatic information in a suitable chronological framework. Without reliable estimates on ages of past events, it is not possible to investigate if they occurred synchronously or some events lagged behind others. Studies to understand the evolution of the Nal region (Chapter 2) have indicated that the lacustrine record (Horizon-1) extends back at least upto a few thousand years whereas the entire 54m core should extend back upto the last major interglacial. The available dating methods, for the time scales involved, are discussed in the following.

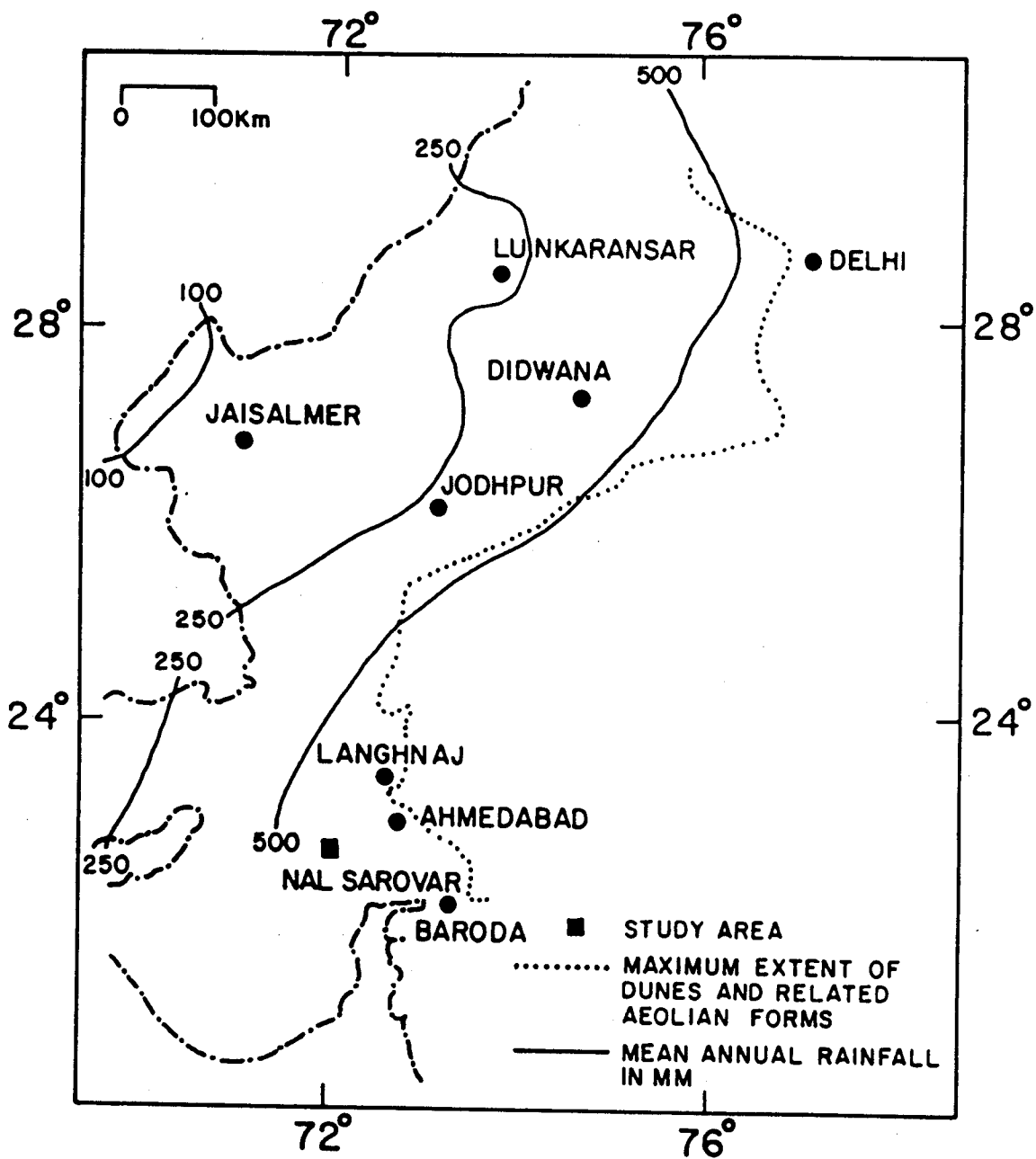


**Fig. 3.1** The extent of fossil aeolian features and isohyet contours in north western India (modified version largely redrawn from Chawla et al., 1992). Sites mentioned in text are indicated.

**$^{210}\text{Pb}$  method:** This method can be used to date sediments upto ~100 years.  $^{222}\text{Rn}$  escapes from the soil into the atmosphere and through a series of short lived daughter products decays into  $^{210}\text{Pb}$  (half life ~22 yrs). This isotope is subsequently removed through precipitation and gets incorporated into the sediments. The decay of  $^{210}\text{Pb}$  is monitored to estimate the age of sediments.

**$^{137}\text{Cs}$  method:** Another method used for dating of young sediments is based on identifying the layer that was deposited in the 1960's when the bomb produced  $^{137}\text{Cs}$  (half life ~30 yrs) activity was the highest.  $^{137}\text{Cs}$  too is incorporated in the sediments through scavenging from the atmosphere by precipitation.

**Radiocarbon method:** In this method, activity of  $^{14}\text{C}$  in the carbon containing matter is used to date sediments younger than ~40ka. Radiocarbon ( $^{14}\text{C}$ ) is produced in the atmosphere by the capture of a cosmic ray produced neutron (n) by nitrogen ( $^{14}\text{N}$ ) resulting in the emission of a proton and creation of  $^{14}\text{C}$  which is then oxidised to  $^{14}\text{CO}_2$ . It is then distributed throughout the atmosphere and all carbon containing reservoirs through carbon cycle. Plants assimilate  $^{14}\text{C}$  during photosynthesis. Animals feed on living plants or take up carbon in a variety of ways. As long as a sample is part of active carbon cycle, its  $^{14}\text{C}$  activity is maintained at a constant level due to equilibrium between intake on one hand and radioactive decay on the other. Thus, all living creatures maintain their  $^{14}\text{C}$  level during their lifetime. After the death of the organism or otherwise removal of the specimen from the active carbon reservoir, the  $^{14}\text{C}$  input ceases. Time of death/removal can be established by determining residual  $^{14}\text{C}$  content of the specimen and its initial activity in the active carbon reservoir, since without fresh intake,  $^{14}\text{C}$  decays with a half life of  $5730 \pm 40$  years.

**Luminescence method:** This method gives the time of last sun exposure of the sediments, prior to deposition. The basic principles of this method and results are discussed in detail in the next Chapter.

For the present study, considering the time scales involved, radiocarbon and luminescence method of dating were used. The experimental procedures employed are described in Appendix C and Appendix E respectively.

### ***3.1.2 Sources of palaeoclimatic information***

The palaeoclimatic information can be derived from a variety of data sources e.g. ocean and lake sediments, ice cores, tree rings etc. A list of data sources with the climatically sensitive variable, range of application, is summarised in Table 3.1.

However, on continents, in most geographical locations, many of these proxy recorders do not often provide long records and it becomes necessary to investigate other systems which may be expected to preserve fairly continuous, long record of palaeoclimate. A particularly promising source is the record preserved in lake sediments from climatically sensitive regions. Lakes have the advantage of providing generally undisturbed, continuous, high resolution palaeoclimatic records. Additionally, they have a far wider geographical distribution; this is especially useful for studying the latitudinal dependence of climate. Hydrological and biological changes within the lake, as well as in its catchment area, are recorded in the sediments, in a variety of ways including the isotopic composition of the organic components preserved in the lake sediments.

### ***3.1.3 Palaeoclimatic studies in north-west India***

From palaeoclimatic perspective, Rajasthan in north-west India, is one of the most extensively studied regions. A variety of proxy climate indicators e.g. pollens, mineralogy, geomorphology, have been used to infer the palaeoclimate. Some of the studies are summarised in the following.

Pollen and geochemical studies in the best studied Didwana lake show oscillating fresh and saline conditions from 9.3 to 7.5ka. Lake levels peaked in the interval 7.5-6.2ka; moderately fresh conditions persisted between 6.2-4.2ka (Wasson et al, 1984; Singh et al, 1990). Between 10.5-3.5ka, the estimated summer precipitation was nearly 2-3 times the present day value (Bryson and Swain, 1981; Swain et al 1983). By about 5ka the Indus valley culture was well established. Paleoclimatic



**Table 3.1. Major palaeoclimatic data sources and their characteristics. (Compiled from Bradley, 1985; Matsumoto, 1991)**

Data Source	Variable measured	Continuity of Evidence	Range (years)	Minimum Sampling Interval (years)	Climate Related Inferences
Ocean sediments	Isotopic composition of planktonic and benthic fossils, floral and faunal assemblages, morphological characteristics of fossils, mineralogical composition and abundance.	Continuous	$10^6$	Depends on sedimentation rate	T, S, B, I, W
Ice cores	Oxygen isotope composition, trace chemistry.	Continuous	$10^5 +$	variable but optimally 1-10 yrs for last $10^4$ yrs	T, C, S <sub>a</sub>
Mountain glaciers	Terminal positions, equilibrium line altitudes.	Episodic	$5 \times 10^4$	-	T, P
Bog or Lake sediments	Stable isotopes, pollen, sedimentology & mineralogy	Continuous	$5 \times 10^4$	50 yrs	T, P, B
Dunes	Sand accumulation and stabilisation phases	Episodic	$5 \times 10^4$	-	P
Tree rings	Ring width anomaly, density, isotopic composition	Continuous	$8 \times 10^3$	1	T, P, S <sub>a</sub>
Historical records	Phenology, weather logs etc.	Continuous	$10^3 +$	1	T, P, B, L
Corals	Stable Isotopes	Continuous	$10^5$	seasonal	T, C, L
Closed basin lakes	Lake level	Episodic	$5 \times 10^4$	-	P

S = Salinity      T = Temperature      I = Ice volume      W = Wind direction and strength      B = Biota  
C = Atmospheric composition      S<sub>a</sub> = Solar activity      P = Effective precipitation      L = Sea level.

reconstruction based on pollen data suggest not only more summer rainfall than present but maximum winter precipitation during the Indus valley culture, 5.5-3.5 ka BP (Bryson and Swain, 1981; Swain et al, 1983). From 4.2ka to present, in Didwana, only an ephemeral lake has persisted (Wasson et al, 1984; Singh et al 1990). Palynological data indicates increased salinity in lakes at ~3.7ka (Singh et al, 1972). However, according to Bryson and Swain (1981), the termination of the wet phase is around 3.5ka in Lunkaransar and 2.5ka in Didwana. At 3ka an extensive arid phase begins with rapid dune building (Singhvi et al 1989; Chawla et al, 1992). Archaeological evidence suggests diminishing aridity around 2ka and re-establishment of a seasonal lake at this time. The estimated summer precipitation in the subsequent period is only half of its pre-arid phase value. In this period highest rainfall amounts have been computed for the period 1.1-0.7ka BP (Bryson and Swain, 1981). Reconstruction of lake level (Wasson et al, 1984) and precipitation (Bryson and Swain, 1981) from Rajasthan are shown in Fig. 3.5.

## 3.2 Present study

In the present study stable isotopic composition of lacustrine organic matter from Nal Sarovar, together with C/N ratios, have been used for palaeoclimatic reconstruction. In the following section a brief account of the basic principles involved and results of present investigations are presented.

### 3.2.1 Basic principles

The application of stable isotopes in palaeoclimatic studies is based on the fact that there are finite differences between isotopic masses of elements (e.g. H, C, N, O) that lead to partitioning of isotopes in any physico-chemical process (Urey, 1947). In isotope geochemistry the concern is with measuring small changes in isotope ratios relative to a standard. The accepted unit of isotopic ratio measurement is 'δ', expressed as parts per mil (‰). Thus,

$$\delta = \frac{R(\text{sample}) - R(\text{standard})}{R(\text{standard})} \times 1000$$

where R denotes the isotopic ratio  $^{18}\text{O}/^{16}\text{O}$ ,  $^{13}\text{C}/^{12}\text{C}$  or D/H as the case may be. In the present study carbon isotopes were used and  $\delta^{13}\text{C}$  values expressed with reference to PDB standard.

Isotopic fractionation is also observed in plant organic matter. Atmospheric carbon dioxide contains approx. 1.1% of  $^{13}\text{C}$ . In the absence of industrial activity, the  $\delta^{13}\text{C}$  value of atmospheric  $\text{CO}_2$  would be  $-7^\circ/\infty$  (Craig, 1957; Keeling, 1961). This forms the reservoir from which the carbon is fixed in organic matter via photosynthesis. During photosynthesis, plants discriminate against  $^{13}\text{C}$  because of small differences in chemical and physical properties imparted by difference in mass. This difference can be used to assign plants to the following groups.

The first category comprises  **$\text{C}_3$  plants** (Craig, 1953; Park and Epstein, 1960), which fix  $\text{CO}_2$  by the action of the enzyme ribulose biphosphate carboxylase (Park and Epstein, 1960). In these plants, the initial chemical product formed during photosynthesis is a three carbon molecule - phosphoglyceric acid, hence the name. This process is called as the **Calvin cycle**.

The  **$\text{C}_4$  plants**, in which  $\text{CO}_2$  is initially taken up through carboxylation of phosphoenolpyruvate, were discovered in the 1960's (Kortschak et al, 1965; Hatch and Slack, 1970). The initial chemical product formed is a four carbon molecule, malic acid. This process is called as the **Hatch-Slack pathway**. Following this discovery, Bender (1968); Smith and Epstein (1971), discovered that  $\text{C}_4$  plants are isotopically distinct from  $\text{C}_3$  plants.

Application of stable isotopes as climatic indicators is based on the differing carbon isotopic values and ecological preferences of the  $\text{C}_3$  and  $\text{C}_4$  type of plants.  $\text{C}_4$  plants favour conditions of aridity and low soil moisture whereas  $\text{C}_3$  plants dominate areas of higher precipitation and higher soil moisture (Tieszen et al, 1979; O'Leary, 1988).

A third group of plants has also been reported which show  $\delta^{13}\text{C}$  values overlapping between those of  $\text{C}_3$  and  $\text{C}_4$  plants (O'Leary, 1981). These comprise desert plants and other succulents which absorb  $\text{CO}_2$  by the pathway known as Crassulacean acid metabolism (Kluge and Ting, 1978; Osmond, 1978) and are known as the **CAM plants**.

A survey of over 1000 published  $\delta^{13}\text{C}$  analysis of whole plants, wood, leaves and seeds (Deines, 1980) showed the following average  $\delta^{13}\text{C}$  values of the three categories of plants

$\text{C}_3$	..	$-27\text{‰}$
$\text{C}_4$	..	$-14\text{‰}$
CAM	..	$-14\text{‰}$ to $-27\text{‰}$

Of the aquatic plants, which are also present in a lake, the floating pond weeds utilise atmospheric  $\text{CO}_2$ , as the diffusion of  $\text{CO}_2$  dissolved in water is several orders of magnitude slower than diffusion of  $\text{CO}_2$  in air (O'Leary, 1988); these plants have  $\delta^{13}\text{C}$  ratios similar to terrestrial plants (Oana and Deevey, 1960). For the submerged aquatics the picture is entirely different as the organic carbon is enriched in  $^{13}\text{C}$  in proportion with the hardness of water (Oana and Deevey, 1960; Smith and Epstein, 1971). With increasing hardness an enrichment in  $^{13}\text{C}$  has been observed in *Chara*, *Potamogeton*, *Nitella* etc. This effect has been attributed to increased utilisation by submerged plants of the bicarbonate component in hard water lakes, instead of dissolved  $\text{CO}_2$ . Any change in hardness of water associated with long term climatic factors could result in a change in  $\delta^{13}\text{C}$  component of up to  $10\text{‰}$  (Stuiver, 1975).

The organic matter in a lake is contributed both by terrestrial and aquatic plants. Hence, for a meaningful interpretation of  $\delta^{13}\text{C}$  variations, it becomes necessary to be able to establish the dominance of either at any particular period of time. To distinguish between organic matter of terrestrial and aquatic origin, carbon to nitrogen ratios have been used (Sweeny et al, 1980; Wetzel, 1983). Autochthonous organic matter (from within the lake) comprising aquatic plants and algae have a C/N ratio of less than 10 (Meybeck, 1982). This is

because organic nitrogen occurs preferentially in proteins and nucleic acids (Blackburn, 1983) which are relatively more abundant in lower plants like aquatic phytoplankton and in bacteria. Higher terrestrial plants have lignin and cellulose which are nitrogen poor; hence allochthonous organic matter (from catchment area) has C/N values which are higher than 20 and may even go as high as 200 (Hedges et al, 1986). Higher values of C/N are indicative of a dominant terrestrial contribution whereas lower values are indicative of a dominant aquatic contribution to the organic matter. Some of the lakes where these techniques have been applied, for palaeoclimatic reconstruction, are lake Biwa, Japan (Nakai and Koyama, 1987); Karewa lake sediments in India (Krishnamurthy et al, 1986); lake Bosumtwi, W. Africa (Talbot and Johannessen, 1992).

**3.2.2 Results and discussion**

**Horizon-3 and Horizon-2**

**Chronology:** Between 3-54m depth, the amount of organic matter was very small (<0.01%). Hence, <sup>14</sup>C dating could be done only on carbonate nodules found occasionally. These gave a date of >38ka at 16m depth and below. The results are shown in table 3.2 below.

**Table 3.2** Radiocarbon dates for Horizon-2 & 3, Nal Sarovar core.

Lab. No.	Radiocarbon Lab. No.	Depth (cm)	<sup>14</sup> C Age (ka) (carbonate)
N-164	PRL-1735	1645-1662	>38
N-167	PRL-1731	1825-1835	>38
N-424	PRL-1720	5465-5485	>38

In the absence of significant organic matter and adequate chronological control, no palaeoclimatic studies were carried out on these two horizons. For Horizon-2, the presence of red beds with calcareous cement is indicative of their formation in an arid environment. The presence of gypsum (at 4m, 5m and 7m depth) is also indicative of aridity. A broad picture of depositional environment emerging from geomorphological and sedimentological studies has already been discussed in Chapter 2 (Section 2.2).

## Horizon-1

**Chronology:** The radiocarbon dates were obtained on bulk organic matter from samples which had been treated by dilute HCl to remove carbonate material (refer to Appendix C for experimental details). Eight samples were dated (see Table 3.3, Fig 3.2) and the estimated age, for any particular depth, was calculated by interpolation using a second order fit to the depth vs. radiocarbon age data, as under,

$$\text{Age (ka)} = -0.00003 * (\text{Depth})^2 + 0.0308 * (\text{Depth}) - 0.037 \quad \dots \text{(equation 3.1)}$$

where "Depth" is in cm.

**Table 3.3** Radiocarbon dates for Horizon-1, Nal Sarovar core.

Lab. No.	Radiocarbon Lab. No.	Depth (cm)	<sup>14</sup> C* Age (years) (organic)
N-1+N-2	PRL (1753+1754)	0-10	Bomb
N-3+N-4	PRL (1755+1756)	10-20	490±110
N-20+N-21	PRL (1773+1774)	58.5-62.5	1780±100
N-52	PRL-1818	124-126	3110±110
N-69+N-70+N-71	PRL-1830	158-164	4400±120
N-76	PRL-1817	207-220	5100±120
N-82	PRL-1876	270-280	5380±130
N-86	PRL-1826	300-309	6750±130

\* <sup>14</sup>C half life is 5730±40 years.

**Stable Isotope studies:** A special glass, vacuum line for gas extraction and C/N analysis was constructed. The same is described in Appendix D along with other experimental procedures involved in δ<sup>13</sup>C and C/N analyses of the sample. Preliminary measurements indicated that only the top 3m of the core had any significant proportion (~1%) of organic matter, thus limiting the study to Horizon-1.

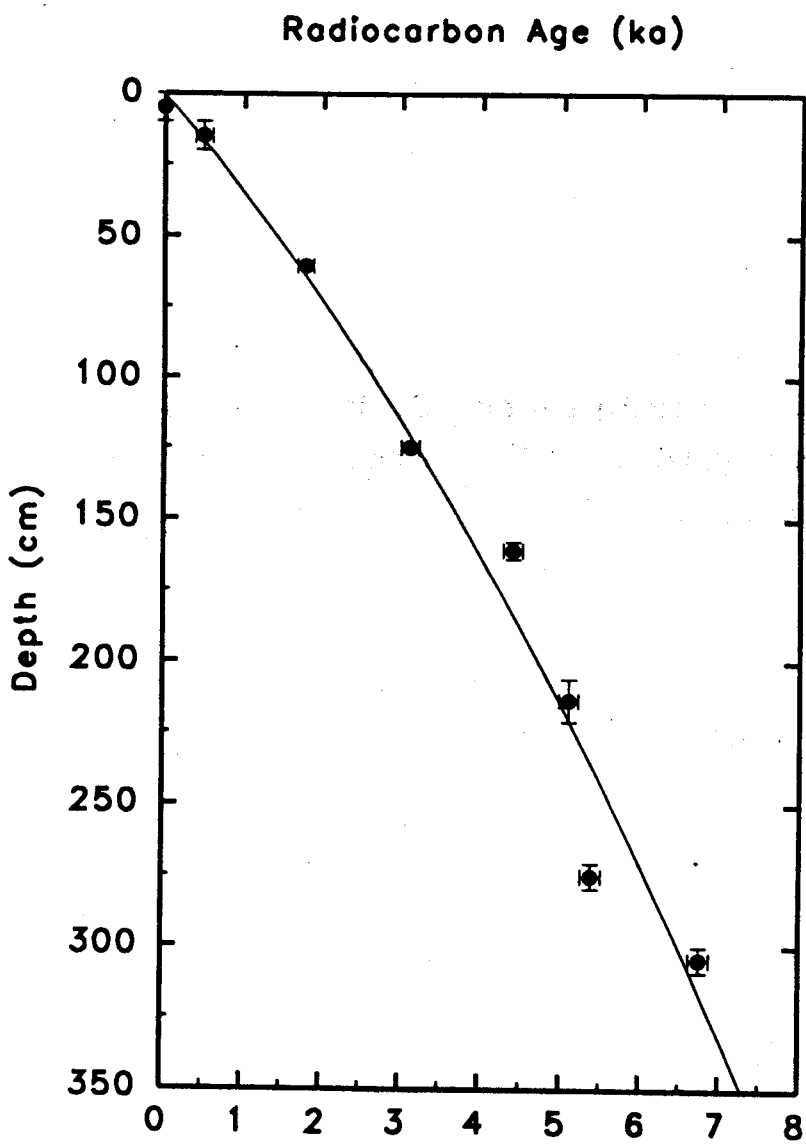


**Fig. 3.2** Plot of radiocarbon dates vs. depth, Nal Sarovar core.

**Modern samples** To investigate the range of  $\delta^{13}\text{C}$  and C/N in terrestrial and aquatic plants, and also to constrain the limits of  $\delta^{13}\text{C}$  variation in submerged plants, a few present day plants from Nal Sarovar were analysed (Table 3.4). Of the present day plants analysed, the terrestrial plant *Cyanadon* showed a C/N value of 24.3 and a  $\delta^{13}\text{C}$  value of  $-13.2\text{‰}$  indicating it to be of  $\text{C}_4$  type plant. The aquatic types showed, as expected, a C/N value  $<10$ . The decayed vegetation matter, 'scum' floating on the surface of the water was also analysed and showed a C/N value of 15.2 indicating contribution from both aquatics as well as from terrestrial plants. The surface sediment however shows a C/N value of 5.9. This indicated that, at least today, the dominant contribution to sediment organic matter in the lake is from aquatic plants.

*Najas* is a free floating plant that takes up  $\text{CO}_2$  chiefly from the atmosphere. The diffusion of  $\text{CO}_2$  into the plants from water is several orders of magnitude slower than in air (O'Leary, 1988). Hence the isotopic signal,  $\delta^{13}\text{C} = -22\text{‰}$ , from *Najas* is dominated by atmospheric  $\text{CO}_2$ . In view of the enrichment of  $10\text{‰}$  for submerged aquatics due to climatic factors (Stuiver, 1975), the maximum enriched value of  $\delta^{13}\text{C}$  that could be expected at Nal Sarovar in totally submerged plants is around  $-12\text{‰}$ .

**Table 3.4** Results of C, N and  $\delta^{13}\text{C}$  analyses on present day samples from Nal Sarovar.

Sample	Habitat	$\delta^{13}\text{C}$ (‰)	C/N
<i>Nitella Sp.</i>	Bottom aquatic	-23.5	8.1
<i>Najas Sp.</i>	Floating aquatic	-22.1	9.9
<i>Cyanadon Sp.</i>	Terrestrial	-13.2	24.3
<i>Cyprus Sp.</i>	Aquatic/terres.	-27.5	nm
Scum	-	-16.8	15.2
Top sediment	-	-21.3	5.9

1. nm = not measured

2. Identification of plant species and habitat by botany dept. Gujarat Univ. Ahmedabad.



**Core Samples** The results of %C, %N,  $\delta^{13}\text{C}$ , C/N analyses on organic matter and % sand in sediments from the Nal Sarovar core samples are shown in Table 3.5. These are also plotted in Fig 3.3 in the form of %C, %N,  $\delta^{13}\text{C}$ , C/N and % sand vs. radiocarbon age. Regression equation 3.1 was used for interpolation of  $^{14}\text{C}$  ages.

The organic matter from Nal Sarovar samples showed a range of  $\delta^{13}\text{C}$  from  $-15\text{‰}$  to  $-23\text{‰}$ . C/N values varied from 6 to 50. Both these factors indicated that there had been variation in the relative contribution from aquatic and terrestrial plants as also in the nature of terrestrial plant population.

**Table 3.5** Results of C, N,  $\delta^{13}\text{C}$  and % sand analyses on samples from Nal Sarovar core.

Lab. No.	Depth (cm)	C (Wt %)	N (Wt %)	C/N	$\delta^{13}\text{C}$ (‰)	Sand (%)
N-1	5	1.43	0.09	15.88	-19.9	4.1
N-4	15	0.91	0.12	7.58	-18.8	3.84
N-5	27	1.03	0.06	17.16	-19.1	1.38
N-8	33	1.00	0.05	20	-18.9	1.42
N-11	39.5	0.95	0.09	10.55	-19.2	4.17
N-13	43.5	0.87	0.08	10.87	-18.2	1.91
N-17	49.5	0.89	0.11	8.09	-18.6	1.55
N-18	53.5	0.90	0.05	18	-18.3	2.17
N-20	57.5	0.90	0.05	18	-18.8	2.02
N-21	59.5	0.77	0.06	12.83	-19.8	1.18
N-23	63.5	0.93	0.06	15.5	-18.2	1.91
N-26	69.5	0.85	0.12	7.08	-18.1	2.33
N-28	73.5	0.89	0.06	14.8	-20.4	2.51
N-31	79.5	0.79	0.06	13.16	-18.8	2.24
N-33	85	1.02	0.09	11.33	-18.9	2.08
N-37	94	1.71	0.12	14.25	-20.0	3.38

... continued

**Table 3.5** Continued

Lab. No.	Depth (cm)	C (Wt %)	N (Wt %)	C/N	$\delta^{13}\text{C}$ (‰)	Sand (%)
N-40	100	0.94	0.09	10.44	-21.4	1.87
N-47	115	0.98	0.15	6.53	-21.9	5.72
N-49	119	0.98	0.05	19.6	-22.8	7.26
N-52	125	1.18	0.06	19.66	-19.8	3.89
N-55	130	1.22	0.09	13.55	-22.9	6.17
N-60	141	0.96	0.05	19.2	-21.7	3.31
N-65	151	1.09	0.06	18.16	-21.6	2.55
N-70	161	0.94	0.06	15.66	-20.9	2.77
N-72	165	1.03	0.07	14.71	-19.3	9.74
N-73	171	1.09	0.08	13.62	-20.4	6.62
N-74	184.5	0.91	0.05	18.2	-19.9	2.91
N-75	201	0.82	0.02	41	-20.6	6.38
N-76	213.5	0.72	0.02	36	-20.6	4.93
N-77	225	1.01	0.02	50.5	-20.5	6.65
N-78	235	1.21	0.06	20.16	-21.9	5.61
N-79	245	1.06	0.05	21.2	-21.7	6.16
N-80	255.5	0.98	0.02	49	-22.8	7.98
N-82	275	0.82	0.09	9.11	-20.7	10.09
N-84	291.5	1.47	0.14	10.5	-17.7	14.94
N-85	296	0.75	0.04	18.75	-16.3	32.22
N-86	304.5	3.31	0.09	17.42	-16.8	39.78
N-87	310.5	0.64	0.03	21.33	-14.9	57.28

**Note**

1.  $\delta^{13}\text{C}$  values are relative to the PDB standard.
2. The experimental procedure and the results of standards are given in Appendix D.
3. Reproducibility on repeated measurements of UCLA standard were 0.2‰

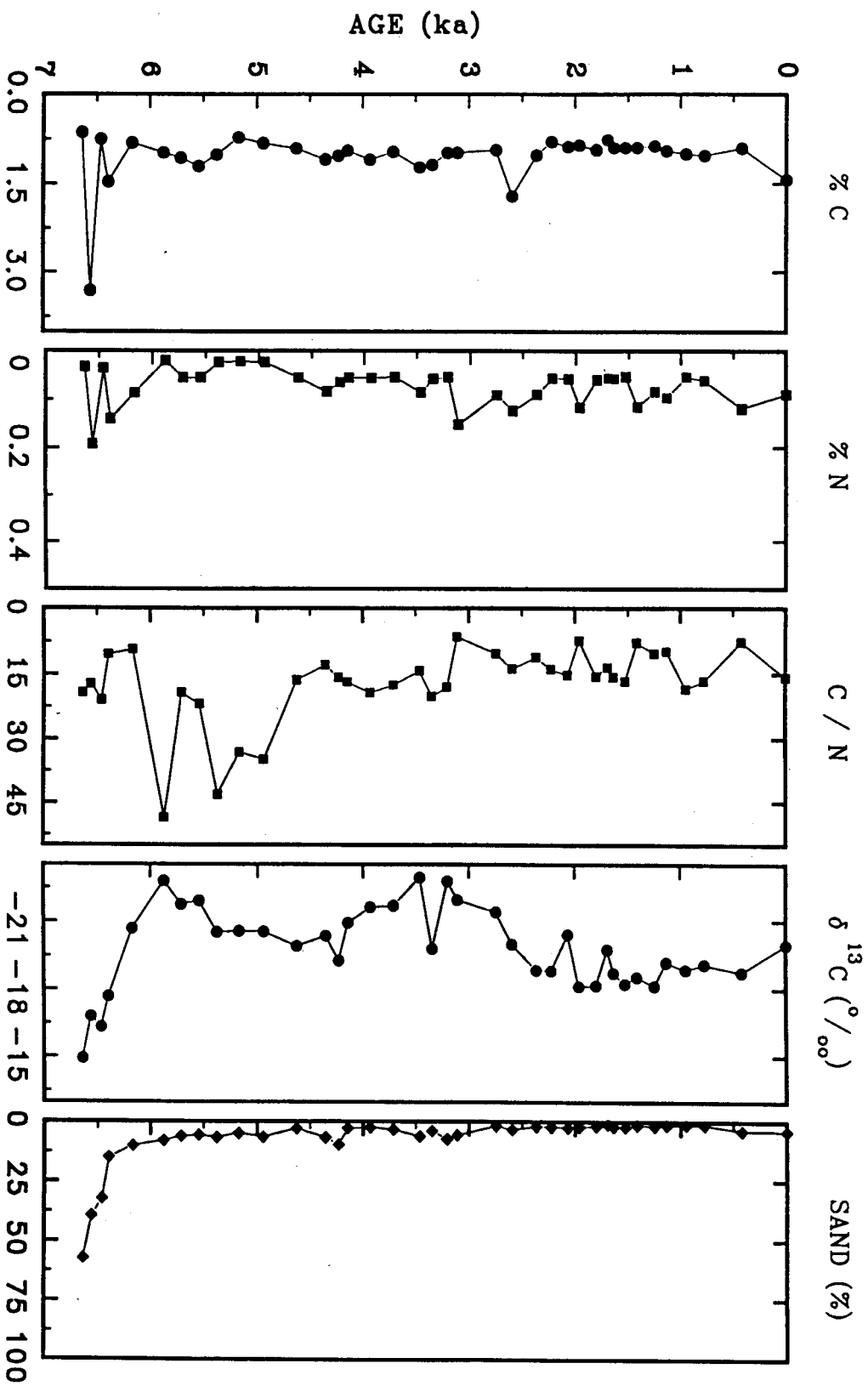


Fig. 3.3 Age variation of %C, %N, C/N,  $\delta^{13}\text{C}$ , and % sand in sediment samples from Nal Sarovar core.

It is possible that the observed variation in C/N vs. age (Fig. 3.3) may be due to loss of nitrogen with age as, nitrogen bearing compounds are more prone to loss during decomposition (Lee and Olson, 1984). The following interpretation assumes that there has not been any loss of nitrogen. This is also supported by plots of nitrogen and carbon versus age which do not show any systematic loss of nitrogen with age. Also, there is a strong correlation between C and N ( $r^2=0.64$ , at 95% confidence interval) suggesting that both C and N are organically bound. Though C/N and  $\delta^{13}\text{C}$  do not show any correlation as a whole, it is possible to identify certain periods where a systematic trend in variation of C/N and  $\delta^{13}\text{C}$  can be observed (Fig. 3.4). The climatic implications of these systematic variations are discussed below. In the following discussion, the terms 'wetter' or 'drier' are with respect to 'present'. Due to inherent errors in radiocarbon dating and of interpolation, the climatic boundaries may have an error of upto  $\pm 250$  years.

**Period 5 (~6.6-6ka):** At the beginning of this period C/N ratios are close to ~20 indicating significant terrestrial contribution to the lake. The  $\delta^{13}\text{C}$  values are enriched ( $\sim -15\text{‰}$ ) indicating a dominance of  $\text{C}_4$  type of vegetation and/or aquatics growing in waters rich in dissolved carbonate. This period also shows a relatively higher proportion of sand (Fig 3.3) which is interpreted to indicate that the surrounding sediments had not yet been stabilised by vegetation and were easily eroded and deposited into the lake.

The climate during early part of this period must have been dry. This is followed by a phase during which there is a decrease in C/N, accompanied by rapid depletion in  $\delta^{13}\text{C}$ , indicating a shift to a wetter climate towards the end of this period.

**Period 4 (6-4.8ka):** High C/N values, at times close to 40, are indicative of an increased contribution of terrestrial plants to the lake sediments. This is accompanied by  $3\text{‰}$  enrichment in  $\delta^{13}\text{C}$ , indicating a small shift towards  $\text{C}_4$  type of vegetation. As noted earlier (Chapter 2; Section 2.2.3.1), fresh water shells of *Bittium* and few land snail shells were found in this zone (Fig. 3.4,

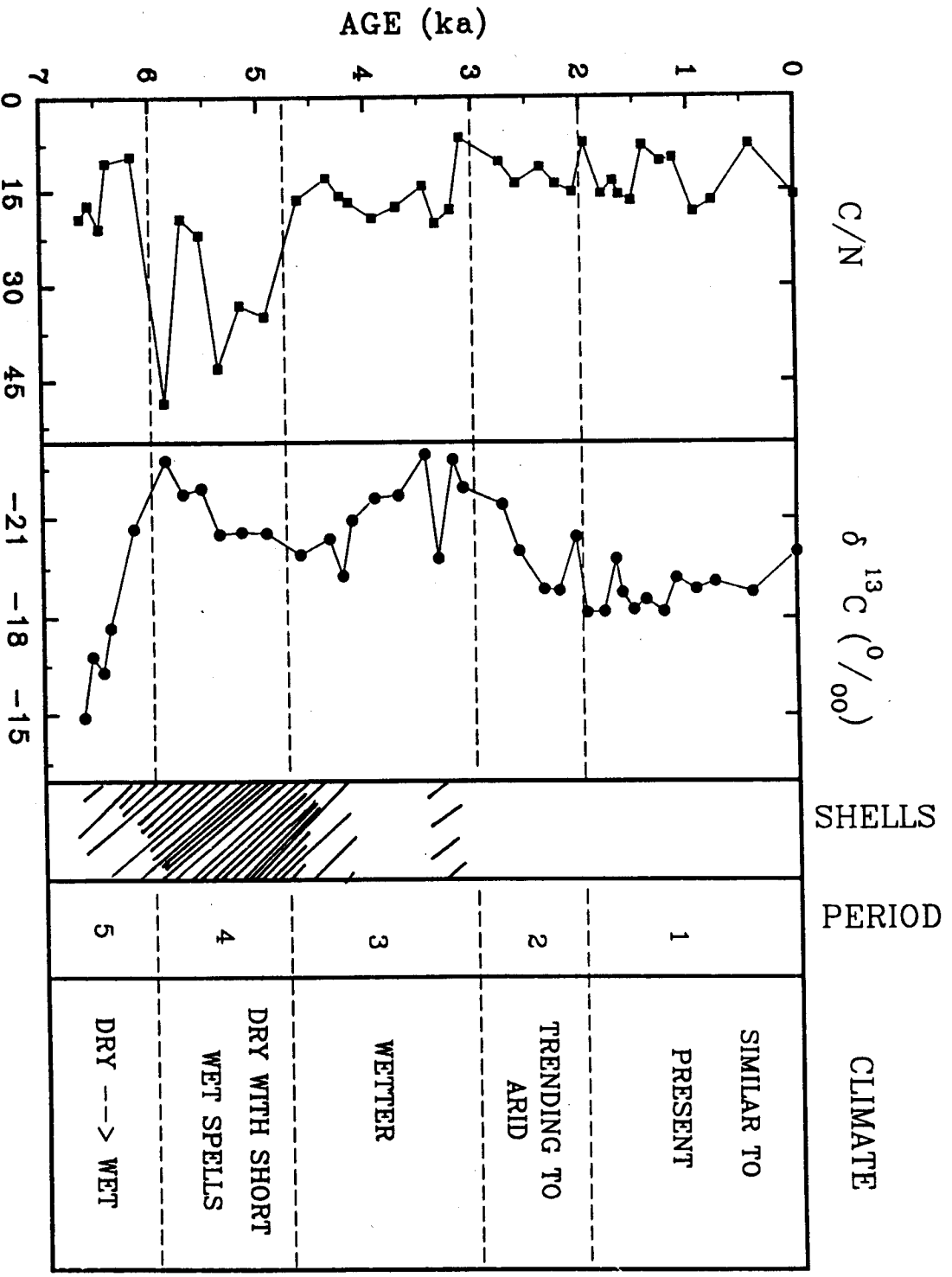


Fig. 3.4 Palaeoclimatic interpretation of C/N and  $\delta^{13}\text{C}$  variations in sediment samples from Nal Sarovar core.

PLATE 3). Based on their presence in large abundance and small size, the lake environment was described as shallow fresh water with periodic drying up of the water body (Jain, pers. comm. 1996).

The almost complete absence of aquatic plants is also indicative of a dry or a shallow lake bed with evenly distributed short wet spells which, though capable of sustaining and bringing in the terrestrial organic matter, were insufficient to sustain aquatic vegetation in the lake. It is likely that the even distribution was achieved by an increase in winter rainfall and decrease in summer rainfall relative to present. Such a shift would explain high C/N and hence absence of aquatic vegetation, yet an abundance of shallow fresh water shells, as also a slight shift towards  $C_4$  type of vegetation. The overall climate in this period can be described as dominantly dry with short wet spells.

**Period 3 (4.8-3ka):** In this period, average C/N ratio declined to ~15 indicating a mixed contribution from both aquatic and terrestrial biota. The  $\delta^{13}C$  values of organic component began to deplete again from the start of this period and reached their lowest around ~3ka.

Increase in aquatic contribution accompanied by depletion in  $\delta^{13}C$  of lake organic matter, indicates a higher lake level. Overall, during this period the climate was wet.

**Period 2 (3-2ka):** Presence of mixed terrestrial and aquatic vegetation was indicated by C/N value of ~15. This, together with, gradual enrichment of  $\delta^{13}C$  values, indicates lower effective precipitation so that the aquatic vegetation was utilising dissolved bicarbonate from the lake.

The overall climate in this period was still wetter than present but the trend towards aridity had begun at 3ka. Present day conditions were reached at about 2ka.

**Period 1 (2ka-Present):** The  $\delta^{13}C$  values did not show any significant variation. C/N ratios showed a generally mixed vegetation but at certain periods the organic matter was increasingly dominated by the aquatic contribution as at 1.9, 1-1.3 and 0.4 ka BP. This, perhaps, represented short

spells when the water level was high. The overall climate in this period was similar to present.

An alternative explanation can also be proposed for the entire data set shown in Fig. 3.4. The lake was established only at ~6.6ka when precipitation minus evaporation increased. In the Period 4 (6-4.8 ka), increased inflow brings in larger amount of terrestrial organic debris. The presence of gastropods, only in this period, could be indicative of standing water conditions, in which case it can be argued that only Period 4 represents standing water conditions. By this reasoning, the subsequent Period 3 (4.8-3 ka) would represent lower inflows of freshwater into the lake; the vegetation, however, remains mesic (requiring medium supply of moisture) according to  $\delta^{13}\text{C}$ . A transitional drying phase occurs between 3 and 2 ka (Period 2) and modern conditions are established at ~2ka.

This re-interpretation, though apparently consistent with the palaeoclimatic history for the comparable period in the Thar desert (Bryson and Swain, 1981; Wasson et al, 1984; Singh et al, 1990), has some arguments against it. As indicated earlier in this section, the habitat of Bittium shells is very shallow water. Also a few fully preserved shells of land snails were found in core and in trenches corresponding to Period 4. There is also a slight enrichment in  $\delta^{13}\text{C}$  indicating a small shift towards  $\text{C}_4$  type of vegetation. C/N values are ~40 indicating negligible contribution from the aquatics which would have been present had the lake levels been higher. All these three factors, gastropod shells,  $\delta^{13}\text{C}$  and C/N on organic matter indicate absence of high lake levels in Period 4. On the other hand, Period 3 (~4.75-3ka) showed a mixed contribution of both terrestrial and aquatic vegetation to organic matter in the lake, as indicated by C/N value of ~15. That Period 3 was wettest is also suggested by lowest values of  $\delta^{13}\text{C}$  (~-23‰) of organic matter which imply a shift towards  $\text{C}_3$  type of plants and/or aquatics growing in fresh waters.

Based on these factors, the alternative interpretation suggesting standing water conditions only in Period 4 has been found to be inadequate to explain the data set of Fig. 3.4. The interpretation suggesting a drier than present period from ~6.6 to ~4.8ka is accepted. This phase was interrupted by a short wet episode at ~6.2 ka. In the period 4.8-3ka the climatic

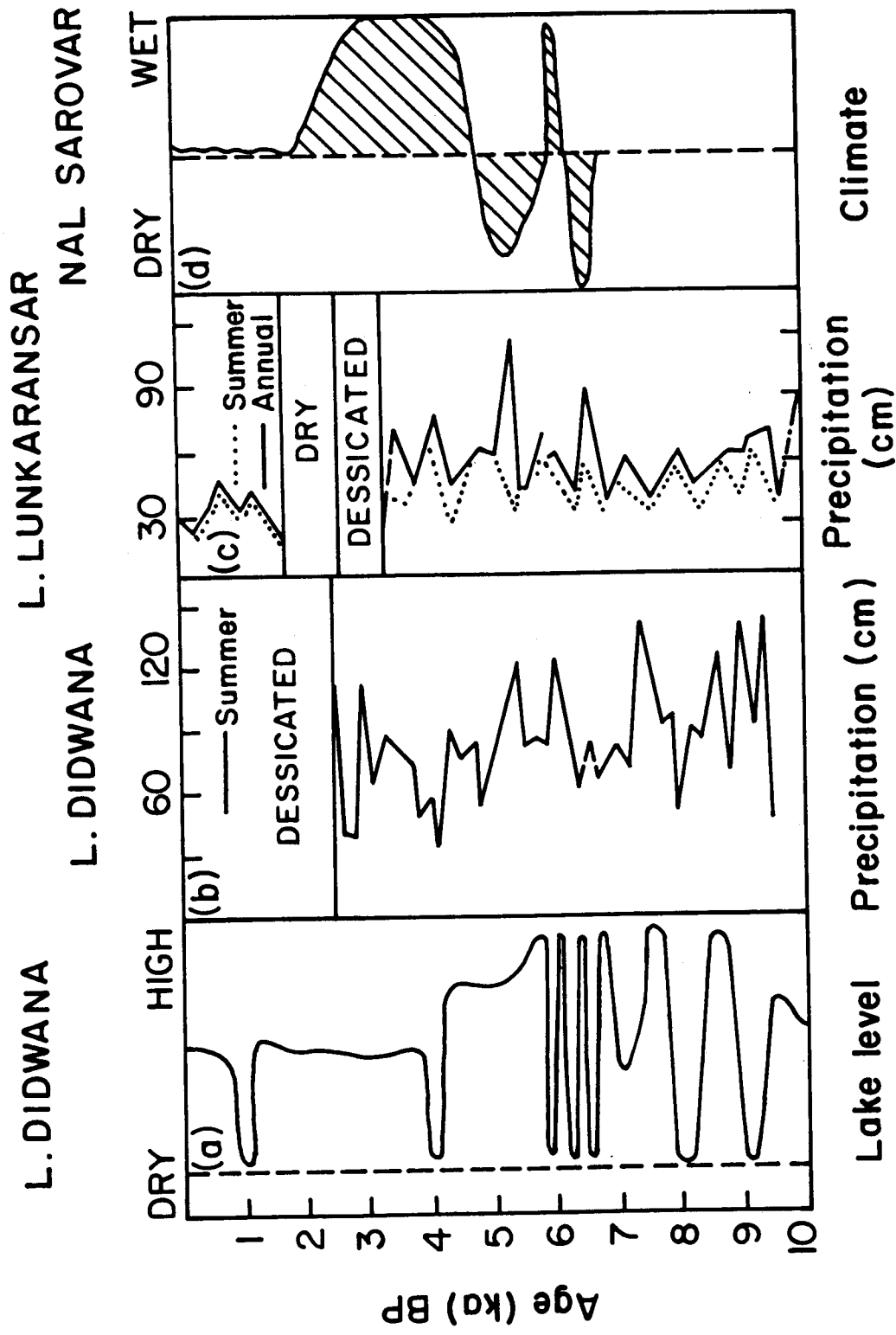


Fig. 3.5 A comparison of palaeoclimatic data from Didwana and Lunkaransar lakes in Rajasthan with Nal Sarovar. (a) Wasson et al, 1984; (b)&(c), Bryson and Swain, (1981).



conditions are inferred to have been wetter than present and the lake generally had fresh water conditions. From 3ka onwards, the aridity seems to increase until the present day climate was established at 2ka.

This climatic interpretation is significantly different from the palaeoclimatic interpretations based on palynological and geochemical data obtained from Lunkaransar (Bryson and Swain, 1981; Swain et al, 1983) and Didwana (Bryson and Swain, 1981; Wasson et al, 1984; Singh et al, 1990) lakes in Rajasthan (Fig. 3.5). The palaeoclimatic record for the period 6.5-4.8ka from both the lakes in Rajasthan showed higher annual rainfall (nearly 2-3 times the present value - Bryson and Swain, 1981; Swain et al, 1983). This is in contradiction to present data for the same period which indicated a shallow lake level, with periodic drying, and an almost complete absence of aquatics, except for a short wet episode ~6.2 ka. It is possible that the inferred uniform distribution of wet spells in Period 4 (6-4.8ka) was achieved through increase in winter precipitation accompanied by a larger decrease in summer rainfall as the overall climate has been inferred to have been dry. Nal lake data, indicating a wetter than present climate in the succeeding period (4.8-3ka), is comparable with the Rajasthan precipitation data which too indicated a higher than present rainfall. While it has not been possible to quantify the Nal lake data in terms of rainfall changes, the observed shifts in C/N ratio and  $\delta^{13}\text{C}$  are not large enough to have been caused by very significant increase in rainfall (2-3 times the present value) in the catchment areas of Nal Sarovar, as has been interpreted by Bryson and Swain (1981), for the Rajasthan lakes for the same period. This inference is drawn by comparison with present day climatic conditions prevailing in the Nal region. Presently, the region receives ~500mm of rainfall from SW monsoon, enough to sustain a water level of ~2m during the wet season. In summer the lake becomes saline and dries up in some years. Had at any time in the past, the increase in rainfall been 2-3 times the present value, the lake levels would have been higher (or the frequency of drying up substantially reduced), aquatic vegetation would have been dominant and this would have shown up as  $\text{C/N} < 10$ . With the exception of Period 4 (where  $\text{C/N} > 20$ ), the C/N values hover around ~15. This clearly indicates that in no period were the aquatics totally dominant which would

have been the case had rainfall been 2-3 times higher, as suggested for Rajasthan lakes.

As indicated in Fig 3.5, the termination of the wet phase is around 3.5ka in Lunkaransar and 2.5ka in Didwana (Bryson and Swain, 1981). However, according to Wasson et al (1984), this wet phase at Didwana ended earlier at 4ka when present day dry conditions were established. Singhvi et al (1989), and Chawla et al (1992), based on TL dating of dune sands, indicated an arid phase with rapid dune building activity at 3ka followed by diminishing aridity at 2ka and establishment of present day conditions. The Nal data also indicates the beginning of aridity around 3ka BP and onset of present day conditions around 2ka BP. There appears to be a general agreement in all data sets regarding establishment of present day conditions ~2 ka BP.

It is possible that the palaeoclimatic variations recorded at Nal Sarovar largely reflect a local picture. At present this can only be checked by the use of other indirect parameters which influence the climate in this region. Nal Sarovar lies in the region where SW monsoon is the most important factor in influencing the climatic record. Sensitivity experiments with GCM's have already shown that albedo changes induced by changing snow cover over Eurasia exert considerable control over the development of continental heat low over Asia, which in turn, affects the strength and duration of the south-west monsoon over the Arabian sea (Barnett et al, 1989). In the past, there is evidence of expanded glacier cover between 5.7-4ka BP in China (Li, 1990) and colder climates between ~5.5-5ka from N. China (Yan and Petit-Maire, 1994). There are also evidences, in Europe, of Holocene glacier expansion at 6.5ka, repeated expansions around 5ka BP (Bradley, 1985 and references therein) and between 3-2.2ka (Denton and Karlen, 1973). These cold periods with expanded glaciers in Eurasia appear to correlate well with the drier periods recorded at Nal lake. This suggests that the monsoon influenced palaeoclimatic record at Nal Sarovar may reflect a regional history of past climatic variations.

## **CHAPTER 4**

### **LUMINESCENCE DATING STUDIES**

In case of Nal Sarovar core samples, the amount of organic matter in the sediments, below 3m depth was very low ( $<0.01\%$ ). Hence radiocarbon dating of organic matter could be attempted only upto 3m (see Section 3.2.2). The radiocarbon dating of the carbonate nodules at depths of 16m and below gave an age of  $>38\text{ka}$ , providing a lower age limit for these sediments. The chronology for sediments below 3m was, therefore, obtained using luminescence dating. In this chapter a brief introduction to luminescence dating is provided along with the results of present study.

Luminescence dating is based on the fact that naturally occurring minerals like quartz and feldspars, among others, act as natural dosimeters and preserve a record of dose/irradiation received through time. Decay of natural radionuclides viz. U, Th and K provides a source of constant irradiation. A short exposure to sunlight can, however, erase the geological luminescence to a zero or near zero value. On burial, reacquisition of luminescence begins which is a function of time and, hence, is proportional to the age i.e. time since last burial, of the sample. Initially the growth of luminescence is linear but with increasing dose, saturation effect occurs. This effect puts an upper limit to the dose and hence the age that can be measured using this technique.

The basic advantage of the method accrues from the fact that the minerals, being sediment constituents, provide an opportunity to date the sediment itself thereby eliminating any ambiguity of correlation of the sample

with the strata. This is in contrast to the radiocarbon method where organics and carbonates associated with the sediment are dated.

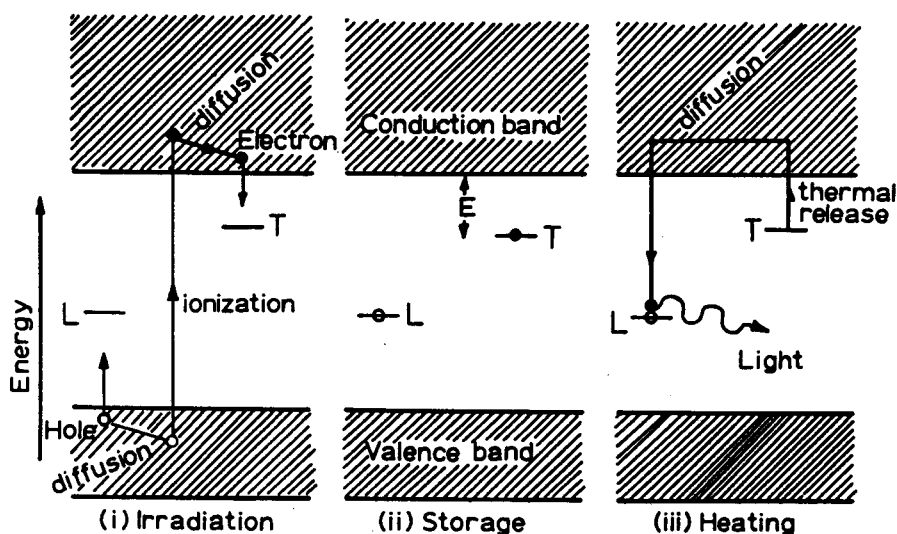
**4.1 Thermal and optically stimulated luminescence**

The phenomenon of stimulated (optical/thermal) luminescence can be explained using the band theory of solids (Fig. 4.1). The interaction of ionising radiation,  $\alpha$ ,  $\beta$  and  $\gamma$  (produced by the decay of radioactive nuclides) with a crystal results in the production of an avalanche of free electrons and holes. Most of these charges combine instantaneously and release energy either thermally and/or optically. A small fraction of free charges, however, gets trapped at various lattice defects in the crystal lattice e.g. vacancies, interstitials etc. The lifetime of these trapped charges varies from  $10^{-4}$  to  $10^9$  a. However, thermal or optical stimulation can cause instantaneous detrapping of charges, some of which radiatively recombine with an opposite charge at an appropriate recombination centre. The emitted luminescence is called as Thermally Stimulated Luminescence/Thermoluminescence (TSL/TL) or Optically Stimulated Luminescence (OSL) depending on the type of stimulation. When optical stimulation is done using infra red light, the emitted luminescence is called as Infra Red Stimulated Luminescence (IRSL). Despite the complexity of the process, it turns out that the total number of trapped charges is proportional to the radiation dose and the final luminescence intensity bears a simple proportional relationship to the radiation dose. This forms the basis of application of luminescence phenomena in dosimetry and dating.

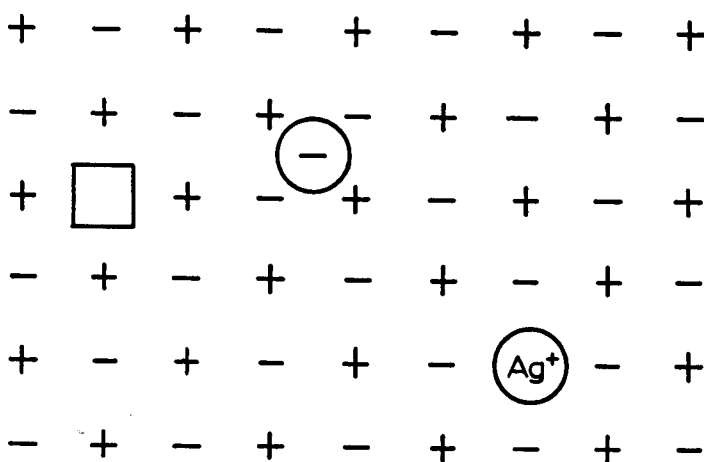
**4.1.1 Age equation**

Given an *ab initio* zero luminescence level, the age equation can be given as

$$\text{Age} = \frac{\text{Total luminescence since last zeroing (L)}}{\text{Luminescence acquisition per year (L/year)}}$$



(a)



(b)

**Fig 4.1** (a) Explanation of the basic process of TL induction using the band theory of solids (after Aitken, 1985). (i) Irradiation by ionising radiation results in the production of free charges some of which get trapped at various defects in the crystal. (ii) Energy 'E' is required for the detrapping of the charges. (iii) Stimulation by heating (or optically) can cause detrapping of these charges some of which recombine radiatively with the opposite charge at a recombination centre 'L' and emit light called as TL or OSL depending on the type of stimulation.

(b) Schematic portrayal of simple types of defects such as negative ion vacancy, interstitial defect and impurities in an ionic crystal (after Aitken, 1974)

$$\text{or, Age} = \frac{L}{\sum_{\alpha, \beta, \gamma, C} (L/D) * (D/y)} \quad \dots (4.1)$$

The above equation can be rewritten as,

$$\text{Age} = \frac{L}{\chi_{\alpha} D_{\alpha} + \chi_{\beta} D_{\beta} + \chi_{\gamma} D_{\gamma} + \chi_c D_c} \quad \dots (4.2)$$

The denominator accounts for the summation of the radiation doses from  $\alpha$ ,  $\beta$ ,  $\gamma$ 's emitted in the decay of radionuclides and cosmic rays. In the equation,  $\chi_i$  is the luminescence sensitivity of the sample and is represented as L/unit dose.  $D_{\alpha}$ ,  $D_{\beta}$ ,  $D_{\gamma}$  and  $D_c$  denote the dose rate due to  $\alpha$ ,  $\beta$ ,  $\gamma$  and cosmic rays respectively. Due to the manner of energy deposition, the high ionisation density and low track length of the alpha particle, the luminescence inducing efficiency of alpha particles is small compared to that of beta or gamma. According to Zimmerman (1971),  $\chi_{\alpha} < \chi_{\beta} = \chi_{\gamma} = \chi_c$  and defining the alpha efficiency factor 'a' as,

$$a = \chi_{\alpha} / \chi_{\beta} \text{ and } Q = L / \chi_{\beta}$$

equation 4.2 can now be rewritten as,

$$\text{Age} = \frac{Q}{aD_{\alpha} + D_{\beta} + D_{\gamma} + D_c} \quad \dots (4.3)$$

where Q is the laboratory  $\beta$  dose that can induce a luminescence level identical to that in the natural sample. It is also known as the equivalent dose (ED). Thus, for the calculation of luminescence age of a sample two parameters have to be measured,

1. The total dose acquired by the sample since the last 'zeroing' event, or its equivalent dose (ED).

2. Dose received per year, i.e. dose rate. This has three components - alpha, beta and gamma which are contributed by U, Th and K in the sample. In addition, the cosmic ray contribution to the dose rate is also considered.

The application of equation 4.3 assumes that there has not been any loss of luminescence with time i.e. that the signal has remained stable.

#### ***4.1.2 Luminescence dating of sediments***

The luminescence age, as discussed above, gives the time elapsed since the last 'zeroing' event. This event is either the most recent thermal event that caused the sample temperature to rise beyond 500°C or the most recent photo-bleaching event caused due to sun exposure of minerals during weathering and transport. It would seem from Fig. 4.2 that a sun exposure of several hours to several minutes is needed to reduce the TL or OSL respectively, to maximum bleachable level value. This assumption is easily satisfied in case of aeolian sediments which are transported over large distances over long durations. However, in case of sediments transported and deposited by water, there always remains a possibility that bleaching to a residual level may not have been achieved (see Section 4.1.3). In such a case, the unbleached geological luminescence can result in an age overestimation.

#### **Estimation of ED**

Estimation of equivalent dose is generally done by constructing a luminescence vs. dose, i.e. the growth curve. The various methods of estimation of ED are briefly discussed below.

1. **Partial bleach method** (Wintle and Huntley, 1980): This method was devised for partially bleached samples. In this method, two growth curves are constructed. For the first, the natural sample is given incremental doses of beta (or gamma) radiation and their TL recorded. For the second, after giving

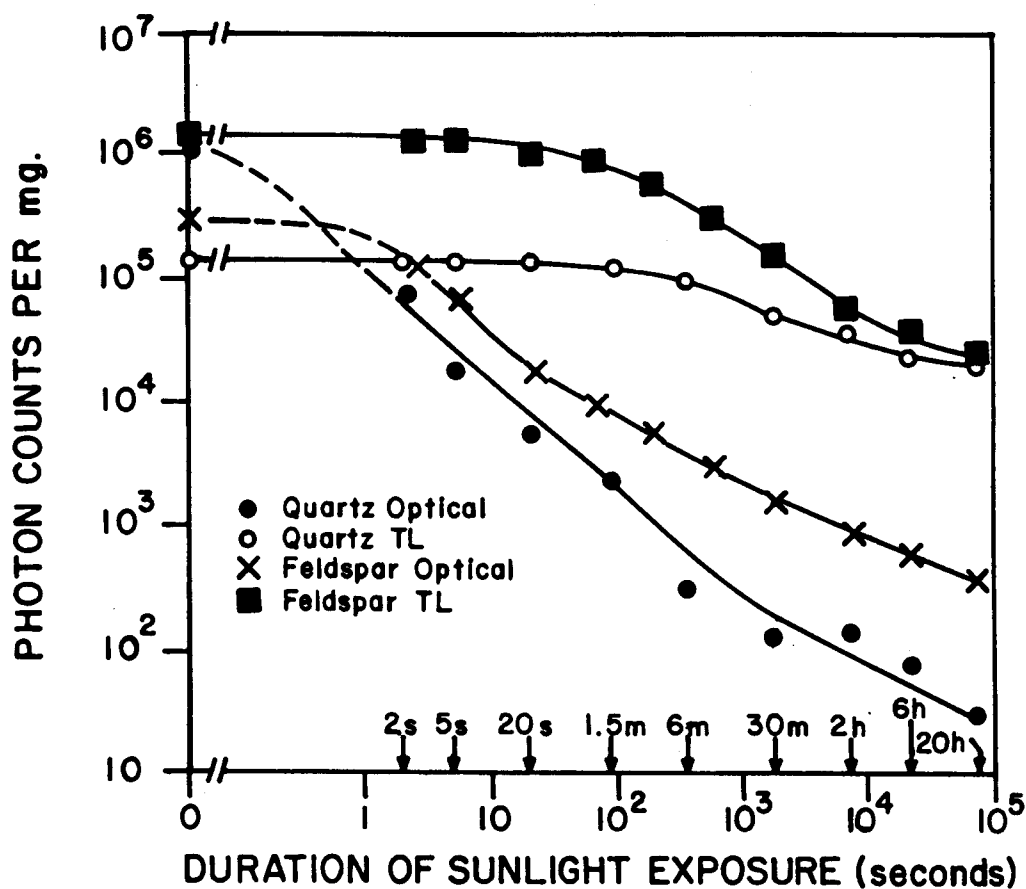


**Fig 4.2** Comparative study of bleaching of quartz and feldspar (after Godfrey-Smith et al, 1988) showing faster bleaching of OSL signal; for OSL, 1% of initial signal was reached for quartz after 10 seconds of sun exposure whereas 9 min were required for a feldspar sample. For TL, exposure time of several hours was needed to reduce the signal. Note reverse sensitivity of minerals to bleaching for OSL and TL.



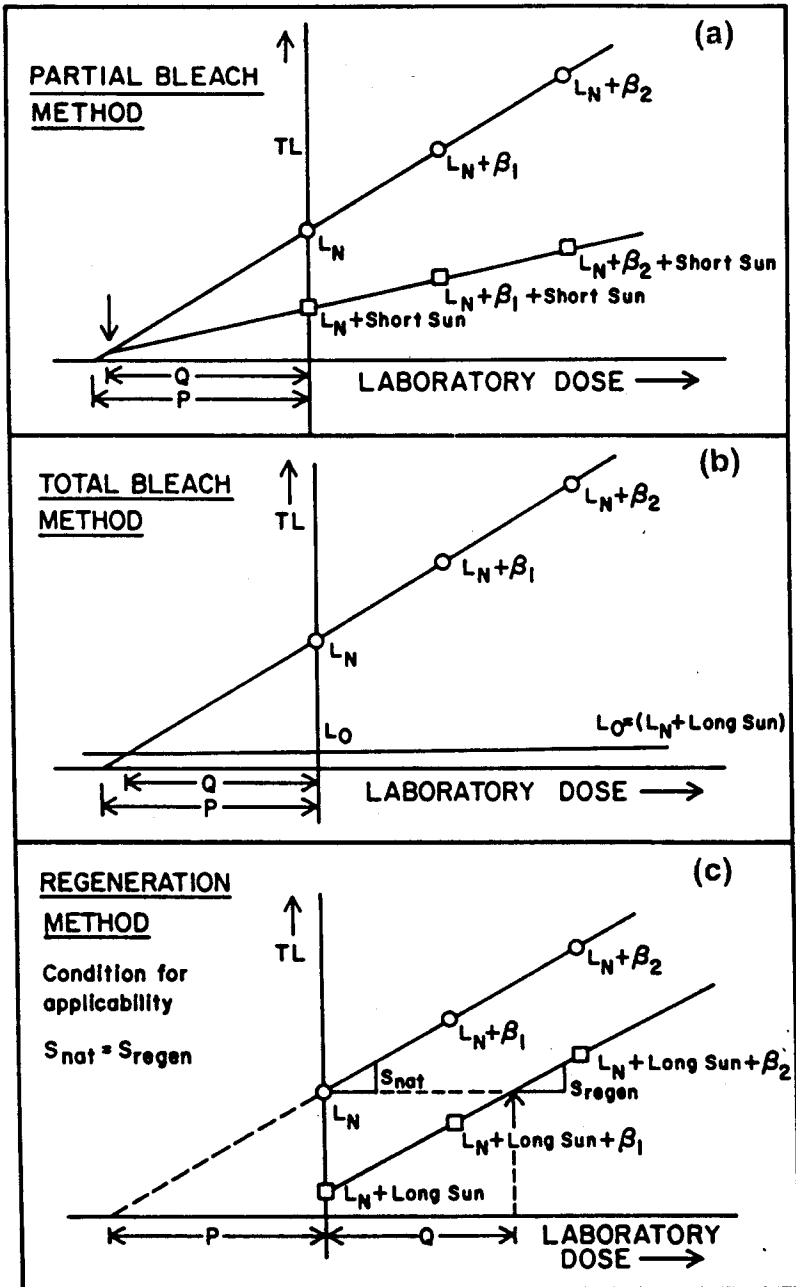


**Fig 4.3** Schematic of methods used in estimation of equivalent dose for sediments. X-axis refers to laboratory dose (after Wintle and Proszynska, 1983).

incremental beta (or gamma) radiation, the samples are additionally given a short sun exposure prior to recording. On the basis that the amount of TL removed by the bleach is a given fraction of the bleachable TL, the intersection of a natural (unbleached) growth curve with the sun bleached curve provides the equivalent dose (Fig 4.3a). The equivalent dose remains unchanged as long as the laboratory sun exposure is smaller than the one received in nature; it increases rapidly once this limit is exceeded.

**2. Total bleach method** (Singhvi et al, 1982): The equivalent dose (ED) is calculated by constructing a TL/OSL growth curve with additive beta or gamma radiation and subtracting from it the residual level (Fig 4.3b) reached after long laboratory light exposure (12 hours), which is presumed to be similar to the level attained prior to deposition.

**3. Regeneration method** (Wintle and Proszynska, 1983): In this method the equivalent dose is determined by comparing the intensity of natural TL signal to the TL signal that is 'regenerated' by laboratory dose on samples which have been sun bleached in the laboratory. The laboratory dose that provides a TL intensity equivalent to that of the natural sample is taken to represent the equivalent dose (Fig 4.3c) provided it is independently established that the laboratory sun bleaching does not alter the luminescence response of the sample. This is checked by comparing slopes of both the additive (obtained by giving incremental beta doses to natural samples) and regenerated (obtained by giving incremental beta doses to sun bleached samples) growth curves. This method is mostly used for well light - bleached aeolian material in which the residual level was reduced to a low level prior to deposition.

### Estimation of dose rate

Dose rate (DR) is a measure of environmental radioactivity of the sediment over a period of time. The estimation of dose rate is generally done using the elemental concentrations of U, Th and K which can be estimated using a variety of physical and radiochemical techniques. The calculated DR is corrected for absorption of alpha, beta and gamma radiation by water in the

sediment. The possible sources of error in DR estimation are (i) long term variations in water content since burial, and (ii) disequilibrium in the decay series. Both of these are discussed subsequently in Section 4.1.4.

In case of OSL, a glance at Fig 4.2 suggests that the time required for zeroing is very short. Thus, in general, most of the sediments can be considered to have been well bleached as far as OSL is concerned. This implies that for OSL dating (Huntley et al, 1985) no correction for residual signal is needed and generally the additive growth curve is sufficient to obtain the equivalent dose. Experimentally, the approach is similar to that in the 'total bleach method' except that no correction for residual level is needed. As the present work was concerned with the dating of fluvial, proximally transported sediments, a brief survey of factors affecting bleaching and dose rate is given below.

#### ***4.1.3 Factors affecting the luminescence signal***

This discussion is structured into two sub themes dealing with: (i) the factors influencing the effectiveness of luminescence zeroing prior to deposition, and (ii) stability of the luminescence signal.

##### **Factors influencing the effectiveness of luminescence zeroing**

For sediments transported and deposited by water, the extent of sun exposure and hence zeroing of geological luminescence depends on a variety of factors as water depth, sediment load, grain size, mineralogy, turbulence and duration of transport of sediments. A brief account of these follows.

**Water depth:** For water laid sediments there is an attenuation of solar spectrum due to absorption by water (Swain and Davis, 1978). Light in the UV to blue region of the spectrum is most effective in evicting electrons from traps but water severely attenuates UV radiation (Jerlov, 1976). Berger and Luternauer (1987), have demonstrated that light intensities at 4m depth in a turbid river are more than  $10^4$  times lower compared to the surface flux and the solar spectrum is severely attenuated below 500 nm and above 690 nm. In

another study involving measurements of underwater spectra for waterlain sediments, Berger (1990), observed that in Lilloet lake (British Columbia), spectra down to 2m are more attenuated at both red and blue ends, with a peak in 560-590 nm range.

**Sediment load:** The net solar spectrum also gets attenuated and shifted towards the red region of the spectral band due to absorption and scattering by solid particulates in water (Jerlov, 1976). The sediment load also varies seasonally. In a study involving measurement of underwater spectra in Fraser river, British Columbia, it was found that, subsequent to a maximum annual discharge in May-June, there was a prominent red component, with a concomitant sharp attenuation of the blue green wavelength. In contrast, during the lower discharge in September, there was proportionately smaller red and larger blue components which have been attributed to differences in relative concentrations of detritus and chlorophyll, (Berger, 1990). In a laboratory experiment, Ditlefson (1992), exposed 2-11  $\mu\text{m}$  size grains to solar spectrum through sediment suspensions (of 75 cm height) for different periods of time. It was found that, for dilute suspensions (0.01-0.02 g/l), more than 50% of the TL signal remained after 20 hours of bleaching but infra red stimulatable luminescence was reduced to 5% in a similar set-up. In more dense suspensions (>0.5 g/l), there was little reduction in either TL or IRSL and bleaching times in excess of 20 hours were needed to reset the luminescence for dating. Thus, the suspended sediments within the water column not only caused spectral attenuation, but also resulted in partial or full filtering of wavelengths between 400-600 nm depending on the turbidity and depth from the surface layer.

**Turbulence:** Laboratory studies (Gemmell, 1985) have indicated that the rate of TL bleaching is inversely related to the speed of flow. Higher flow speeds result in lower photo-bleaching rates and vice versa. This was attributed to the effects of flow turbulence in keeping sediments in suspension, thereby reducing the penetration of UV radiation, and to the re-entrainment of partially bleached or unbleached sediments into the flow.

**Grain size:** Grains in an alluvial deposit may have been derived from different parts of the catchment area, e.g. from soils in the upper part of the catchment area, from actively weathering bedrock or from earlier alluvial deposits being reworked. During transport, different grain sizes are likely to have had different histories of light exposure on account of different sources, length and duration of transport, modes of transport and deposition. Fine grains are carried closer to the top of water surface and settle slowly; these have a greater probability of exposure to a wider spectra and getting bleached. The coarser grains being moved close to the river bed are likely to be exposed only to a restricted spectra (due to the effect of suspended sediment load and greater depth) resulting in insufficient bleaching. It is thus likely that the constituent grains, of different sizes, within the same deposit, may have had different degree of pre-depositional exposure and different residual levels of luminescence at the time of burial. In a study of known age glacio-lacustrine sediments of British Columbia, it was observed (Berger, 1988) that only the fine grained facies (clayey) which were deposited by slow rain out from suspension gave correct ages.

**Mineralogy:** It is now known that different minerals respond differently to photo-bleaching (Bailiff et al, 1977; Debenham and Walton, 1983; Mejdahl, 1985). Comparative studies of bleaching by sunlight for OSL and TL have been reported by Godfrey-Smith et al, (1988). They observed that for OSL, 1% of the initial signal was reached in 10 seconds for quartz and 9 min for a sample of feldspar. For TL, the minerals show a reverse sensitivity to bleaching (Fig. 4.2).

The foregoing discussion clearly shows that in the case of fluvially transported sediments, the extent of zeroing is uncertain. For such a dating effort, the TL partial bleach method which involves a very short sun exposure or OSL method is to be preferred. In cases where both the partial bleach and OSL methods have been applied to the sediments, a general agreement between the two was observed (Duller, 1992; Balescu and Lamothe, 1994; Rao, 1996). As an improvement to partial bleach method, Berger (1990), recommended laboratory bleaching, after blocking the shorter wavelengths. This was successfully used in several instances for dating of partially bleached

sediments. There are exceptions, however, where even the approach of restricted bleaching did not yield meaningful results in the case of known age samples (Berger and Easterbrook 1993; Berger, 1988; Forman and Ennis, 1991).

### *Stability of the luminescence signal*

**Long term stability:** Kinetic studies indicate that the high temperature ( $>250^{\circ}\text{C}$ ) TL signal of feldspar and quartz has a mean life of 1-10 Ma (Aitken, 1985). However, regeneration ages on fine grain fraction of loess from Europe showed an agreement with known ages only up to 50-100ka (Debenham, 1985; Wintle, 1985b). Beyond this, ages were consistently underestimated. Studies on IRSL dating of feldspars also indicated limiting ages (Rao, 1996). Debenham (1985), explained this underestimation in TL ages as being due to time dependent decay of luminescence centres. On the other hand Rendall and Townsend (1988), have attributed the underestimation effect to sensitivity changes resulting from exposure to laboratory light. Efforts have been made to correct the dates assuming a mean lifetime of TL signal (Debenham, 1985; Wintle, 1990).

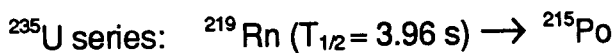
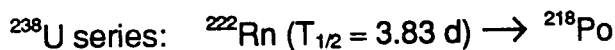
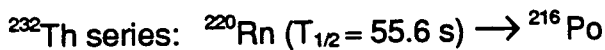
**Anomalous fading:** Some samples exhibit, over a short time, a loss of signal which, on the basis of kinetic considerations, is expected to be stable over a much larger period. This phenomenon, called anomalous fading, was first reported by Wintle (1973). In some cases, loss of TL signal of even 50% over a storage period of one week has been observed. This obviously has important implications for dating as it substantially affects the ages. In particular, it was found that volcanic feldspars can show serious fading (Guerin and Valladas, 1980). The following explanations have been suggested to explain anomalous fading: (i) Tunnelling of charges from traps to recombination centres due to their volume overlap (Wintle, 1973;1977; Visocekas, 1979; Huntley, 1985a). (ii) Templer (1985), explained fading in zircons by suggesting that recombination proceeded via an excited state shared between traps and recombination centres. To facilitate the isolation of stable signal, often a pre-heat at  $150^{\circ}\text{C}$ - $200^{\circ}\text{C}$  for times ranging up to few hours is used.

#### 4.1.4 Factors affecting the dose rate

These are discussed below.

**Water content:** Water in sediments, though itself devoid of radioactivity, absorbs part of the radiation which would have otherwise reached the grains. Thus, the net radiation dose is lower than calculated from the abundance of U, Th and K in the sediment. Therefore, a correction to account for the higher stopping power of water for  $\alpha$ ,  $\beta$ ,  $\gamma$  as compared to air is applied (Zimmerman, 1971). Although the amount of attenuation is calculated using 'as found' values, the variation of water content through geological time and its actual estimation constitute the single largest uncertainty. The saturation level, as determined by the porosity of the sample, sets an upper limit for this effect on age.

**Disequilibrium effects:** Another factor that affects the dose rate estimation is the disequilibrium in the decay series of U and Th. The two elements have long decay chains, involving radioisotopes with significantly different geochemistry. It is likely that given a specific geochemical environment, daughter members may be leached out or precipitated, e.g. U and Th have short lived gaseous member Rn in their decay series, as indicated below,



In each of the above cases, escape of the radon gas is a possibility. This process is speeded up by the action of water (Desai, 1975). If radon is lost then not only is the Rn activity less but activities of all subsequent members are also lower. Escape is more likely with  $^{222}\text{Rn}$  because of its half life of 3.8 days. Others isotopes because of their short half lives are more likely to decay into non mobile daughters before escape. For 100% escape of  $^{222}\text{Rn}$ , there is a 25% decrease in annual dose for fine grains (Aitken, 1985).

There can be other causes of disequilibrium too. Radium may be leached out by the action of ground water. Also, uranium and thorium occur in

nature in tetravalent oxidation state and their ions have similar ionic radii ( $U^{+4}=1.05\text{\AA}$  and  $Th^{+4}=1.10\text{\AA}$ ). Consequently the two elements can substitute extensively for each other. However, under oxidising conditions U forms the uranyl ion (valency +6) which forms water soluble compounds. Therefore, U is a mobile element under oxidising conditions and may be separated from Th which exists only in the tetravalent state and whose compounds are generally insoluble in water. In case of calcium carbonate, U is incorporated at the time of deposition but not thorium. Also, both  $^{230}\text{Th}$  and  $^{231}\text{Pa}$  form insoluble hydroxides so that these are removed from ground water as soon as they are produced. This can result in an excess of  $^{230}\text{Th}$  in river sediments which is found to increase with a decrease in grain size (Scott, 1968).

## 4.2 Present Study

Samples from Nal Sarovar core were dated with OSL method using IR stimulation. The experimental procedures are discussed in Appendix E. A total of 11 samples were dated using IRSL method. Of these, two samples were additionally dated using partial bleach method.

### 4.2.1 Results

The results of luminescence dating are shown in Table 4.1. A few of the typical sample results are shown in Fig. 4.4 and Fig. 4.5. Fig. 4.4 shows the IRSL growth curve for sample N-143. The estimated ED is  $55\pm5$  Gy (Fig 4.4a). Fig. 4.4b shows the IRSL ages for different IR stimulation times. An average age of the sample over the plateau was computed as  $47\pm8$  ka. Similar results are shown for sample N-168 in Fig. 4.5 (a, b).

In some cases, where a sufficient amount of sample was available for processing, coarse grained IRSL dating was attempted; for N-102 ( $150\text{--}250\mu$ ) and N-127 ( $90\text{--}150\mu$ ). The IRSL data for coarse grains, however, showed a large scatter ( $\sim 20\%$ ) between identically treated discs even after normalisation. Similar large data scatter was observed during partial bleach TL dating, using 10min of sunlight bleaching, on  $4\text{--}11\mu$  fraction of samples N-143 and N-102.



**Table 4.1** Results of luminescence and dosimetry measurements on samples from Nal Sarovar core.

Lab. No.	Depth (m)	ED <sup>1</sup> (Gy)	U <sup>2</sup> (ppm)	Th <sup>2</sup> (ppm)	K <sup>3</sup> (%)	$\alpha$ efficiency 'a'	H <sub>2</sub> O in situ (%)	Dose Rate <sup>4</sup> (Gy/ka)	Age <sup>1</sup> (ka)
N-99	3.90-3.93	88±5	1.25±.35	3.29±1.2	0.44	0.07	7	1.365	64±8
N-102	4.27-4.47	198±24	1.86±.55	5.86±1.9	1.17	0.06	7.4	2.501	79±12
N-105	4.77-5.22	257±5	1.4±0.6	6.3±2.06	0.98	0.07	7	2.276	113±8
N-127	9.07-9.20	40±4 (87)	0.78±.33	3.74±1.12	0.29	0.07	7.6	1.091	37±10 (80)
N-143	12.17-12.25	55±5	1.45±.33	3.67±1.13	0.22	0.05	5.8	1.167	47±8
N-167	18.25-18.35	251±18 (272)	1.8±.53	5.09±1.8	0.46	0.06	6.9	1.731	145±9 (160)
N-168	18.35-18.42	156±3	1.37±.26	2.34±.93	0.33	0.07	7	1.138	136±9
N-226	23.81-24.00	165±7	3.33±.84	5.89±2.8	0.59	0.06	12.7	2.372	69±9
N-288	32.78-32.90	227±9	2.86±.62	4.78±2.13	0.56	0.07	16.4	2.160	97±9
N-412	49.95-50.00	202±11	2.21±.56	6.28±1.91	0.47	0.06	9.8	2.00	101±10
N-424	54.65-54.85	156±11	1.89±.43	5.46±1.48	0.27	0.07	5.9	1.705	92±9

1. IRSL data for fine grained fraction. The figures in brackets indicate the values obtained using TL partial bleach (10min) method.
2. Measured by  $\alpha$  counting.
3. Measured using Atomic Absorption Spectrometry.
4. The dose rate has been calculated using an average value of 'as found' and saturation water content.

# SAMPLE NO. N-143

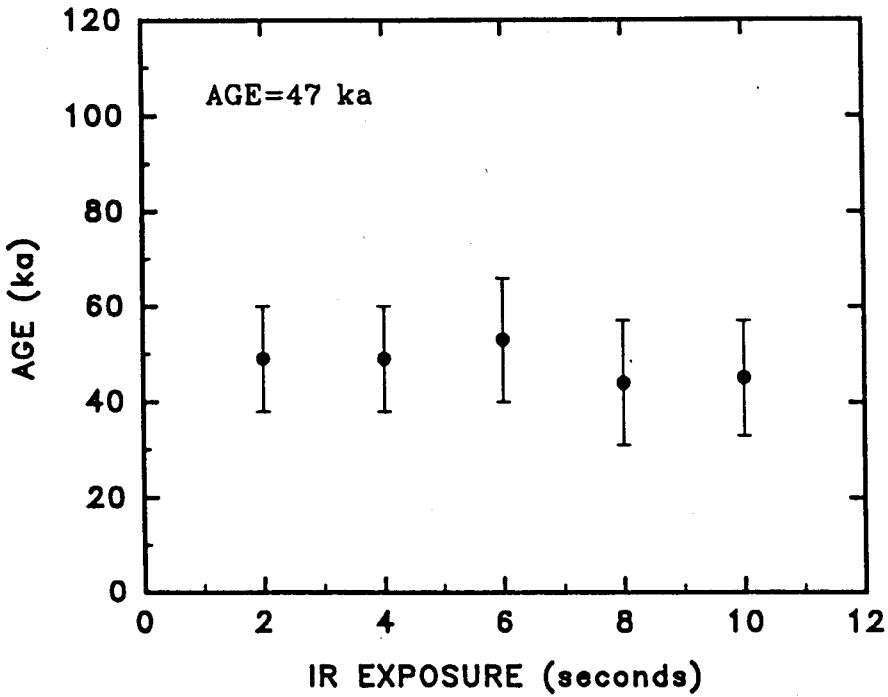
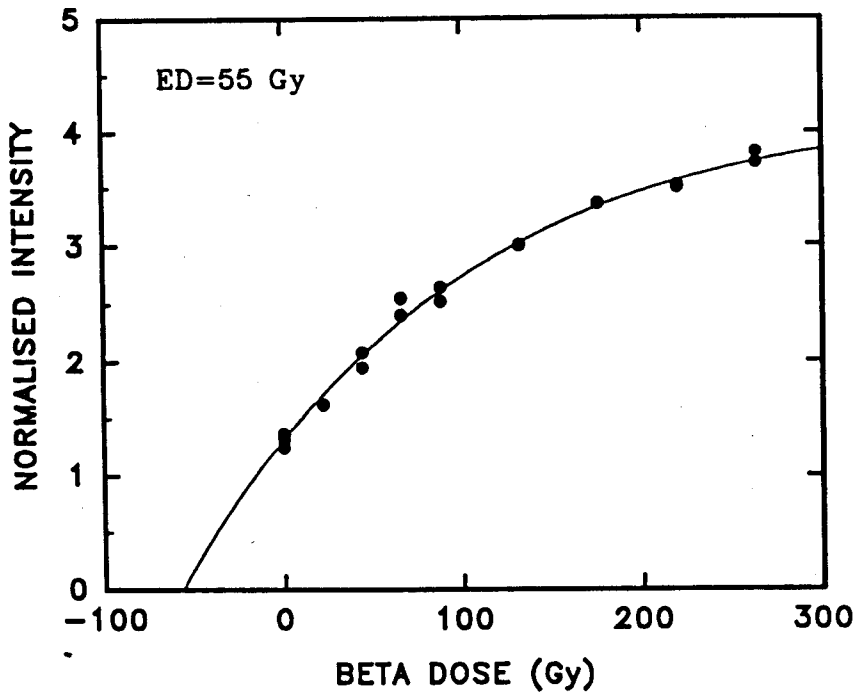
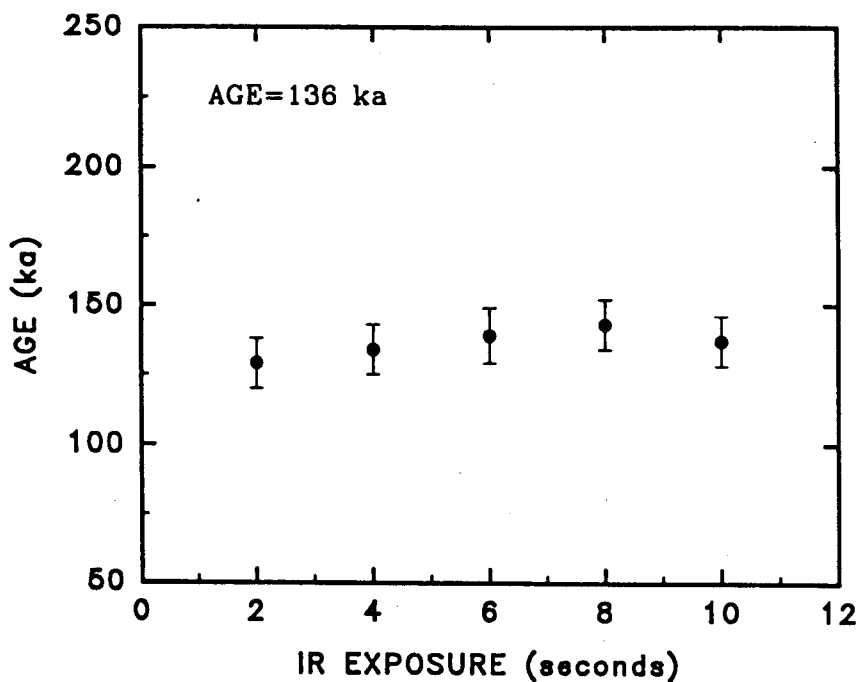
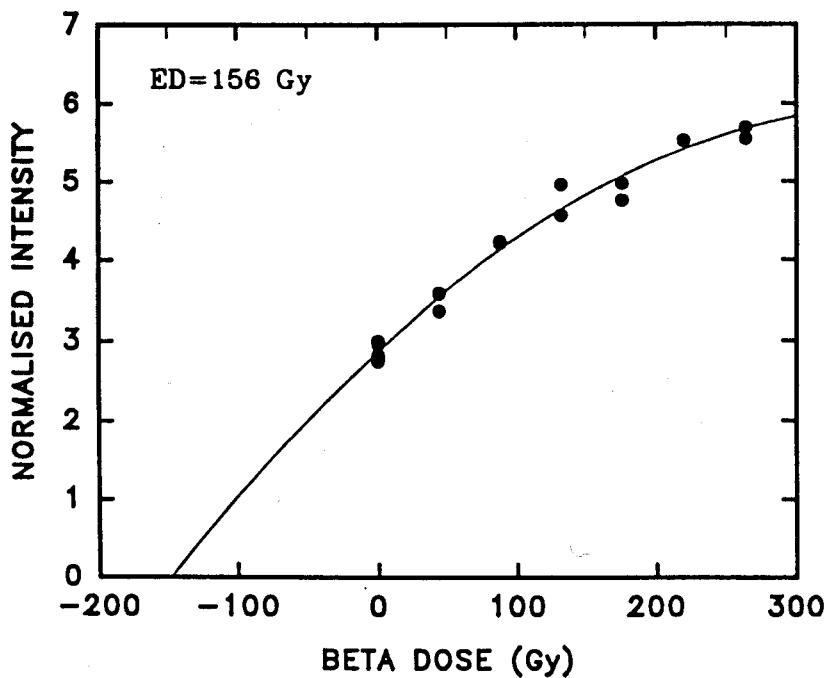


Fig. 4.4 IRSL growth curve and age plateau for N-143. Also indicated are the mean values of ED and age.

# SAMPLE NO. N-168



**Fig 4.5** IRSL growth curve and age plateau for sample N-168. Also indicated are the mean values of ED and age.

This indicated that these samples contained a mixture of grains that were exposed to sunlight for very different periods of time. This could occur if, (i) distance of transport was very short or (ii) aeolian (well bleached) sediments were mixed with fluvial (partially bleached) sediments. When such samples are irradiated in the laboratory, the grains, being on different parts of their growth curves will show a large scatter in the TL/IRSL (Duller, 1994).

Both well bleached (dunes to east and north-east) and partially bleached (fluvial sediments to east) sediments could have acted as source for Horizon-2, of Nal Sarovar core, based on heavy mineral analysis (Section 2.2.3). But since the dunes were formed from reworked fluvial material, it is not possible, at this stage, to say which/both of these possibilities, namely, short distance transport or multiple sources could have caused the observed scatter in luminescence data.

The IRSL ages, on fine grained (4-11  $\mu\text{m}$ ) fraction of various samples studied, and their depths are graphically shown in Fig 4.6. An increase in dates with depth is observed though some samples give dates that do not follow the general trend line. The salient features of this study are discussed below.

#### **4.2.1.1 Salient features of results**

1. The samples in the sand layer (Horizon-2) showed a large scatter with some dates higher than the stratigraphically older Horizon-3 (Fig. 4.6). Also, the IRSL age of  $79 \pm 12$  ka at 4m depth is inconsistent with the radiocarbon age of  $\sim 7$ ka (Section 3.2.2) obtained on the organic matter at  $\sim 3$ m depth. This is because Horizon-2 grades into Horizon-1 and there is no evidence of a hiatus between the two.
2. An apparent saturation effect is visible in dates for Horizon-3, with the dates at  $\sim 32$ m and below hovering around  $\sim 90$  ka.
3. Partial bleach TL dates, on 4-11 $\mu$  size, with bleaching time of 10min, could be calculated for two samples in Horizon-2. The sample at 9m (N-127) depth

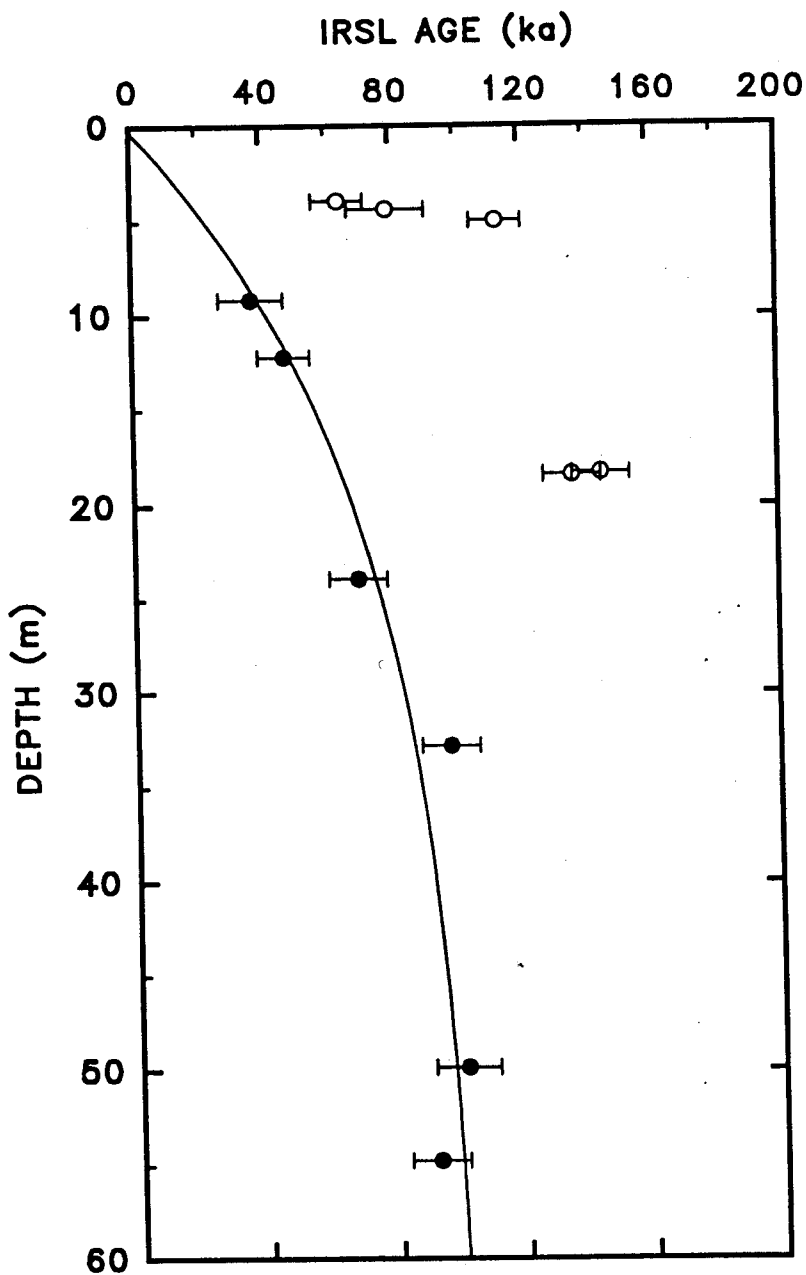


**Fig 4.6** Variation of IRSL dates with depth in Nal Sarovar core. The open circles represent the anomalous dates (see text for discussion). The filled circles represent the dates used for interpolation.

gave a partial bleach date of  $\sim 80$  ka which is higher than the IRSL age of  $37 \pm 10$  ka. Fig. 4.7 gives the results of partial bleach dating of the sample N-127. The TL glow curves for this sample are shown in Fig. 4.7a for different treatments of the sample i.e. N, N+S(10 min), N+220 $\beta$ . The additive and partial bleach growth curves at 340°C are shown in Fig. 4.7b. The age was estimated from the ED vs. temperature plot (Fig. 4.7c) over the plateau region 310°C to 350°C. Another sample at  $\sim 18$ m depth (N-167) was also TL dated using ten minutes partial bleach. It gave a partial bleach date of  $\sim 160$  ka which is comparable to the IRSL date of  $145 \pm 13$  ka. Even though there appears to be an agreement between the IRSL and TL dates for the sample N-167, this date does not fit into the sequence. It appears that the sample at  $\sim 18.3$ m depth (N-167), had undergone little pre-depositional sun exposure and it is likely that these dates correspond to an older event prior to deposition in NaI. In contrast, the sample at  $\sim 9$ m (N-127) depth had been partially exposed to sunlight (probably a restricted spectrum) which, though sufficient to zero the geological IRSL, was not adequate to reset the geological TL.

An attempt was made to identify the cause of observed scatter in the IRSL dates on fine grained samples in the sand horizon (Fig. 4.6). In the earlier Section (4.1), it was noted that the age estimation could be affected by any one or more of the following: (a) anomalous fading, (b) disequilibrium in decay series, (c) variation in water content subsequent to burial and (d) insufficient zeroing of geological luminescence prior to deposition.

#### **4.2.1.2 Tests for anomalous fading and disequilibrium**

Tests on the samples (see Appendix E) with a storage of 3 months indicated an absence of anomalous fading. A typical anomalous fading test is shown in Fig. 4.8. It is seen that identically treated sample aliquots show, within narrow limits of scatter, no fading of signal even after 3 months storage.

Gamma spectrometry using HPGe detectors was undertaken to check for disequilibrium in the decay series of U and Th (see Appendix E). Disequilibrium was found to be absent in all cases. Only for samples N-167 and

# SAMPLE NO. N-127

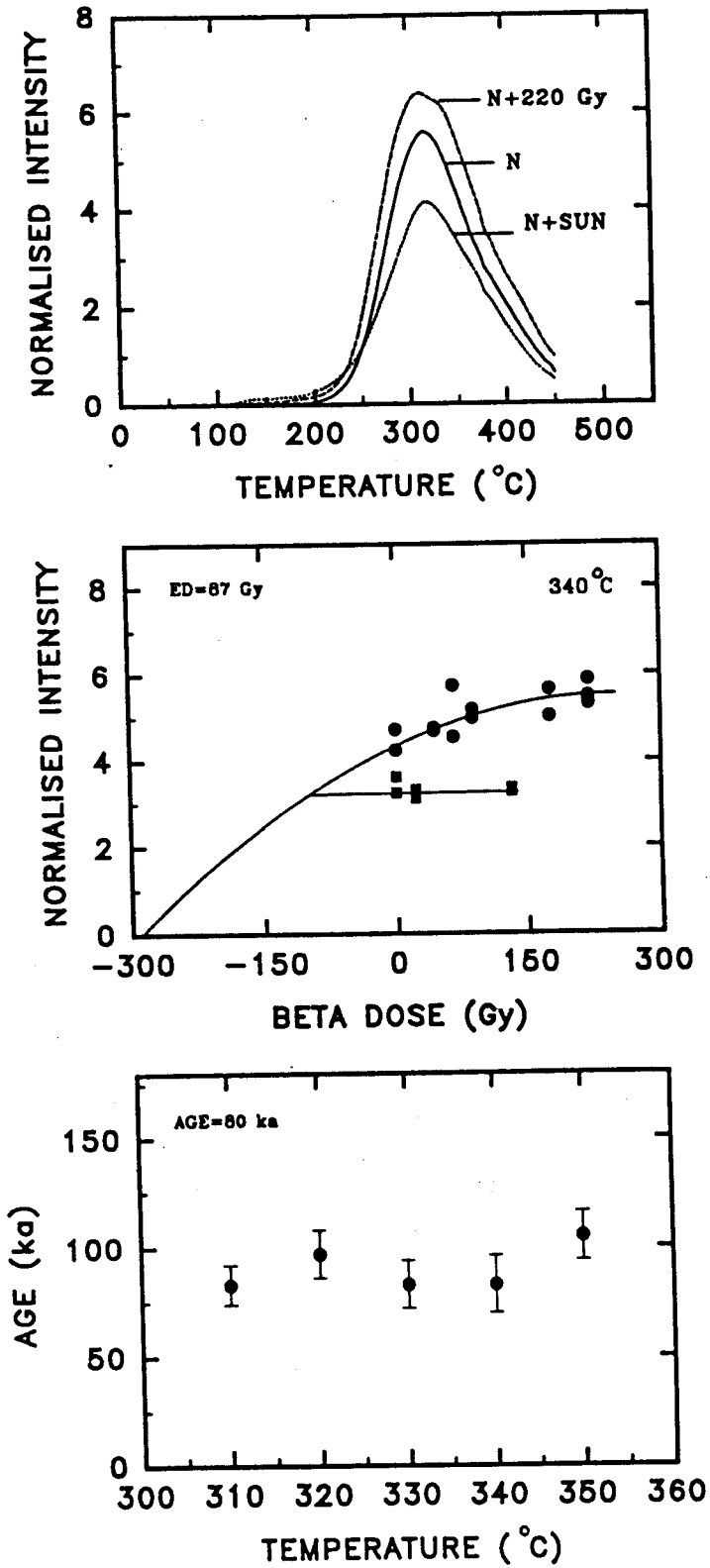
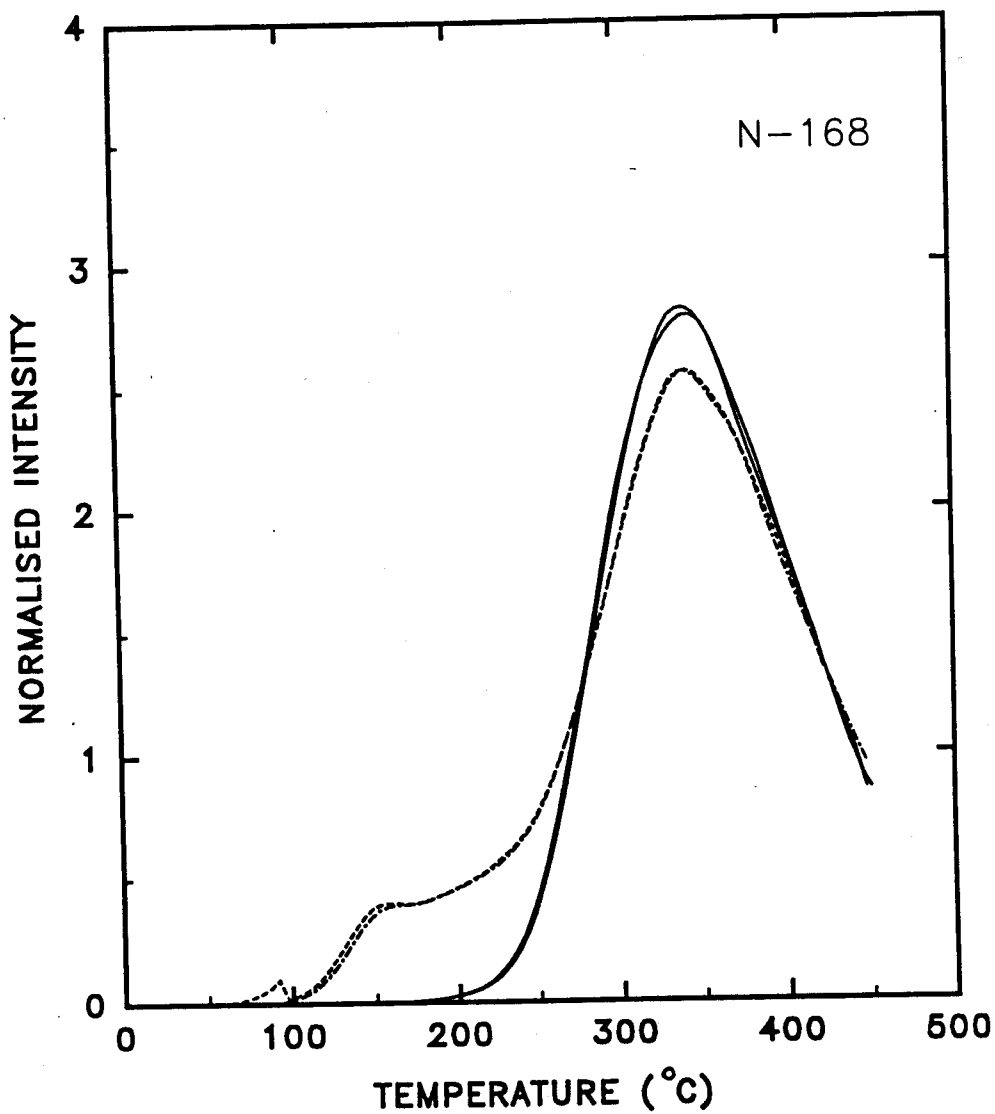


Fig 4.7 (a) Glow curves, (b) growth curves and (c) age plateau, for partial bleach dating (10 min sun exposure) of sample N-127.



**Fig 4.8** Result of anomalous fading test on a typical sample. The dashed lines show the TL of two aliquots immediately after irradiation of 44Gy. The continuous lines show the TL record of two other aliquots of the same sample similarly irradiated 3 months previously.



N-424, there is a small difference in the U concentration as determined from peak intensities of  $^{235}\text{U}$  and  $^{214}\text{Bi}$  (Table 4.2); the two values, however, do not affect the IRSL dates significantly to explain the scatter.

#### **4.2.2 Discussion**

Saturation water content was determined for samples, one each from the sandy layer (16%) and silty clay layer (30%). A correction for dose rate, using saturation water content, was found insufficient to explain the observed anomaly in the IRSL age data beyond 20%.

The anomalous higher IRSL dates are confined to the sand horizon which was deposited by a high energy transporting regime. As discussed in Section 4.1.3, in case of transport in a dense suspension and/or turbulent transport, there is very little reduction of either TL or IRSL. Insufficient zeroing of the geological signal for such samples is a possibility. Such a possibility in the case of Nal core samples was also indicated by the scatter in the coarse grained IRSL and fine grained partial bleach data of sediments from Horizon-2. Also, in the present case, an indication of higher energy of transporting medium was found in the coarser sand size of the samples showing anomalous ages as compared to the samples which lie on the trend line (Table 4.3).

To the east of Nal lies the Cambay Graben which is known to have experienced tectonic activity during the Late Quaternary (Sareen et al, 1993; Sridhar et al, 1994). The heavy mineral assemblage of the sand layer is typical of a mixed granitic and/or metamorphic provenance indicating that the source area for sand in the 4-18m layer, at least, has remained confined mainly to the east and north-east of Nal Sarovar. A tectonically induced uplift in the Cambay Graben would result in the rejuvenation of the rivers which then begin to downcut previously deposited sediments. It is also possible that the sediments showing anomalous dates are reworked older samples which were deposited

**Table 4.2** Estimation of U and Th on samples from Nal Sarovar core by  $\gamma$  counting in different parts of decay chain. Also given are the estimates from  $\alpha$  counting.

Lab No.	U (ppm) - $\gamma$ spectrometry				Th (ppm) - $\gamma$ spectrometry					U (ppm)	Th (ppm)
	$^{235}\text{U}$ (185)*	$^{214}\text{Pb}$ (295)*	$^{214}\text{Bi}$ (609)*	$^{214}\text{Bi}$ (1120)*	$^{212}\text{Pb}$ (238)*	$^{208}\text{Tl}$ (583)*	$^{228}\text{Ac}$ (338)*	$^{228}\text{Ac}$ (911)*	$^{228}\text{Ac}$ (968)*	$\alpha$ counting	$\alpha$ counting
N-99	1.15	1.43	1.37	1.33	4.98	4.94	4.94	4.73	4.01	1.25 $\pm$ 0.35	3.29 $\pm$ 1.2
N-102	1.56	1.4	1.62	1.54	6.4	6.8	7.33	7.19	6.32	1.86 $\pm$ 0.55	5.86 $\pm$ 1.90
N-105	1.43	1.54	1.5	1.35	5.3	5.17	5.15	5.27	4.23	1.40 $\pm$ 0.6	6.30 $\pm$ 2.06
N-143	1.16	1.15	1.28	1.15	3.6	3.44	3.59	3.31	3.27	1.45 $\pm$ 0.33	3.67 $\pm$ 1.10
N-167*	1.52	1.88	1.83	1.99	2.2	2.5	2.2	2.54	2.51	1.8 $\pm$ 0.53	5.09 $\pm$ 1.80
N-226	1.88	2.04	2.01	1.66	9.08	8.88	10.43	10.21	9.07	3.33 $\pm$ 0.84	5.89 $\pm$ 2.80
N-288**	1.74	1.78	2.03	2.39	10.81	11.11	13.26	11.91	10.79	2.86 $\pm$ 0.62	4.78 $\pm$ 2.10
N-412	1.87	2.06	2.32	2.18	10.47	10.88	12.6	10.68	10.11	2.21 $\pm$ 0.56	6.28 $\pm$ 1.90
N-424	1.45	1.84	1.81	1.87	6.7	6.83	7.38	6.79	7.04	1.89 $\pm$ 0.43	5.46 $\pm$ 1.50

Errors in measurement are 10%.

\* Numbers in brackets indicate the energy (keV) of  $\gamma$  emitted by the isotope.

\* Th is underestimated by  $\gamma$  counting. IRSL age from Th ( $\gamma$ ) is 173ka as compared to IRSL age of 145ka from Th ( $\alpha$ ).

\*\* Th is overestimated by  $\gamma$  counting. IRSL age from Th ( $\gamma$ ) is 80ka as compared to IRSL age of 97ka from Th ( $\alpha$ ).

**Table 4.3** Mean grain size of samples from sandy horizon that have been dated by the luminescence method.

Lab No.	Mean size	Sediment type	Measured IRSL date (ka)	Estimated* IRSL date (ka)
N-99	0.86 $\phi$	coarse sand	64	18
N-105	0.93 $\phi$	coarse sand	113	23
N-127	1.33 $\phi$	medium sand	37	38
N-143	1.16 $\phi$	medium sand	47	48
N-167	0.93 $\phi$	coarse sand	145	65

\* Estimated from best fit to the minimum IRSL age vs depth data.

by flood events; these were inadequately zeroed prior to deposition and hence reflect older ages. Evidence of older exposed deposits, found in cliffy sections; entrenched rivers and fault controlled river courses, have been reported (Sridhar, 1995; Tandon et al, 1996).

Thus, in view of (i) absence of anomalous fading; (ii) absence of disequilibrium in the samples, and (iii) the possibility of inadequate pre-depositional zeroing, the minimum dates consistent with stratigraphy have been accepted. The dates of intermediate samples have been obtained by interpolation between the accepted dates. With this assumption, the measured IRSL age of the red bed at 12m depth in Nal Sarovar core is 47 $\pm$ 8 ka. This is in agreement with the TL/OSL age 58 $\pm$ 5 ka of similar red bed found at Vijapur near Ahmedabad (Tandon et al, 1996). This is significant since this red bed has a regional occurrence and is used as a marker horizon (Pant and Chamyal, 1993) for Late Quaternary deposits in Gujarat. The interpolated date of the sample at 18m depth is ~65 ka indicating an age of >65 ka for underlying Horizon-3 which fits in fairly well with the >73ka (isotope stage 5 age) assigned

to this deposit on the basis of field evidence. Since all the dates below 32m hover around ~90ka, it is likely that this feature is due to luminescence saturation effect (see Section 4.1.3). The age determined for sample at ~54m depth (sample no. N-424) is  $90 \pm 12$  ka which is likely to be older as it has been underestimated to some extent due to luminescence saturation effect.

## **CHAPTER 5**

### **SUMMARY, SYNTHESIS AND FUTURE PERSPECTIVES**

This study was carried out with the dual objectives of understanding the evolution of Nal region, in terms of an interplay of regional tectonism and eustatic sea level changes, and to decipher its Holocene palaeoclimatic history. The Nal region is important because it lies within the palaeo-Thar margin and is a potential site for palaeoclimatic investigations. Owing to its low elevation, proximity to the Gulfs of Kachchh and Khambhat, and also to the tectonically active Cambay Graben, it is likely that both eustatic sea level changes and tectonism have played a role in the evolution of this region. It was, therefore, essential to reconstruct the evolutionary history of this region to provide a framework for any future study.

As described in the previous chapters, a variety of techniques including remote sensing, subsurface lithological correlation, sedimentological and mineralogical analyses, radiocarbon and luminescence dating, were used to decipher the evolutionary history of the region. For palaeoclimatic reconstruction,  $\delta^{13}\text{C}$  and C/N ratio analyses on organic matter were also carried out.

In the following, the salient results of various studies are first summarised. This is followed by a synthesis of all the data to reconstruct an evolutionary model for the Nal region. Within this framework, palaeoclimatic reconstruction for the past ~7ka, using  $\delta^{13}\text{C}$  and C/N, is also presented.

## **5.1 Summary**

The salient results of this study, using various techniques, are summarised below,

### ***5.1.1 Remote sensing and field studies***

1. Rivers on the western, Saurashtra side, have large valleys though the present flow through them is seasonal.
2. On the Saurashtra side, evidence of the last major interglacial transgression was found in the form of inland deltas. The palaeo-strandline is, presently, at  $\sim +15\text{m msl}$ .
3. There is no evidence of any major uplift, in the delta region, subsequent to delta formation.
4. Several abandoned river channels were found to the east of the Nal region.
5. Evidence of Holocene transgression was found as older mud flats on both the western (Saurashtra) and the eastern (Ahmedabad) side of Gulf of Khambhat.
6. Deranged drainage pattern was found in older mud flats.

### ***5.1.2 Sub surface lithological studies***

1. The lithology on the eastern side of the Nal region was dominated by sand with intercalations of clay/silty clay.
2. In the vicinity of Nal Sarovar, and in the N-S direction, extending from the Little Rann of Kachchh to Dholera near the Gulf of Khambhat, a change in lithology to a layer of sand (5-35m) underlain by a thick sequence (40-55m) of clay/silty clay was seen.
3. In the Nal region, the RL of the top and bottom of sand layer varies from +14 to -30m, while that of the underlying silty clay layer is +3m to -75m.

### **5.1.3 Core studies**

1. The core raised from Nal Sarovar comprised of three horizons: Horizon-3 (54-18m), Horizon-2 (18-3m) and Horizon-1 (3-0m). The base of Horizon-3 was not reached in the core.
2. Horizon-3 comprised of silty clay/clayey silt, Horizon-2 was dominantly sand and Horizon-1 comprised silty clay/clay.
3. Mineralogical studies indicated the source of sediments in Horizon-3 to be from south and/or west; Horizon-2 and Horizon-1 to be dominantly from east.
4. Radiocarbon dating on organic matter indicated the age, of the base of Horizon-1, to be ~7ka. Carbonate nodules from 16m depth and below gave  $^{14}\text{C}$  date of >38ka. IRSL dating indicated that Horizon-2 was deposited between 7--65 ka. Based on IRSL dating and other studies, the deposition of Horizon-3 was assigned to oxygen isotope stage 5.
5. Stable isotope ( $\delta^{13}\text{C}$ ) and C/N studies indicated the climate to be drier than present between ~6.6-6ka. From 6-4.8ka, while the overall climate was dry, the rainfall was inferred to be more evenly distributed. The climate was wetter than present in the period 4.8-3ka. From 3ka, the trend towards aridity began and present day conditions were established around 2ka.

## **5.2 Synthesis**

Based on the results of various investigations carried out, as described in previous chapters and summarised above, it is possible to develop a model for the geomorphic evolution of the region covering the entire low lying tract between the Gulf of Khambhat and the Gulf of Kachchh including the Nal Sarovar.

## **5.2.1 Geomorphic evolution of Nal region**

### **STAGE 1**

During the last major interglacial when the sea level was higher, a shallow sea linked the Gulf of Khambhat with the Gulf of Kachchh. The palaeo-deltas and the palaeo-strandline observed to the west of Nal Sarovar (upto 30km inland, at ~+15m msl respectively) were formed during the period of last major interglacial transgression (isotope stage 5e, ~125ka). At that time, and also during the entire isotope stage 5 (127-73ka), the low lying Nal region was covered with a shallow sea having a dominant input of sediments from the Saurashtra peninsula and/or Gulf of Khambhat. The presence of smectite as a dominant (>70%) mineral phase in the sediments of Horizon-3 implies that the sediment input, at the present location of the Nal Sarovar, from the eastern side was small. This, probably, was due to the depositional front of the rivers draining the north and central Gujarat being farther east in the Cambay Graben. There may have been breaks in the sediment deposition, during the sub-stages of isotope stage 5, linked to the fall of the sea level. The IRSL dating, however, suggests that the deposition of the silty clay (Horizon-3) in this region ceased when the sea level finally dropped at the beginning of isotope stage 4. Owing to the limitations of the dating methods available, it has not been possible to give a more precise time of break up of this connection.

A schematic representation of the geography of the Nal region during last major interglacial transgression is given in Fig. 5.1.

### **STAGE 2**

With the lowering of base level, the depositional front of fluvial input from the east, probably also aided by tectonic uplift in the region of Cambay Graben, could now advance westwards. This is suggested by the presence of a layer of sand (Horizon-2), with its source in the east, as confirmed by the characteristic



STAGE - I

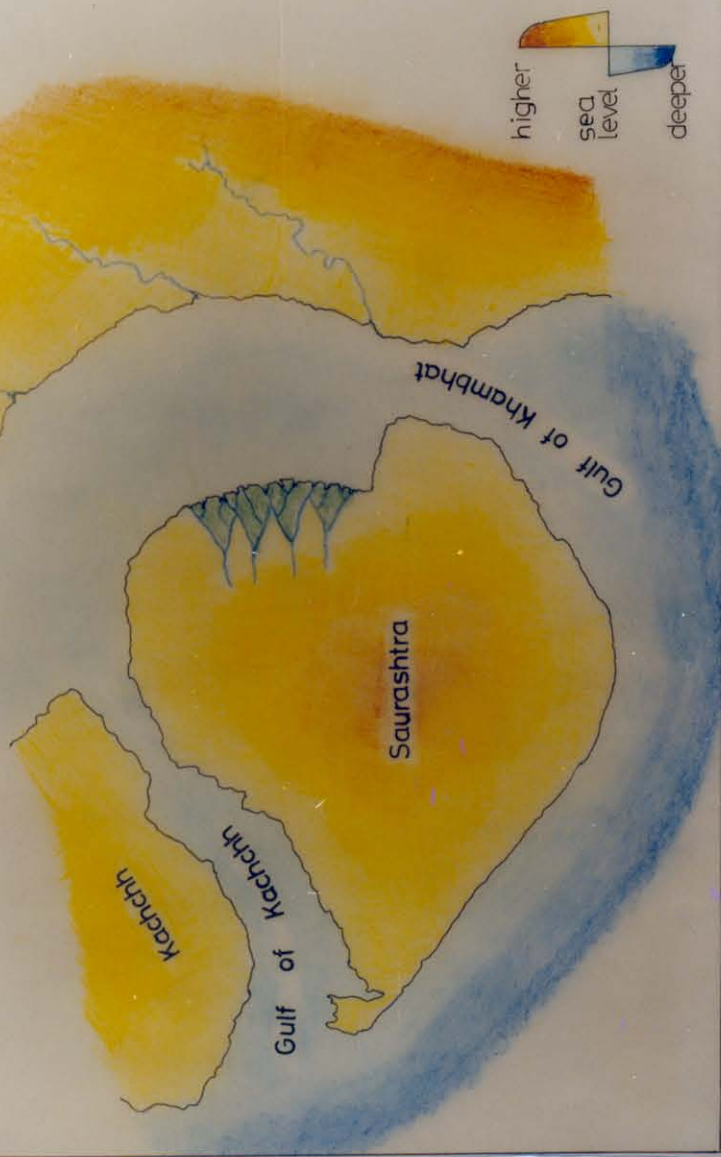


**Fig. 5.1** Schematic representation of geography of the Nal and surrounding regions during the period of last major interglacial transgression (in Stage 1 of evolution of Nal region).

heavy mineral assemblage. The thickness of this layer varies from 5-35m, increasing towards the southern part of the Nal region. The deposition of sand was not continuous as is indicated by the presence of a red bed and evaporite minerals. This sedimentary material was most likely brought in by flash floods and had little sun exposure so that the TL/OSL signal from the previous depositional history was not erased. Alternatively, it is possible that the region to the east of Nal Sarovar was tectonically uplifted some time subsequent to the deposition of Horizon-3 and pre-existing sediments from farther east were rapidly eroded and redeposited in the low level narrow land corridor, that still remained, linking the Little Rann of Kachchh and the Gulf of Khambhat. It may be noted that the Cambay Graben lying to the east of Nal Sarovar was topographically the lowest elevation and had acted as a sediment sink at least until the Miocene. Presently, this area has a surface elevation of +80 m to +100 m and the low elevation area has shifted to Nal Sarovar which is +13 m to +16 m msl. Evidences of Late Quaternary tectonism in the Cambay Graben has been reported in the form of entrenched rivers, cliffy sections, fault controlled river courses.

The Stage 2 of evolution of the Nal region spans the interval ~73-7ka. A schematic representation of the geography of the Nal region, during the LGM, is given in Fig. 5.2.

### **STAGE 3**

As a result of the combined influence of (i) westward advance of the sedimentation front; (ii) tectonism and; (iii) the post glacial sea level rise, the Nal Sarovar came to within a few metres of its present elevation at about 7ka when it became a closed basin. The present Nal Sarovar, therefore, originated as a result of westward advance of the sedimentation front until it could no longer advance due to the presence of high land of Saurashtra. At that time either due to sedimentation process alone or aided by tectonism, the west flowing rivers shifted their courses and presently only the abandoned channels remain. The present day rivers are entrenched in their courses indicating the role of tectonism. Other studies also indicate that the present river

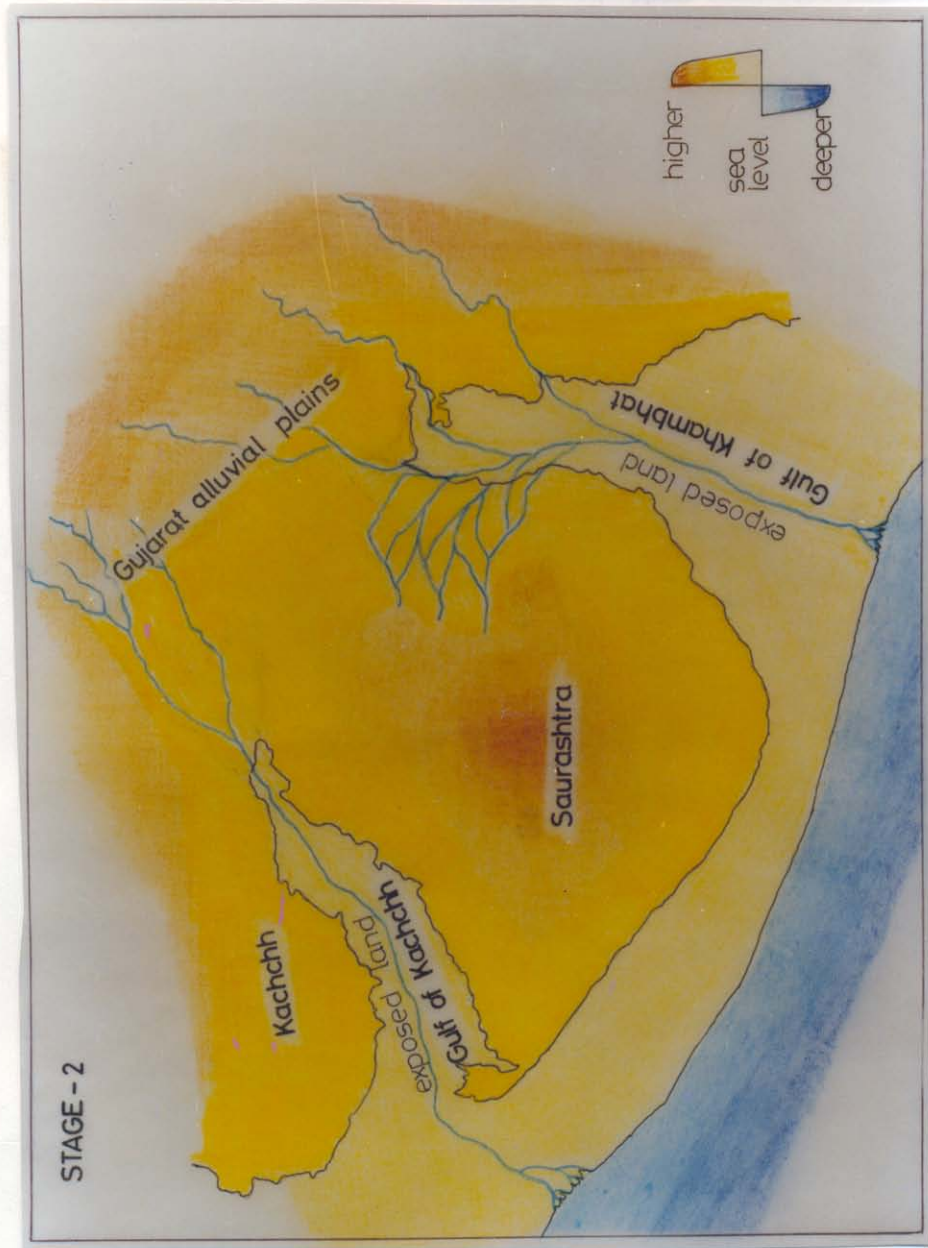


**Fig. 5.2** Schematic representation of the geography of the Nal and surrounding regions during the period (~18ka BP) of last glacial maximum (LGM) regression (in Stage 2 of evolution of Nal region)

courses may have been acquired during the Late Quaternary. The mud flats, present to the south of Nal, represent the Holocene transgressions in the area.

A schematic representation of the geography of the Nal region during the Holocene transgression is given in Fig. 5.3.

In view of the distance, and elevation difference, that separates the Nal region from the reported exposed sections in Sabarmati, Mahi and Narmada rivers, as also the limitations of working with a core, it is difficult to establish correlation of these sections with the Nal region, particularly in view of limited chronological control. It was, however noted in Chapter 2 (Section 2.2.3.1), that red beds were encountered in the Nal core between 10-14m. The IRSL dating of a sample (N-143) at ~12m depth in the core gave a date of  $47 \pm 8$  ka. This is to be compared with the TL/OSL date,  $58 \pm 5$  ka, of a similar red bed found at Vijapur, near Ahmedabad. It is significant since this red bed has a regional occurrence and has been used as a marker horizon for Quaternary alluvial sediments. In view of the limited available chronological data, both from river sections and the Nal region, it maybe premature to attempt detailed correlation at this stage.

### ***5.2.2 Palaeoclimate of Nal region during last 7ka***

The  $\delta^{13}\text{C}$  and C/N ratio of the organic matter (Horizon-1), that was deposited in the Nal Sarovar basin, provide a qualitative picture of the palaeoclimatic variations in the region. The studies indicate that the period from ~6.6-6ka was generally drier than present with the exception of a short wet phase around 6.2ka. From 6-4.8ka the rainfall was lower than present but more evenly distributed, probably as a result of a slight increase in winter rainfall. From 4.8-3ka the climate was wetter than present. The trend towards aridity began around 3ka and present day conditions set in ~2ka BP. This picture is somewhat different to the one deciphered by earlier workers from Rajasthan lakes for the period 6.5-4.8ka when, in opposition to the wetter climate in Rajasthan, the climate here was drier. From 4.8ka to present however the climatic changes in this region are similar to those in Rajasthan. Also, a general agreement between periods of glacier expansion in Eurasia and drier periods in



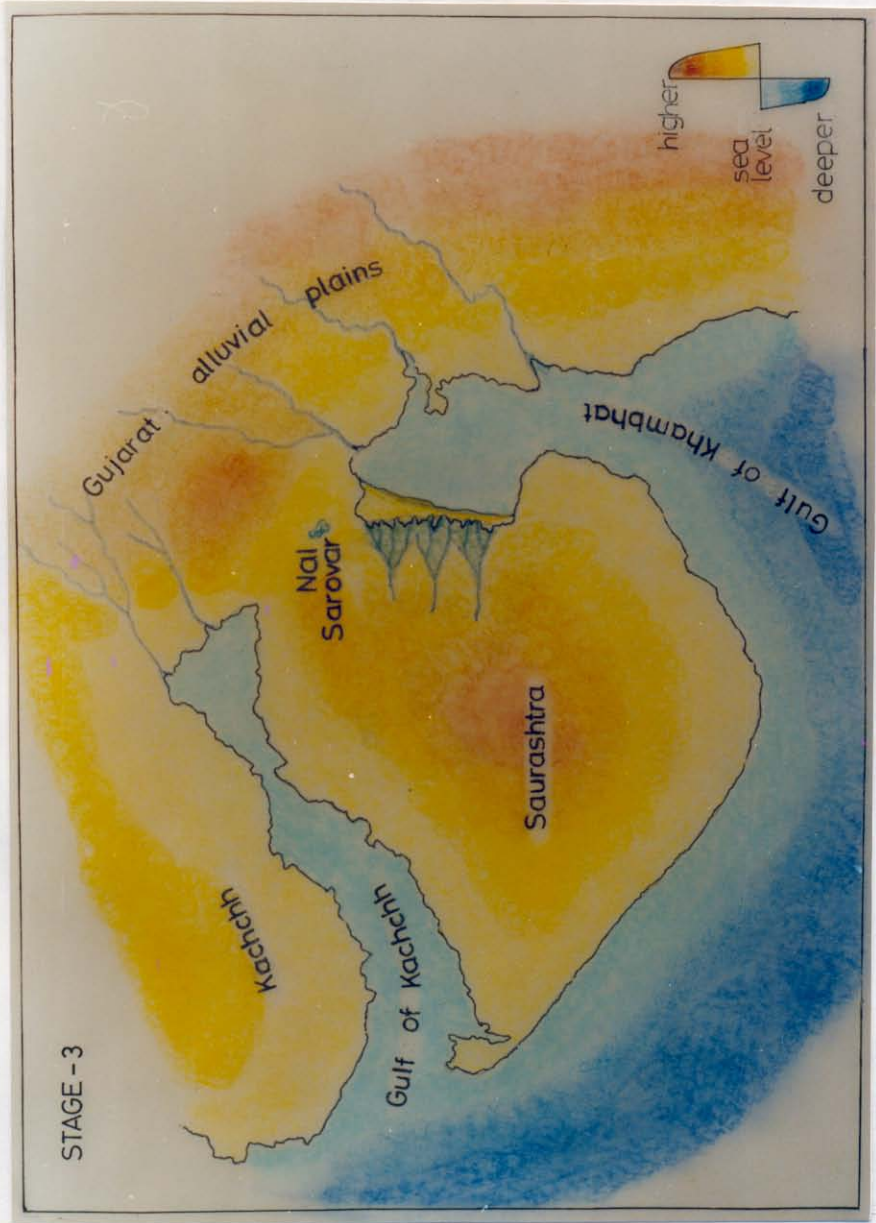


**Fig. 5.3** Schematic representation of the geography of the Nal and surrounding regions during the period (~5ka BP) of Holocene transgression (in Stage 3 of evolution of Nal region)

Nal Sarovar is observed. This suggests that the palaeoclimatic record from Nal is a regional feature.

### **5.3 Future perspectives**

This thesis has yielded an understanding of the interplay of eustasy and tectonism in the evolution of Nal region and has provided a framework for further work in this region. Some of the studies were beyond the scope of the present work as they require extensive investigations, but need to be pursued later, are listed below:

- \* The amount of organic material in these sediments was small and obtained radiocarbon dates for much of the sequence were beyond the normal radiocarbon dating range. Therefore, recourse was taken to luminescence dating. In some samples, insufficient bleaching of sediments and in some others saturation effects were identified. The ages of different horizons and events in the evolutionary history of the region, therefore, had to be inferred through a combination of  $^{14}\text{C}$ , TL/OSL dating, geomorphological data and globally established chronology of sea level variations.

More studies are required for further validating the chronology using a variety of approaches e.g., dating of different minerals, OSL partial bleach and TL partial bleach using restricted spectrum for bleaching.

- \* There is also a need to establish a more definitive chronology for the inland deltas. The limited field work undertaken during this study did not yield any suitable radiocarbon or uranium/thorium series dating material. TL/OSL was not attempted keeping in view the difficulties faced earlier.
- \* Additional drill cores, in the Little Rann of Kachchh through Nal Sarovar to Gulf of Khambhat corridor, have been raised to study the facies variation through grain size and mineralogical variations in this corridor. As expected, the lithological sequence is similar to the Nal Sarovar core. Detailed investigations on these cores are needed.

No fossils have been found in the  $>63\mu$  size fraction even in the Horizon-3 which, based on the considerations of sedimentology, mineralogy, eustatic sea level changes, chronology and stratigraphic correlation has been inferred to have been deposited in a shallow sea linking the Little Rann of Kachchh and the Gulf of Khambhat. The study of microfossils ( $<63\mu$ ) on this core as well as the others raised may prove useful.

As the marine sediments have a higher concentration of boron in comparison to terrestrial sediments, such studies need to be carried out on the sediments from Horizon-3 to confirm their marine origin.

## **APPENDIX A**

### **Sampling Procedures**

Following types of samples were collected for this study:

1. Samples from surface sediments and exposed sections.
2. Samples from trenches.
3. Samples from Nal Sarovar core.

All the samples were labelled and sealed in the field, with the records maintained in a field log book. Locations of these samples were marked on copies of toposheets. In most cases, photographs of the field location were also taken. Since most laboratory analyses for this work have been carried out on samples recovered from core drilling, the sampling procedure for these are described in detail.

The core for this study was raised in June 1992 with the help of the Directorate of Geology and Mining (DGM), Govt. of Gujarat. Owing to a weak monsoon the previous year, the water level was already low and the lake had completely dried up by the time the coring operation was in progress. The core was raised from the deepest part of the lake to ensure an undisturbed near surface record. A tungsten carbide drill bit, with a 5cm internal diameter (ID) core tube, was used for the purpose of drilling. After about every 1.5m of drilling, the core was raised and the sample removed from the casing tube either by hammering it on a clean surface (in case of sand horizons) or by hydraulic forcing (in case of clayey horizon). After about every 3m of drilling (more frequently in case of sand horizon) a casing (ID = 7.5cm) was lowered and the bore hole washed with water before deeper drilling.

Nearly all the samples from clayey horizon showed greater length than the actual depth drilled. While in the field the samples were labelled as sub samples of any particular drilling length, the actual depth of each subsection was estimated by distributing the excess recovered length between different sub samples in proportion to their individual recovered lengths.



The samples were partitioned in the field itself, as soon as they were received. The depth of the sample, its length and the down core direction was recorded accurately on the sample as well as in the logbook. The samples were then packed in polythene bags, labelled and sealed in the field itself. Samples for Thermoluminescence (TL) and Optically Stimulated Luminescence (OSL) dating were specially picked up from depths where lithological changes were observed. To avoid the possibility of changes in water content of samples as a result of bore hole washing, the samples for luminescence studies were collected from the lowermost portion of the core raised during any drilling run. These were then tightly wrapped in aluminium foil and sealed in airtight polythene bags to prevent water loss. As discussed earlier (Chapter 4) a correct estimate of water content of the sample is essential for calculation of TL/OSL ages.

A list of samples with their field number, laboratory number and corrected depth is given in Table A1.

The litholog was prepared in the field itself on the basis of visual, hand specimen estimate of grain size, colour etc. After arrival in the lab selected samples were subjected to a detailed laboratory analyses and the final litholog prepared.

**Table A.1** Details of Nal Sarovar core samples.

Lab. No.	Field No.	Depth* (cm)
N-1	NS 0-10	0-10
N-2	NS 0-10	0-10
N-3	NS 10-20	10-20
N-4	NS 10-20	10-20
N-5	NS 24.5-29.5	24.5-29.5
N-6	NS 29.5-30.5	29.5-30.5
N-7	NS 30.5-32	30.5-32
N-8	NS 32-34	32-34
N-9	NS 34-36.5	34-36.5
N-10	NS 36.5-38.5	36.5-38.5
N-11	NS 38.5-40.5	38.5-40.5
N-12	NS 40.5-42.5	40.5-42.5
N-13	NS 42.5-44.5	42.5-44.5
N-14	NS 44.5-46.5	44.5-46.5
N-15	NS 46.5-48.5	46.5-48.5
N-16	NS 48.5-50.5	48.5-50.5
N-17	NS 50.5-52.5	50.5-52.5
N-18	NS 52.5-54.5	52.5-54.5
N-19	NS 54.5-56.5	54.5-56.5
N-20	NS 56.5-58.5	56.5-58.5
N-21	NS 58.5-60.5	58.5-60.5
N-22	NS 60.5-62.5	60.5-62.5
N-23	NS 62.5-64.5	62.5-64.5
N-24	NS 64.5-66.5	64.5-66.5
N-25	NS 66.5-68.5	66.5-68.5
N-26	NS 68.5-70.5	68.5-70.5
N-27	NS 70.5-72.5	70.5-72.5
N-28	NS 72.5-74.5	72.5-74.5
N-29	NS 74.5-76.5	74.5-76.5
N-30	NS 76.5-78.5	76.5-78.5
N-31	NS 78.5-80.5	78.5-80.5
N-32	NS 80.5-83.5	80.5-83.5
N-33	NS 83.5-86.5	83.5-86.5
N-34	NS 86.5-90.0	86.5-90.0
N-35	NS 90-92	90-92
N-36	NS 92-93	92-93
N-37	NS 93-95	93-95
N-38	NS 95-97	95-97

Lab. No.	Field No.	Depth* (cm)
N-39	NS 97-99	97-99
N-40	NS 99-101	99-101
N-41	NS 101-103	101-103
N-42	NS 103-105	103-105
N-43	NS 105-107	105-107
N-44	NS 107-110	107-110
N-45	NS 110-112	110-112
N-46	NS 112-114	112-114
N-47	NS 114-116	114-116
N-48	NS 116-118	116-118
N-49	NS 118-120	118-120
N-50	NS 120-122	120-122
N-51	NS 122-124	122-124
N-52	NS 124-126	124-126
N-53	NS 126-127	126-127
N-54	NS 127-129	127-129
N-55	NS 129-131	129-131
N-56	NS 131-133	131-133
N-57	NS 133-135	133-135
N-58	NS 135-138	135-138
N-59	NS 138-140	138-140
N-60	NS 140-142	140-142
N-61	NS 142-144	142-144
N-62	NS 144-146	144-146
N-63	NS 146-148	146-148
N-64	NS 148-150	148-150
N-65	NS 150-152	150-152
N-66	NS 152-154	152-154
N-67	NS 154-156	154-156
N-68	NS 156-158	156-158
N-69	NS 158-160	158-160
N-70	NS 160-162	160-162
N-71	NS 162-164	162-164
N-72	NS 164-166	164-166
N-73	NS 166-177	166-177
N-74	NS 177-195	177-195
N-75	NS 195-207	195-207
N-76	NS 207-220	207-220

\* Depth is given as measured from surface

**Table A.1** continued

Lab. No.	Field No.	Depth* (cm)
N-77	NS 220-230	220-230
N-78	NS 230-240	230-240
N-79	NS 240-250	240-250
N-80	NS 250-261	250-261
N-81	NS 261-270	261-270
N-82	NS 270-280	270-280
N-83	NS 280-290	280-290
N-84	NS 290-293	290-293
N-85	NS 293-300	293-300
N-86	NS 300-309	300-309
N-87	NS 309-312	309-312
N-88	NS 312-317	312-317
N-89	NS 317-322	317-322
N-90	NS 322-327	322-327
N-91	NS 327-331	327-331
N-92	NS 331-341	331-341
N-93	NS 341-351	341-351
N-94	NS 351-363	351-363
N-95	NS 363-373	363-373
N-96	NS 373-384	373-384
N-97	NS 384-388	384-388
N-98	NS 388-390	388-390
N-99	NS 390-393	390-393
N-100	NS 393-417	393-417
N-101	NS 417-427	417-427
N-102	NS 427-447	427-447
N-103	NS 447-463	447-463
N-104	NS 463-477	463-477
N-105	NS 477-522	477-522
N-106	NS 522-540	522-540
N-107	NS 540-552	540-552
N-108	NS 552-562	552-562
N-109	NS 562-572	562-572
N-110	NS 572-584	572-584
N-111	NS 584-595	584-595
N-112	NS 595-600	595-600

Lab. No.	Field No.	Depth* (cm)
N-113	NS 600-610	600-610
N-114	NS 610-625	610-625
N-115	NS 625-647	625-647
N-116	NS 647-672	647-672
N-117	NS 672-685	672-685
N-118	NS 685-702	685-702
N-119	NS 702-717	702-717
N-120	NS 717-732	717-732
N-121	NS 732-745	732-745
N-122	NS 745-760	745-760
N-123	NS 760-775	760-775
N-124	NS 775 -790	775-790
N-125	NS 870-887	870-887
N-126	NS 887-907	887-907
N-127	NS 907-920	907-920
N-128	NS 920-937	920-937
N-129	NS 937-950	937-950
N-130	NS 950-965	950-965
N-131	NS 965-987	965-987
N-132	NS 987-1000	987-1000
N-133	NS 1000-1025	1000-1025
N-134	NS 1025-1052	1025-1052
N-135	NS 1052-1065	1052-1065
N-136	NS 1065-1102	1065-1102
N-137	NS 1102-1122	1102-1122
N-138	NS 1122-1152	1122-1152
N-139	NS 1152-1165	1152-1165
N-140	NS 1165-1184	1165-1184
N-141	NS 1184-1199	1184-1199
N-142	NS 1199-1217	1199-1217
N-143	NS 1217-1225	1217-1225
N-144	NS 1225-1247	1225-1247
N-145	NS 1247-1272	1247-1272
N-146	NS 1272-1285	1272-1285
N-147	NS 1285-1299	1285-1299
N-148	NS 1299-1324	1299-1324

Table A.1 continued:

Lab. No.	Field No.	Depth* (cm)
N-149	NS 1324-1346	1324-1346
N-150	NS 1346-1366	1346-1366
N-151	NS 1366-1392	1366-1392
N-152	NS 1392-1405	1392-1405
N-153	NS 1405-1430	1405-1430
N-154	NS 1430-1455	1430-1455
N-155	NS 1455-1485	1455-1485
N-156	NS 1485-1515	1485-1515
N-157	NS 1515-1539	1515-1539
N-158	NS 1539-1552	1539-1552
N-159	NS 1552-1565	1552-1565
N-160	NS 1565-1592	1565-1592
N-161	NS 1592-1602	1592-1602
N-162	NS 1602-1615	1602-1615
N-163	NS 1615-1645	1615-1645
N-164	NS 1645-1662	1645-1662
N-165	NS 1662-1675	1662-1675
N-166	NS 1675-1775	1675-1775
N-167	NS 1825-1835	1825-1835
N-168	NS 1835-1842	1835-1842
N-169	NS 1842-1852	1842-1852
N-170	NS 1852-1857	1852-1857
N-171	NS 1857-1862	1857-1862
N-172	NS 1862-1867	1862-1867
N-173	NS 1867-1874	1867-1874
N-174	NS 1874-1879	1874-1879
N-175	NS 1879-1884	1879-1884
N-176	NS 1884-1889	1884-1889
N-177	NS 1889-1894	1889-1894
N-178	NS 1894-1899	1894-1899
N-179	NS 1899-1904	1899-1904
N-180	NS 1904-1909	1904-1909
N-181	NS 1909-1914	1909-1914
N-182	NS 1914-1920	1914-1920
N-183	NS 1920-1925	1920-1925
N-184	NS 1925-2025/7	1925-1945

Lab. No.	Field No.	Depth* (cm)
N-185	NS 1925-2025/6	1945-1953
N-186	NS 1925-2025/5	1953-1965
N-187	NS 1925-2025/4	1965-1981
N-188	NS 1925-2025/3	1981-1997
N-189	NS 1925-2025/2	1997-2016
N-190	NS 1925-2025/1	2016-2025
N-191	NS 2025-2135/9	2025-2036
N-192	NS 2025-2135/8	2036-2050
N-193	NS 2025-2135/7	2050-2063
N-194	NS 2025-2135/6	2063-2076
N-195	NS 2025-2135/5	2076-2090
N-196	NS 2025-2135/4	2090-2098
N-197	NS 2025-2135/3	2098-2109
N-198	NS 2025-2135/2	2109-2119
N-199	NS 2025-2135/1	2119-2135
N-200	NS 2135-2235/16	2135-2140
N-201	NS 2135-2235/15	2140-2145
N-202	NS 2135-2235/14	2145-2150
N-203	NS 2135-2235/13	2150-2157
N-204	NS 2135-2235/12	2157-2165
N-205	NS 2135-2235/11	2165-2171
N-206	NS 2135-2235/10	2171-2176
N-207	NS 2135-2235/9	2176-2184
N-208	NS 2135-2235/8	2184-2192
N-209	NS 2135-2235/7	2192-2198
N-210	NS 2135-2235/6	2198-2204
N-211	NS 2135-2235/5	2204-2210
N-212	NS 2135-2235/4	2210-2216
N-213	NS 2135-2235/3	2216-2222
N-214	NS 2135-2235/2	2222-2228
N-215	NS 2135-2235/1	2228-2235
N-216	NS 2235-2400/11	2235-2252
N-217	NS 2235-2400/10	2252-2264
N-218	NS 2235-2400/9	2264-2277
N-219	NS 2235-2400/8	2277-2290
N-220	NS 2235-2400/7	2290-2306

Table A.1 continued

Lab. No.	Field No.	Depth* (cm)
N-221	NS 2235-2400/6	2306-2322
N-222	NS 2235-2400/5	2322-2332
N-223	NS 2235-2400/4	2332-2347
N-224	NS 2235-2400/3	2347-2364
N-225	NS 2235-2400/2	2364-2381
N-226	NS 2235-2400/1	2381-2400
N-227	NS 2400-2560/9	2400-2422
N-228	NS 2400-2560/8	2422-2444
N-229	NS 2400-2560/7	2444-2463
N-230	NS 2400-2560/6	2463-2484
N-231	NS 2400-2560/5	2484-2497
N-232	NS 2400-2560/4	2497-2518
N-233	NS 2400-2560/3	2518-2533
N-234	NS 2400-2560/2	2533-2550
N-235	NS 2400-2560/1	2550-2560
N-236	NS 2560-2750/11	2560-2570
N-237	NS 2560-2750/10	2570-2588
N-238	NS 2560-2750/9	2588-2608
N-239	NS 2560-2750/8	2608-2625
N-240	NS 2560-2750/7	2625-2638
N-241	NS 2560-2750/6	2638-2657
N-242	NS 2560-2750/5	2657-2676
N-243	NS 2560-2750/4	2676-2699
N-244	NS 2560-2750/3	2699-2715
N-245	NS 2560-2750/2	2715-2737
N-246	NS 2560-2750/1	2737-2750
N-247	NS 2750-2870/10	2750-2758
N-248	NS 2750-2870/9	2758-2768
N-249	NS 2750-2870/8	2768-2781
N-250	NS 2750-2870/7	2781-2793
N-251	NS 2750-2870/6	2793-2805
N-252	NS 2750-2870/5	2805-2820
N-253	NS 2750-2870/4	2820-2832
N-254	NS 2750-2870/3	2832-2847
N-255	NS 2750-2870/2	2847-2861
N-256	NS 2750-2870/1	2861-2870

Lab. No.	Field No.	Depth* (cm)
N-257	NS 2870-2990/11	2870-2882
N-258	NS 2870-2990/10	2882-2897
N-259	NS 2870-2990/9	2897-2907
N-260	NS 2870-2990/8	2907-2917
N-261	NS 2870-2990/7	2917-2927
N-262	NS 2870-2990/6	2927-2936
N-263	NS 2870-2990/5	2936-2948
N-264	NS 2870-2990/4	2948-2959
N-265	NS 2870-2990/3	2959-2971
N-266	NS 2870-2990/2	2971-2981
N-267	NS 2870-2990/1	2981-2990
N-268	NS 2990-3140/7	3021-3045
N-269	NS 2990-3140/6	3045-3059
N-270	NS 2990-3140/5	3059-3079
N-271	NS 2990-3140/4	3079-3094
N-272	NS 2990-3140/3	3094-3119
N-273	NS 2990-3140/2	3119-3127
N-274	NS 2990-3140/1	3127-3140
N-275	NS 3140-3290/14	3140-3153
N-276	NS 3140-3290/13	3153-3164
N-277	NS 3140-3290/12	3164-3173
N-278	NS 3140-3290/11	3173-3178
N-279	NS 3140-3290/10	3178-3188
N-280	NS 3140-3290/9	3188-3195
N-281	NS 3140-3290/8	3195-3204
N-282	NS 3140-3290/7	3204-3217
N-283	NS 3140-3290/6	3217-3226
N-284	NS 3140-3290/5	3226-3241
N-285	NS 3140-3290/4	3241-3254
N-286	NS 3140-3290/3	3254-3266
N-287	NS 3140-3290/2	3266-3278
N-288	NS 3140-3290/1	3278-3290
N-289	NS 3290-3420/9	3290-3305
N-290	NS 3290-3420/8	3305-3320
N-291	NS 3290-3420/7	3320-3332
N-292	NS 3290-3420/6	3332-3353

**Table A.1** continued

Lab. No.	Field No.	Depth* (cm)
N-293	NS 3290-3420/5	3353-3368
N-294	NS 3290-3420/4	3368-3387
N-295	NS 3290-3420/3	3387-3398
N-296	NS 3290-3420/2	3398-3408
N-297	NS 3290-3420/1	3408-3420
N-298	NS 3420-3540/11	3420-3426
N-299	NS 3420-3540/10	3426-3437
N-300	NS 3420-3540/9	3437-3445
N-301	NS 3420-3540/8	3445-3457
N-302	NS 3420-3540/7	3457-3470
N-303	NS 3420-3540/6	3470-3484
N-304	NS 3420-3540/5	3484-3501
N-305	NS 3420-3540/4	3501-3518
N-306	NS 3420-3540/3	3518-3524
N-307	NS 3420-3540/2	3524-3531
N-308	NS 3420-3540/1	3531-3540
N-309	NS 3540-3690/12	3540-3553
N-310	NS 3540-3690/11	3553-3564
N-311	NS 3540-3690/10	3564-3575
N-312	NS 3540-3690/9	3575-3589
N-313	NS 3540-3690/8	3589-3603
N-314	NS 3540-3690/7	3603-3614
N-315	NS 3540-3690/6	3614-3626
N-316	NS 3540-3690/5	3626-3640
N-317	NS 3540-3690/4	3640-3658
N-318	NS 3540-3690/3	3658-3672
N-319	NS 3540-3690/2	3672-3688
N-320	NS 3540-3690/1	3688-3690
N-321	NS 3690-3840/10	3690-3691
N-322	NS 3690-3840/9	3691-3706
N-323	NS 3690-3840/8	3706-3723
N-324	NS 3690-3840/7	3723-3745
N-325	NS 3690-3840/6	3745-3762
N-326	NS 3690-3840/5	3762-3774
N-327	NS 3690-3840/4	3774-3785
N-328	NS 3690-3840/3	3785-3804

Lab. No.	Field No.	Depth* (cm)
N-329	NS 3690-3840/2	3804-3831
N-330	NS 3690-3840/1	3831-3840
N-331	NS 3840-3980/10	3840-3853
N-332	NS 3840-3980/9	3853-3869
N-333	NS 3840-3980/8	3869-3884
N-334	NS 3840-3980/7	3884-3903
N-335	NS 3840-3980/6	3903-3914
N-336	NS 3840-3980/5	3914-3931
N-337	NS 3840-3980/4	3931-3950
N-338	NS 3840-3980/3	3950-3960
N-339	NS 3840-3980/2	3960-3974
N-340	NS 3840-3980/1	3974-3980
N-341	NS 3840-3980/0	-
N-342	NS 3980-4180/13	3980-3989
N-343	NS 3980-4180/12	3989-4001
N-344	NS 3980-4180/11	4001-4015
N-345	NS 3980-4180/10	4015-4033
N-346	NS 3980-4180/9	4033-4053
N-347	NS 3980-4180/8	4053-4073
N-348	NS 3980-4180/7	4073-4094
N-349	NS 3980-4180/6	4094-4106
N-350	NS 3980-4180/5	4106-4120
N-351	NS 3980-4180/4	4120-4141
N-352	NS 3980-4180/3	4141-4154
N-353	NS 3980-4180/2	4154-4170
N-354	NS 3980-4180/1	4170-4180
N-355	NS 4180-4360/14	4180-4195
N-356	NS 4180-4360/13	4195-4209
N-357	NS 4180-4360/12	4209-4222
N-358	NS 4180-4360/11	4222-4244
N-359	NS 4180-4360/10	4244-4257
N-360	NS 4180-4360/9	4257-4274
N-361	NS 4180-4360/8	4274-4271
N-362	NS 4180-4360/7	4271-4281
N-363	NS 4180-4360/6	4281-4294
N-364	NS 4180-4360/5	4294-4309

**Table A.1 continued**

Lab. No.	Field No.	Depth* (cm)
N-365	NS 4180-4360/4	4309-4320
N-366	NS 4180-4360/3	4320-4331
N-367	NS 4180-4360/2	4331-4346
N-368	NS 4180-4360/1	4346-4360
N-369	NS 4360-4560/13	4360-4373
N-370	NS 4360-4560/12	4373-4388
N-371	NS 4360-4560/11	4388-4402
N-372	NS 4360-4560/10	4402-4419
N-373	NS 4360-4560/9	4419-4430
N-374	NS 4360-4560/8	4430-4451
N-375	NS 4360-4560/7	4451-4470
N-376	NS 4360-4560/6	4470-4489
N-377	NS 4360-4560/5	4489-4501
N-378	NS 4360-4560/4	4501-4511
N-379	NS 4360-4560/3	4511-4522
N-380	NS 4360-4560/2	4522-4543
N-381	NS 4360-4560/1	4543-4560
N-382	NS 4560-4790/16	4560-4576
N-383	NS 4560-4790/15	4576-4592
N-384	NS 4560-4790/14	4592-4608
N-385	NS 4560-4790/13	4608-4623
N-386	NS 4560-4790/12	4623-4638
N-387	NS 4560-4790/11	4638-4654
N-388	NS 4560-4790/10	4654-4666
N-389	NS 4560-4790/9	4666-4677
N-390	NS 4560-4790/8	4677-4692
N-391	NS 4560-4790/7	4692-4709
N-392	NS 4560-4790/6	4709-4719
N-393	NS 4560-4790/5	4719-4738
N-394	NS 4560-4790/4	4738-4757

Lab. No.	Field No.	Depth* (cm)
N-395	NS 4560-4790/3	4757-4762
N-396	NS 4560-4790/2	4762-4781
N-397	NS 4560-4790/1	4781-4790
N-398	NS 4790-5000/15	4790-4803
N-399	NS 4790-5000/14	4803-4820
N-400	NS 4790-5000/13	4820-4836
N-401	NS 4790-5000/12	4836-4850
N-402	NS 4790-5000/11	4850-4865
N-403	NS 4790-5000/10	4865-4881
N-404	NS 4790-5000/9	4881-4901
N-405	NS 4790-5000/8	4901-4910
N-406	NS 4790-5000/7	4910-4928
N-407	NS 4790-5000/6	4928-4943
N-408	NS 4790-5000/5	4943-4957
N-409	NS 4790-5000/4	4957-4976
N-410	NS 4790-5000/3	4976-4986
N-411	NS 4790-5000/2	4986-4995
N-412	NS 4790-5000/1	4995-5000
N-413	NS 5284-5485/12	5285-5300
N-414	NS 5284-5485/11	5300-5316
N-415	NS 5284-5485/10	5316-5333
N-416	NS 5284-5485/9	5333-5348
N-417	NS 5284-5485/8	5348-5366
N-418	NS 5284-5485/7	5366-5381
N-419	NS 5284-5485/6	5381-5396
N-420	NS 5284-5485/5	5396-5414
N-421	NS 5284-5485/4	5414-5431
N-422	NS 5284-5485/3	5431-5448
N-423	NS 5284-5485/2	5448-5465
N-424	NS 5284-5485/1	5465-5485

## **APPENDIX B**

### **Experimental Procedures For Sedimentological And Mineralogical Analyses**

#### **B.1 Textural analysis**

The core samples were subjected to grain size analysis. In the sand layer, about 60-80g. sample was taken. This was subjected to sequential 10% HCl and 30% v/v hydrogen peroxide treatment to remove the carbonates and organics. The sample was then wet sieved through 62.5 $\mu$  sieve (BSS No. 240). The finer than 62.5 $\mu$  was used to determine the amount of silt and clay using standard pipette analysis method (Carver, 1971) employing the principle of Stoke's settling. The sand-silt-clay percentages were then computed. Results are given in Table B.1

#### **B.2 Heavy mineral separation**

Heavy minerals were separated from the sand fraction of the sample using bromoform ( $\rho=2.85$ ). The samples were transferred to a separating funnel which had been filled with bromoform. After a few hours time, the heavy mineral fraction was collected in a beaker and washed. The remaining bromoform was kept aside for further use. The heavy minerals were mounted on glass slides and identified under a petrological microscope.

#### **B.3 X- Ray diffraction**

This was used for the identification of clay minerals to determine the provenance for Horizon-1 and Horizon-3. Calcium carbonate and organic matter were removed by dilute acetic acid and 6% v/v hydrogen peroxide respectively. Clay fraction ( $<2\mu$ ) was collected using Stoke's settling principle and concentrated by centrifugation. It was then pipetted onto glass slides and dried. The slides were scanned between  $3^\circ$  to  $30^\circ$  ( $2\theta$ ) at



1°/min/cm using a  $\text{CuK}_\alpha$  source. The clay minerals were identified from the charts using the powder diffraction data file, published by International Centre for Diffraction Data, Pennsylvania.

Smectite has a broad peak in the region, 7.3° to 5.9° (2 $\theta$ ). However the peak for vermiculite also appears in this region (6.22°). The presence of smectite was confirmed using glycolation method. To the natural clay sample, 1N  $\text{MgCl}_2$  was added and left overnight. The next day this mixture was washed with distilled water. A slide was subsequently prepared from this clay sample. This slide was then kept in a dessicator with ethyl glycol at 60°C for 6 hours. If the peak in the natural slide is of smectite and not vermiculite, the treated slide will show the widening of the peak.

Also both kaolinite and chlorite have the same peak at 12.4° (2 $\theta$ ). Differentiation of kaolinite and chlorite was carried out using the thermal treatment. To the natural slide was added a 1N solution of KCl and left overnight. The next day this mixture was washed with double distilled water and a slide prepared. This slide was then heated to 550°C. The peak remains if the mineral is chlorite.

For the purpose of semi-quantification, the area under the peak was graphically computed. Using the following formula (Biscaye, 1965), relative clay mineral percentages calculated,

$$\text{smectite} + 4 * (\text{illite}) + 2 * (\text{kaolinite}) + 2 * (\text{chlorite}) = 100\%$$

The results are given in Table B2.

**Table B.1** Results of grain size analyses\* on samples from Nal Sarovar core.

Lab no.	Depth (cm)	Sand (%)	Silt (%)	Clay (%)
N-4	10-20	3.84	31.19	64.97
N-34	86.5-90	3.38	14.20	82.42
N-75	195-207	7.33	31.78	60.89
N-83	280-290	14.41	45.47	40.42
N-99	390-393	85.98	10.9	3.12
N-100	393-417	64.62	27.53	7.85
N-105	477-522	91.34	6.95	1.71
N-107	540-552	82.79	10.31	6.90
N-113	600-610	64.43	24.44	11.13
N-118	685-702	70.04	13.72	16.24
N-124	775-790	44.76	37.62	17.62
N-126	887-907	65.90	26.60	7.50
N-127	907-920	71.59	19.32	9.09
N-132	987-1000	73.49	22.71	3.82
N-136	1065-1102	51.15	39.03	9.82
N-143	1217-1225	81.07	10.81	8.12
N-147	1285-1299	37.26	49.87	12.87
N-148	1299-1324	41.96	43.95	14.09
N-153	1405-1430	80.46	15.27	4.27
N-155	1455-1485	42.26	48.73	9.01
N-156	1485-1515	54.46	31.83	13.71
N-160	1565-1592	41.68	24.68	33.64
N-166	1675-1775	82.33	3.59	14.08
N-168	1835-1842	35.85	35.62	28.53
N-184	1925-1945	6.20	70.70	23.10
N-197	2098-2109	48.23	22.78	28.99
N-225	2364-2381	41.09	18.85	40.06
N-226	2381-2400	5.36	33.83	60.81
N-227	2400-2422	4.73	55.26	40.01
N-229	2444-2463	5.28	82.52	12.2
N-249	2768-2781	1.95	37.25	60.80

\* For graphical presentation see Fig 2.17.

**Table B.1 continued:**

<b>Lab No.</b>	<b>Depth (cm)</b>	<b>Sand (%)</b>	<b>Silt (%)</b>	<b>Clay (%)</b>
N-268	3021-3045	11.75	28.43	59.82
N-288	3278-3290	3.35	39.98	56.67
N-350	4106-4120	12.73	23.31	63.96
N-378	4501-4511	11.61	32.27	56.12
N-397	4781-4790	30.21	30.33	39.46
N-411	4986-4995	17.96	29.1	52.94
N-412	4995-5000	18.46	35.75	45.79
N-424	5465-5485	53.91	6.89	39.20

**Table B.2** Results of clay mineral analyses\* on samples from Nal Sarovar core.

Lab No.	Depth (cm)	Smectite (%)	Kaolinite (%)	Chlorite (%)	Illite (%)
N-4	10-20	12.96	7.79	5.20	74.05
N-34	86.5-90	7.57	8.56	4.47	79.40
N-75	195-207	8.29	7.2	4.86	79.56
N-83	280-290	8.52	5.78	4.62	81.08
N-100	393-417	12.09	7.46	3.74	76.71
N-105	477-522	52.09	9.71	8.49	29.71
N-113	600-610	55.76	8.85	2.21	33.18
N-118	685-702	53.04	10.33	6.19	30.44
N-124	775-790	42.59	14.68	4.77	37.96
N-126	887-907	67.15	9.66	4.35	18.84
N-132	987-1000	68.40	5.10	1.70	24.80
N-136	1065-1102	70.30	5.91	1.97	21.82
N-147	1285-1299	74.78	5.22	2.61	17.39
N-148	1299-1324	62.14	6.19	3.10	28.57
N-155	1455-1485	64.92	4.16	2.61	28.51
N-156	1485-1515	51.43	7.27	7.01	34.29
N-227	2400-2422	52.89	5.82	5.36	35.93
N-229	2444-2463	97.53	1.19	0.44	0.84
N-249	2768-2781	97.96	0.57	0.45	1.02
N-268	3021-3045	76.47	7.86	3.89	11.76
N-288	3278-3290	98.23	1.18	0.59	-
N-350	4106-4120	98.69	0.66	0.65	-
N-378	4501-4511	94.87	3.44	1.69	-
N-412	4995-5000	97.45	1.82	0.73	-
SPM**	-	29.82	21.59	6.48	42.11

\* For graphical presentation see Fig 2.18.

\*\* Suspended sediment from flood water of Sabarmati river at Ahmedabad (Sept. 1994).

## **APPENDIX C**

### **Experimental Procedures For Radiocarbon Dating**

The radiocarbon dating requires determination of the residual  $^{14}\text{C}$  content in the sample. This value is then translated into an age that is an estimate of time elapsed since the given sample was removed from the environment in which it was in equilibrium with respect to  $^{14}\text{C}$ . The following steps are involved in the procedure:

C.1 Pre-treatment of the sample.

C.2 Preparation of sample for  $^{14}\text{C}$  activity measurement.

C.3 Estimation of the residual  $^{14}\text{C}$  activity.

C.4 Age determination.

#### **C.1 Sample pre-treatment**

Some degree of post depositional alteration of sample often occurs in nature. The purpose of pre-treatment is to isolate a fraction that is most likely to have remained unaltered. For lake mud, in the case of this study, it usually involved dilute acid wash to remove secondary carbonate material. Subsequently the sample was washed repeatedly with distilled water and dried.

#### **C.2 Preparation of sample for counting**

Following chemical reactions are involved:

*C.2.1 Carbon dioxide preparation.* This involved the use of a specially prepared vacuum line. For organic samples,  $\text{CO}_2$  was released by combustion in a flow of oxygen. For carbonate samples, the  $\text{CO}_2$  was released by treatment of powdered sample with  $\text{H}_3\text{PO}_4$ .

Once the  $\text{CO}_2$  gas was obtained, the next step involved its chemical and physical purification. The following sequence was followed, as described in Gupta and Polach (1985),

- KI/I<sub>2</sub> solution for oxidation/decomposition of phosphorus, nitrogen and sulphur.
- Solution of 0.1N AgNO<sub>3</sub> for the precipitation of chlorides and other halides and acidic vapours.
- Solution of K<sub>2</sub>Cr<sub>2</sub>O<sub>7</sub>/H<sub>2</sub>SO<sub>4</sub> for final oxidation of traces of CO and trapping of SO<sub>3</sub>.
- Silica gel to trap the moisture.

Carbonate samples are relatively clean. The CO<sub>2</sub> from their acid hydrolysis was dried by passing through two dry ice/alcohol or acetone cooled traps. The purified CO<sub>2</sub> was frozen and then expanded in glass bottles.

**C.2.2 Acetylene synthesis:** This was accomplished in two steps. The first step involved reaction of sample CO<sub>2</sub> with molten Li, inside a reaction vessel, to form lithium carbide. In the second step, lithium carbide was hydrolysed to yield C<sub>2</sub>H<sub>2</sub>.

**C.2.3 Benzene synthesis:** The C<sub>2</sub>H<sub>2</sub> was trimerised to C<sub>6</sub>H<sub>6</sub> by letting the frozen C<sub>2</sub>H<sub>2</sub> sublime slowly onto an activated vanadium catalyst in an evacuated column. Complete conversion of the C<sub>2</sub>H<sub>2</sub> gas into benzene took ~8 hours. To recover the benzene subsequently, the column was heated at 110°C and benzene collected under vacuum in a liquid nitrogen cooled trap. The frozen benzene was aerated, allowed to melt at room temperature, transferred to a storage vial and refrigerated.

### C.3 Measurement of activity

The activity of sample carbon, converted into benzene, was measured using liquid scintillation counter (LKB Wallace 1220 Quantulus). The counter had photomultiplier tubes which sensed light signals produced by decay of <sup>14</sup>C in benzene. As such <sup>14</sup>C decay will not produce light. Hence, organic scintillators were dissolved in the sample prior to counting. The sample was counted for about 2500 min.

## C.4 Age determination

Having measured the residual radiocarbon activity of a sample, the  $^{14}\text{C}$  age was estimated by relating the measured residual activity ( $A_{\text{SN}}$ ), to the original equilibrium  $^{14}\text{C}$  activity of the reservoir ( $A_{\text{ON}}$ ), that supplied the sample. The relationship based on radioactive decay equation is given as

$$A_{\text{SN}} = A_{\text{ON}} \exp(-\lambda t)$$

where  $t$  = years elapsed since the sample was removed from the equilibrium condition in the  $^{14}\text{C}$  reservoir.

$$\lambda = \text{decay constant of } ^{14}\text{C} = 0.693/t_{1/2}.$$

$$t_{1/2} = \text{half life of } ^{14}\text{C} = 5730 \pm 40 \text{ years.}$$

The reservoir activity is supposed to be represented by a wood grown before 1890 AD, and hence unaffected by fossil or bomb produced  $\text{CO}_2$ . The Primary Modern Reference Standard ( $A_{\text{ON}}$ ) for radiocarbon dating is a 1950 batch of oxalic acid from the U.S. National Bureau of standards. 95% activity of the primary reference standard corresponds to activity of wood grown in AD 1890. In the PRL radiocarbon laboratory, a specially prepared batch of sucrose, pre-calibrated with primary oxalic acid standard, was used as a standard for modern  $^{14}\text{C}$  activity comparison.

For details of standard procedures involved in checking efficiency of counting, statistical monitoring and age calculations, reference is made to Gupta and Polach (1985).

Results of  $^{14}\text{C}$  dating of Nal Sarovar samples are given in Tables 3.2 and 3.3.

## **APPENDIX D**

### **Experimental Procedures For $\delta^{13}\text{C}$ And C/N Analyses**

Details of experimental techniques involved in the  $\delta^{13}\text{C}$  and C/N analyses of organic matter present in the sediments are described in this appendix. These are dealt with under the following sections:

D.1 Calibration of the gas extraction assembly line.

D.2 Sample pre-treatment and gas extraction.

D.3 Mass spectrometric measurements.

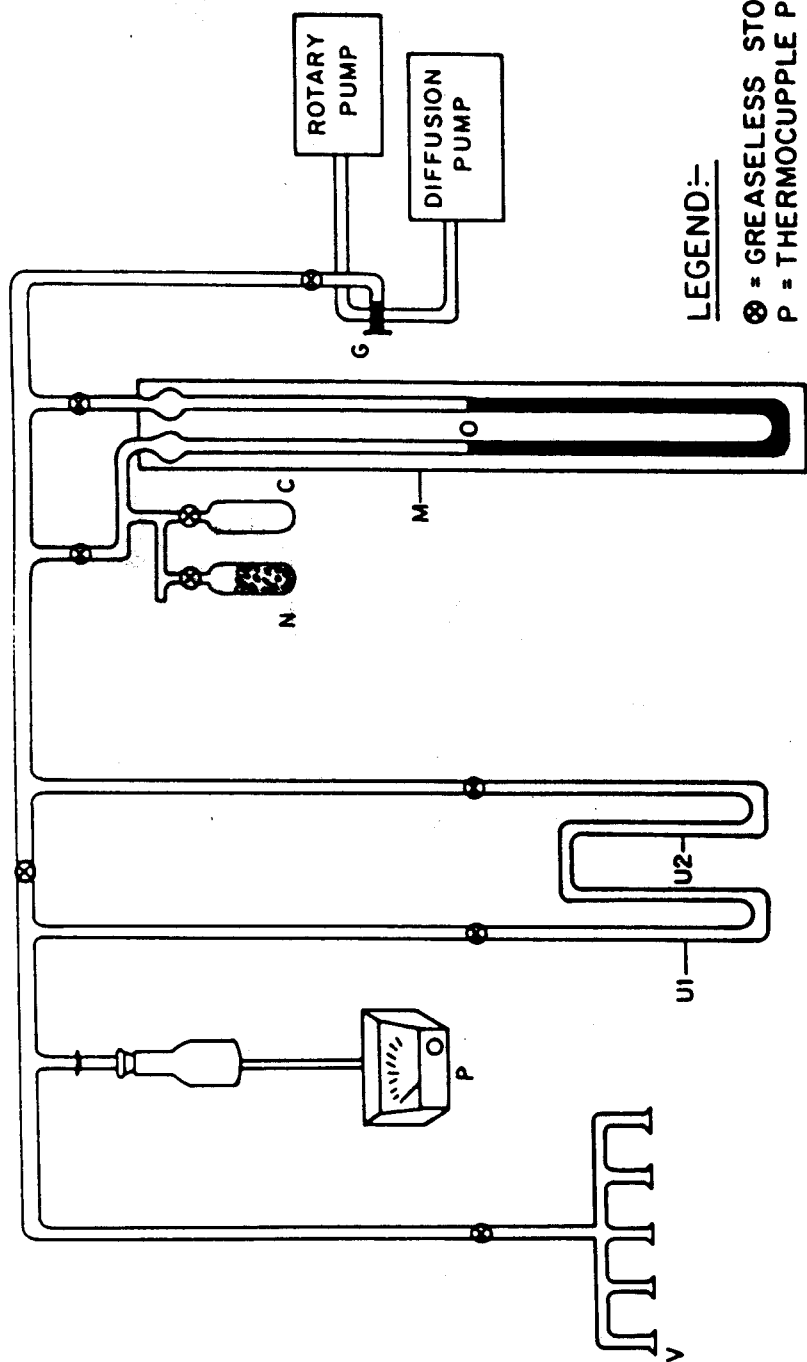
#### **D.1 Calibration of the assembly line:**

A schematic diagram of the glass gas extraction line, especially constructed for this work, is shown (Fig. D.1).

Experiments were undertaken to calibrate the gas extraction line by constructing a plot of P (pressure as measured in the manometer tube) vs micromoles of gas (nitrogen or  $\text{CO}_2$ ) in a fixed volume (manometer and glass/quartz tube). For this purpose a gas bottle of known volume was taken. After evacuation to  $10^{-3}$  torr, it was filled with purified  $\text{N}_2$  gas at a known pressure from a  $\text{N}_2$  gas cylinder. The purification step involved passing the  $\text{N}_2$  gas from the cylinder through liquid nitrogen ( $\text{LN}_2$ ) cooled tubes, U1 and U2, to remove any impurity of  $\text{CO}_2$  or water that may be present. Using the gas law, the number of micromoles of purified gas in the bottle was calculated. All the gas in the  $\text{N}_2$  bottle was then released into the evacuated assembly line. The  $\text{N}_2$  was absorbed onto the charcoal finger (labelled N in Fig. D.1) at  $\text{LN}_2$  temperature. Once all the gas had been so collected, the manometer tube was closed and the charcoal finger torched to released the  $\text{N}_2$ . Upon cooling to room temperature, the pressure in the manometer tube was measured and the gas pumped away. The charcoal finger was torched again and kept ready for the next lot. A series of such measurements gave a plot of  $P(\text{N}_2)$  vs Micromoles of  $\text{N}_2$  (Fig. D.2).

A similar procedure was followed for obtaining the calibration curve for  $\text{CO}_2$  gas with the difference that the gas was collected in the glass finger





**LEGEND:-**

- ⊗ = GREASELESS STOPCOCK
- P = THERMOCUPPLE PRESSURE GAUGE
- U1, U2 = ARMS OF U TUBE
- N = CHARCOAL FINGER
- C = CO<sub>2</sub> TRAP
- M = MERCURY MANOMETER
- G = GREASED STOPCOCK
- V = SAMPLE INLET

**Fig D.1 Assembly line for extraction of Carbon dioxide and Nitrogen.**

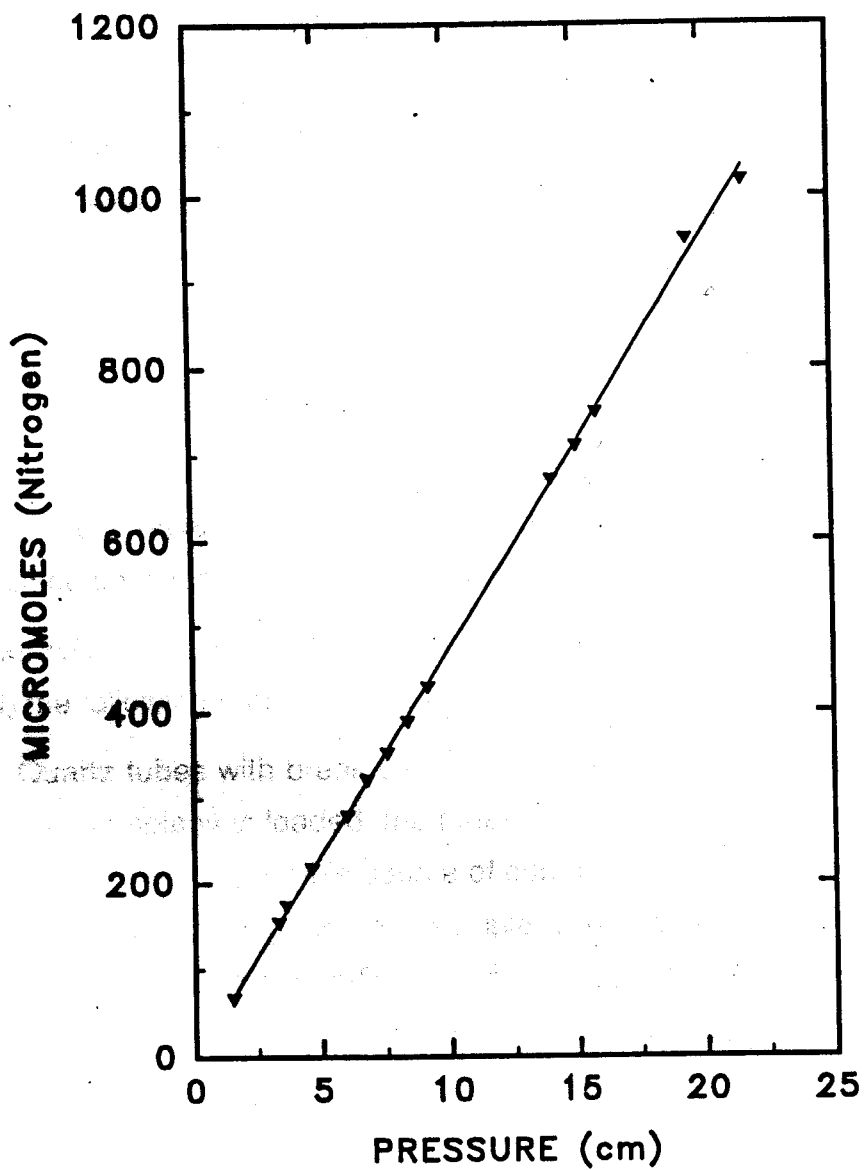


Fig. D.2 Calibration curve for determination of nitrogen.

(labelled C in Fig. D.1). The calibration curve for carbon dioxide is shown in Fig. D.3.

In both the cases, the efficiency of gas absorption/freezing was monitored using a thermocouple pressure gauge.

## **D.2 Sample pre-treatment and gas extraction:**

**B1. Sample pre-treatment:** Since the aim of this study was to analyse the organic fraction of the sediments for  $\delta^{13}\text{C}$  and C/N values, the first step was to remove inorganic carbon from each sample. The carbonate minerals constitute the main source of inorganic carbon in the sample. To remove them, a 10% Hydrochloric acid treatment is repeatedly given to 1g of dried and powdered sample. Dilute HCl was added till the reaction was over. A fresh batch of acid was then added and the samples left overnight to ensure complete removal of all the carbonates. Once the acid reaction was over the samples were repeatedly washed with double distilled water and dried at 70°C. Dried samples were powdered and stored in clean dry vials.

**B2. Extraction of  $\text{CO}_2$  and  $\text{N}_2$  from organic matter:** For the extraction of  $\text{CO}_2$  and  $\text{N}_2$  the following procedure was used.

Quartz tubes with break seals were used for combustion of samples. Before the sample was loaded, the tubes were left overnight in a furnace at 600°C to remove any possible source of contamination. About 400mg of pre-treated, accurately weighed, dry sample was loaded into a quartz tube (10mm OD, 8mm ID, 10cm long ) with break seal at one end. Alongwith the sample, about 1g of pure E-Merck copper oxide was added which acted as a oxygen donor for the oxidation of the sample. This copper oxide, in wire form, had been baked previously at 400°C for 10 hours to remove any traces of organic matter which might have been present. The quartz tube with the sample and CuO was then evacuated to  $10^{-3}$  Torr for at least 3 hours and then sealed under vacuum. The sealed quartz tube containing the sample and CuO was then inserted into stainless steel jackets, to ensure uniform heating, and heated to 800°C for 6 hours in a furnace.

With each batch of 7 sample tubes a Urea ( $\text{NH}_2\text{CO.NH}_2$ ) and a UCLA glucose standard was also processed to monitor the combustion

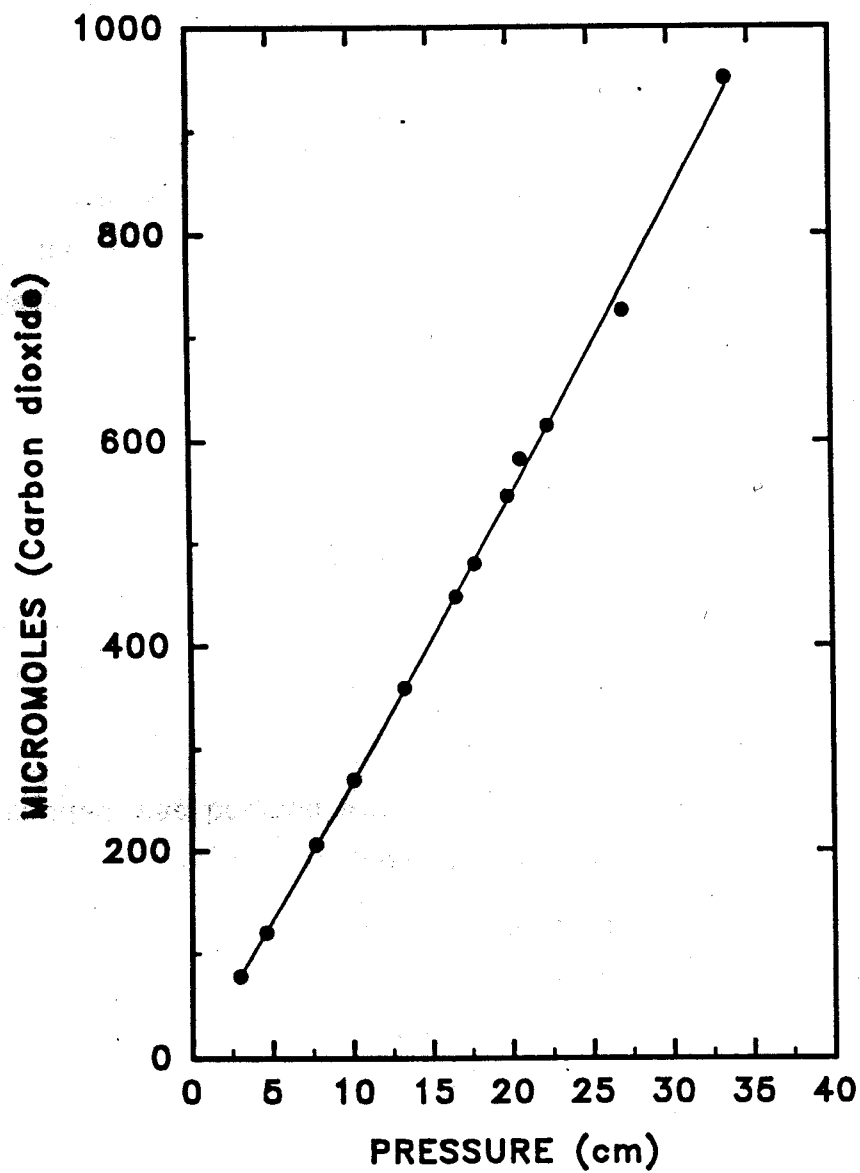


Fig. D.3 Calibration curve for determination of carbon dioxide.

efficiency. The yield for UCLA glucose was over 90%. Urea was used as a standard to monitor the reproducibility of %C and %N whereas UCLA glucose was used to monitor the reproducibility of  $\delta^{13}\text{C}$ . Blanks were periodically measured and found to be less than 3 micromoles as compared to the total gas yield of around 300 micromoles.

The cooled quartz tube, with a stainless steel ball resting on its break seal, was contained in a glass tube and introduced into the vacuum line through valve 'V'. After evacuation the break seal was cracked open by moving the steel ball using an external magnet. The released gases comprising water vapour,  $\text{CO}_2$  and  $\text{N}_2$  were made to pass through the U tubes, U1 and U2, which had been cooled to liquid nitrogen temperature to trap water vapour and  $\text{CO}_2$ . The  $\text{N}_2$  gas was trapped on the charcoal contained in a quartz finger 'N' at liquid nitrogen temperature. The manometer valve was closed and the  $\text{N}_2$  released by torching. After cooling, the yield was measured by reading the manometer. Knowing the weight 'w' of the sample and number of micromoles 'n' of nitrogen the yield was calculated as,

$$\% \text{ Nitrogen} = 2.8 \cdot n / w$$

The nitrogen was pumped away and the charcoal finger torched again, evacuated and kept ready for the next sample.

$\text{CO}_2$  was separated from water vapour by replacing the liquid nitrogen trap around U1 and U2 by a alcohol - liquid nitrogen slurry maintained at  $-90^\circ\text{C}$ . The  $\text{CO}_2$  was collected in the glass finger and the yield measured. If 'c' is the number of micromoles of carbon dioxide produced, the carbon content of the sample was calculated using the formula,

$$\% \text{ Carbon} = 1.2 \cdot c / w$$

### D.3 Mass spectrometric measurements

After extraction, the  $\text{CO}_2$  gas samples were taken to the mass spectrometer laboratory and again purified using a alcohol- $\text{LN}_2$  slurry trap. In principle, a mass spectrometer may be divided into four different parts: (1) double inlet system, which is used to introduce the sample and the

reference gas; (2) An ion source where ions are formed (thermally or by electron impact), accelerated and focused into a narrow beam; (3) mass analyser, where the beams emerging from the ion source are subjected to a magnetic field due to which the ions are deflected into circular paths, the radius of which is proportional to square root of Mass/charge, and (4) ion collector, where the separated ions are collected in the ion detector and converted into an electrical pulse which is then fed into an amplifier.

The relative variations of the isotopic composition of different samples can be measured with high accuracy, with respect to a reference sample which is introduced into the mass spectrometer alternately with the sample under investigation, using a double inlet system. While analysing CO<sub>2</sub> by mass spectrometry, different ionic species with the same molecular weight will interfere with each other and corrections were applied for the same using the Craig (1957), equations.  $\delta^{13}\text{C}$  was measured using a VG micromass 602D mass spectrometer, relative to tank CO<sub>2</sub> which served as an internal standard. Knowing the value of tank CO<sub>2</sub> with respect to PDB, the  $\delta^{13}\text{C}$  value of sample wrt PDB was calculated using the equation,

$$\delta^{13}\text{C}_{\text{PDB}}^{\text{X}} = \delta^{13}\text{C}_{\text{TC}}^{\text{X}} + \delta^{13}\text{C}_{\text{PDB}}^{\text{TC}} + 10^{-3} \delta^{13}\text{C}_{\text{TC}}^{\text{X}} \delta^{13}\text{C}_{\text{PDB}}^{\text{TC}}$$

where X=sample, TC=tank CO<sub>2</sub>.

In this case,  $\delta^{13}\text{C}_{\text{PDB}}^{\text{TC}} = -22.17\text{‰}$ , a value close to the  $\delta^{13}\text{C}$  value of the sample being measured.

## Results of standards

Results of  $\delta^{13}\text{C}$  (‰) measurements on UCLA glucose:

- Mean =  $-10.12 \pm 0.19$ , n=14
- Value obtained at UCLA =  $-9.78 \pm 0.14$

Results of %C and %N measurements on Urea (NH<sub>2</sub>.CO.NH<sub>2</sub>)

% Nitrogen:	measured = $47 \pm 2$ (n=11)	expected = 46.62
% Carbon:	measured $19.7 \pm 0.6$ (n=8)	expected = 19.98

## **APPENDIX E**

### **Experimental Procedures For Luminescence Dating**

The principles of luminescence dating have already been discussed in Chapter 4 (section 4.1). In this appendix, are described, the experimental procedures followed for sample collection, estimation of equivalent dose (ED) and dose rate.

#### **E.1 Sample collection**

It has already been mentioned earlier (appendix A) that core sections selected for luminescence dating were wrapped in aluminium foil and stored in airtight polythene bags as soon as they were raised. The core length varied from 5-20 cm and was 5 cm in diameter. Owing to the time lag between sample raising and its covering, the outer skin of the core had been exposed to light. However subsequent processing of sample was done under subdued red light after removing the outer 1 cm skin of the core sample and cutting 2 cm off from the ends of the core. The skin was discarded to avoid any possibility of contamination. The end portions were used for alpha counting (to determine U and Th contents), Gamma spectrometry (U/Th series disequilibrium checking), AAS (K content estimation) and water content estimations. Only the central unexposed portion was taken for equivalent dose estimation.

#### **E.2 Laboratory procedures for determination of ED**

The methods for estimation of ED have been discussed in Chapter 4 (Section 4.1.2). For the construction of growth curves, aliquots/discs of the same sample must be given different treatments. The procedures for preparation of aliquots are described below. The entire process was done under subdued red light illumination.

◆

## E.2.1 Sample preparation

**Selection of grain size and mineral phase:** For the purpose of dating, finer fraction ( $4-11\mu$ ) comprising of silt was preferred since they are likely to have been in suspension longer and more likely to have been bleached during transport. The silts comprised about 10-30% in Horizon-2 and also constitute a significant fraction in Horizon-3. For a few samples, in Horizon-2, coarse grained dating of feldspars was also attempted. This method was not generally applied since very little feldspar was found in the sand sized fraction. Feldspar mineral phase was generally preferred since they saturate at larger doses and are more useful for dating older sediments. The infra red stimulated luminescence (IRSL) dating was used for obtaining the ages of samples in the present study. For a few samples, Thermoluminescence (TL) dating using partial bleach method was also attempted.

**Sample pre-treatment:** Samples were sequentially treated with 1N HCl to remove the carbonates, 30% v/v hydrogen peroxide to remove the organic matter and 0.01N sodium oxalate solution to deflocculate the sample. All the treatments were continued till the reactions were over and sample was washed with distilled water in between the steps.

**Preparation of discs:** For convenience of handling, aliquots of sample were prepared by depositing the separated size onto 1cm diameter aluminium/steel discs. These discs had been cleaned earlier using emery paper to ensure uniform distribution of sample on its surface. Both the fine grain and the mineral inclusion technique were used.

**Fine-grain technique:** In this technique, (Zimmerman, 1971) the samples were suspended in a 6cm column of acetone. The  $4-11\mu$  size fraction was separated using Stoke's settling in acetone. One and a half minutes time was required for the  $>11\mu$  size fraction to settle. To separate  $<4\mu$  size, again a settling time of 15 minutes was given and the overlying filtrate removed. The material settled at the base of test tube was the required  $4-11\mu$  size fraction. Different aliquots of



the sample were prepared by re-suspending the sample in either acetone or alcohol and pipetting on to aluminium discs. These discs were dried in the oven at 45°C. In view of difficulties of separation of required mineral phases, e.g. quartz or feldspar, at this size, specific optical windows (by use of suitable filters) were used to discriminate against and/or select emissions of a particular mineral phase (Debenham and Walton, 1983).

**Coarse grain technique:** This technique was developed initially for studying 90-125µm quartz inclusions (Fleming, 1970) and is also called as the mineral inclusion technique. This technique has been extended to study the large K-feldspar inclusions too (Mejdahl and Winther-Nielson, 1983). After sample treatment, the coarser size fraction was dried and sieved to obtain the required size (95-150µm) fraction. The magnetic minerals were then removed using a hand magnet followed by isodynamic separation using a Franz magnetic separator. Since, in both quartz and feldspar, only the outer ~20µm skin was exposed to  $\alpha$  radiation, it was removed by an appropriate HF acid etch. The two mineral phases were separated using heavy liquid (sodium polytungstate) density separation ( $d > 2.65$  to float quartz and  $2.58 < d < 2.65$  to isolate the K-feldspar).

Even though the process for preparation of discs was same, there were small differences in sensitivities between discs either due to variation in the sample amount or due to differing luminescence sensitivities of the grains which caused a scatter in the luminescence output. For this purpose, sample normalisation, described below, is done. In the present study only short shine normalisation was used but the other methods are mentioned for the sake of completeness.

## **E.2.2 Sample normalisation**

**Short shine normalisation:** This relies on the fact that it is possible to measure the initial OSL signal of a sample without significantly reducing the geological

optical signal. Each aliquot, prior to any treatment, was given 0.5 seconds of IR stimulation. This signal was subsequently used for normalisation.

**Weight normalisation:** This is used for mineral inclusion method and involves dividing the luminescence signal of each aliquot by the weight of the sample present in that aliquot. Implicit in the use of this method is the assumption that the luminescence characteristics of grains in the aliquot are similar. However, this may not be strictly true and in some cases when the luminescence characteristics are dominated by a small number of bright grains, weight normalisation is not very successful.

**Zero glow normalisation:** Zero glow normalisation was first suggested by Aitken and Bussel (1979). It takes advantage of the fact that due to the short lifetime of the 110°C peak, it is absent in all the natural samples. Each aliquot was given a test dose that is small compared to its palaeodose and the intensity of the 110°C peak measured. This TL is a measure of the overall sample response of the aliquot as influenced by differences in weight, spreading and proportions of the bright grains present. Because of its short lifetime, the peak is liable to decay significantly within a few minutes and hence a standardised schedule for irradiation and recording has to be adopted.

### **E.2.3. Sample treatment**

The samples treatment consisted of irradiations ( $\beta$  and  $\alpha$ ) for estimation of ED, and pre heat.

**Irradiation:** Beta irradiations were given on an automated time controlled fifteen seater irradiator (Littlemore Inc.) using a 25 mCi  $^{90}\text{Sr}/^{90}\text{Y}$   $\beta$  source. The dose rate was 2.2 Gy/min for fine grains. Alpha irradiations were made on a manually timed, evacuated six seater irradiation system using an  $^{241}\text{Am}$  source (Singhvi and Aitken, 1978) of strength 220  $\mu\text{Ci}$ .

**Pre Heat :** Just prior to recording (TL or OSL), all samples were pre-heated at 160° C for 6 hours to remove unstable part of the signal. The system consisted of a heavy brass block fixed in a temperature controlled furnace. The

block has small slit in which the sample aliquots were placed on a copper plate and inserted.

#### **E.2.4 Calculation of 'a' value**

The  $\alpha$  efficiency factor 'a' was calculated using the formula,

$$a = \beta \text{ (Gy)} / (13 * S * y)$$

where,  $\beta$  is the dose that gives the TL intensity equal to that given by  $y$  (minutes) of  $\alpha$  exposure from an  $^{241}\text{Am}$  source of strength 'S' (given in  $\mu\text{m}^2 \text{ min}^{-1}$ ) (Aitken and Bowman, 1975).

Since in this study chiefly IRSL method of dating has been used, the 'a' value was also obtained from the IR stimulation of  $\alpha$  and  $\beta$  irradiated samples. The natural luminescence was zeroed using IR long shine (5 min) and also by long sun bleach. The alpha efficiency factor was determined for sample N-127 by both, long sun and IR regeneration, methods and found to be the same within  $1\sigma$ . For other samples subsequently, sun regenerated IR growth curves were constructed for both  $\alpha$  and  $\beta$  doses and the 'a' value calculated. The estimated 'a' values are given in Table 4.1.

#### **E.2.5. Anomalous fading test**

In the present case, the primary provenance is dominated by metamorphic and volcanic rocks. Since IRSL dating was done on the feldspars, there was a possibility of samples exhibiting anomalous fading. All the samples were checked for anomalous fading. Two sample aliquots were given 20min beta exposure and the TL recorded immediately along with another set of two aliquots which had been identically irradiated 3 months previously. This was considered as optimum test since it has been found that the samples which show fading in the IRSL signal also show fading in TL (Spooner, 1993).

#### **E.2.6 Luminescence measurement**

**OSL measurements:** OSL system comprising a rotatable sample holder with a capacity of 16 discs was used. The IR source consisted of 14 GaAs

LED's arranged in series which emit light at  $880 \pm 80$  nm. The source was operated using a programmable constant current DC supply. The detector consisted of a bialkali photomultiplier tube (9635QA) connected to a photon counting system, the output of which was recorded through EG&G 4096 channel ACE-MCS card coupled to an IBM/PC-486. The signal was filtered using Corning 5-58(blue pass)+7-59(violet pass) and Chance Pilkington HA3 (IR rejecting) combination. The background was typically 150 cps as compared to the sample signal of a few thousand cps.

**TL measurements:** These were made on an automated TL system (Daybreak). The system comprised of a heating arrangement and the emissions were detected using a PMT tube (EMI 9635 QA) through UG11 (ultraviolet pass) +HA3 filters. Since in case of NaI the samples were very bright, Neutral Density (ND) filters of different transmission powers were additionally used. All the measurements were carried out in pure Nitrogen atmosphere and a heating rate of  $5^{\circ}\text{C/s}$  was used.

### **E.3 Laboratory procedure for measurement of dose rate**

The dose rate is a measure of the environmental radioactivity of the sediment over a period of time. Nearly all the dose rate is provided by uranium, thorium decay series and potassium-40. The following procedures were used for dose rate estimation.

**AAS:**  $^{40}\text{K}$  was estimated using by Atomic Absorption Spectrometry (AAS). Samples were digested by sequential treatment of HF,  $\text{HClO}_4$ ,  $\text{HNO}_3$  and HCl. The solutions were then diluted to bring them to the linear portion of the absorbance curve. The absorption spectra were recorded on the Perkin-Elmer 305 atomic absorption spectrometer.

**$\alpha$  counting:** U and Th were measured using thick source alpha counting. The samples were crushed, and spread onto a ZnS(Ag) scintillator. All the measurements were made using an alpha counter (Daybreak 582). The counting system was calibrated using standard sand 105A with 10.2 ppm U, as

described by Aitken (1985). Typical background rates were  $\sim 0.2$  counts/ks for a counting area of  $13.85 \text{ cm}^2$ .

**$\gamma$  spectrometry:** To determine disequilibrium, if any, in the decay chains of U and Th gamma spectrometry was carried out. Samples were sealed in plastic vials using araldite and stored for a period of 2-3 weeks to allow the radon to build up. Subsequently high energy gamma counting using a p type Ge(Li) well type detector with a multi channel analyser was done. The standard used for calibration had U=5.69 ppm., Th=14.5 ppm and K=2.63%. The amount of  $^{235}\text{U}$  was determined using gamma counting of the sealed sample and that of U computed by comparison with the standard; U was also calculated by counting a post  $^{222}\text{Rn}$  daughter,  $^{214}\text{Bi}$ . A discrepancy in the U concentration as determined by both these methods will be indicative of disequilibrium. Similarly, the concentration of  $^{232}\text{Th}$  was determined by counting two of its post  $^{220}\text{Rn}$  daughters -  $^{208}\text{Tl}$ ,  $^{212}\text{Pb}$  and one pre  $^{220}\text{Rn}$  daughter  $^{228}\text{Ac}$ , and comparing with the standard which is in equilibrium. The amount of  $^{40}\text{K}$  was also computed by gamma spectrometry. The values show agreement with that obtained from AAS.

#### **E.4 Water content estimation**

About 30gm of sample was weighed and kept in oven to dry at  $60^\circ\text{C}$  in order to determine 'as found' water content. The results are given in Table 4.1. For the purpose of determining the saturation water content, a chunk of sample was oven dried and tightly wrapped in aluminium foil to ensure no free space for water. Over a period of few days, distilled water was added from a dropper to the sample. Once this amount was absorbed, water was added again. This continued till the sample was saturated and a thin film of water stayed on the surface - this was carefully removed. The difference in weights before and after addition of water gave an estimate of the saturation water content.

## E.5 Data analysis

The OSL intensity was normalised with respect to short shine and the growth curve constructed by fitting a polynomial or a saturating exponential curve to the data. The ED was obtained from the intersection of the additive growth curve with the x- axis for different IR exposure times (Chapter 4, Section 4.1.2). The weighted average of ED values over the plateau was used.

The 'a' value was computed by constructing both  $\beta$  and  $\alpha$  regeneration growth curves and using the equation (Section E.2.4) given by Aitken and Bowman (1975).

The dose rate was calculated from the relative contributions of  $\alpha$ ,  $\beta$ , and  $\gamma$ s from U, Th and K using standard tables (Aitken, 1985). A correction to account for the higher stopping power of water for  $\alpha$ ,  $\beta$ ,  $\gamma$  as compared to air is applied (Zimmerman, 1971). An average of 'as found' and saturation water content was used for dose rate calculations.

The luminescence age was subsequently calculated using equation 4.3. The errors on age were computed according to the procedures discussed in Aitken (1985). The reported ages represent the calculated mean of the age over the plateau. The quoted error on age is the minimum measured error over the age plateau. The results are given in Table 4.1.

## REFERENCES

- Agrawal, D.P. and Gupta, S.K. (1988). Climatic changes in India during the last 700,000 years. In *The Palaeoenvironment of east Asia from the mid-Tertiary*, 1. Whyte, P. et al (eds). pp: 488-499. Hong Kong Univ., Hong Kong.
- Agrawal, D.P., Dodia, R., Kotlia, B.S., Razdan, H. and Sahni, A. (1989). The Plio-Pleistocene geologic and climatic record of the Kashmir valley, India: A review and new data. *Palaeogeogr., Palaeoclimatol., Palaeoecol.* **73**. pp: 267-286.
- Ahmad, F. (1986). Geological evidence bearing on the origin of Rajasthan Desert (India). *Proc. Ind. Natn. Sci. Acad.* **52A**. pp: 1285-1306.
- Aitken, M.J. (1974). *Physics and archaeology*. Clarendon press, Oxford.
- Aitken, M.J. (1985). *Thermoluminescence dating*. Academic press, Oxford.
- Aitken, M.J. and Bowman, S.G.E. (1975). Thermoluminescent dating: assessment of alpha particle contribution. *Archaeometry*. **17**. pp: 132-138.
- Aitken, M.J. and Bussel, A.J. (1979). Zero glow monitoring (ZGM). *Ancient TL*. **6**. pp: 13-15.
- Allchin, B., Goudie, A. and Hedge, K. (1978). *The prehistory and paleogeography of the Great Indian Desert*. Acad. Press.
- Bailiff, I.K., Bowman, S.G.E., Mobbs, S.F. and Aitken, M.J. (1977). The phototransfer technique and its use in thermoluminescence dating. *J. of Electrostatics*. **3**. pp: 269-280.
- Balescu, S. and Lamothe, M. (1994). Comparison of TL and IRSL age estimates of feldspar coarse grains from waterlain sediments. *Quat. Sci. Rev.* **13**. pp: 437-444.

- Barnett, T.P., Dumenil, L. and Latif, M. (1989). The effect of Eurasian snow cover on regional and global climatic variations. *J. Atmos. Sci.* **46(5)**. pp: 661-685.
- Bender, M.M. (1968). Mass spectroscopic studies of carbon -13 variations in corn and other grasses. *Radiocarbon*. **10**. pp: 468-472.
- Berger, G.W. (1988). Dating of Quaternary events by luminescence in 'Dating Quaternary Sediments' Easterbrook D.J. (ed) *Geol. Soc. of America*. **227**. pp: 13-50.
- Berger, G.W. (1990). Effectiveness of natural zeroing of the thermoluminescence in sediments. *J. Geophys. Res.* **95**. pp: 12375-12397.
- Berger, G.W. and Easterbrook, D.J. (1993). Thermoluminescence dating tests for lacustrine, glaciomarine, and floodplain sediments from western Washington and British Columbia. *Can. Jour. Earth Sci.* **30**. pp: 1815-1828.
- Berger, G.W. and Luternauer, J.J. (1987). Preliminary fieldwork for thermoluminescence dating studies at Fraser river delta, British Columbia. *Geological Survey of Canada paper*. **87-1A**. pp: 901-904.
- Bhaskaran, M., Rajagopalan, G. and Somayajulu, B.L.K. (1989).  $^{230}\text{Th}/^{234}\text{U}$  dating of the Quaternary carbonate deposits of Saurashtra, India. *Chem. Geol.* **79**. pp: 65-82
- Bhattacharya, A. (1989). Vegetation and climate during the last 30,000 years in Ladakh. *Palaeogeogr., Palaeoclimatol., Palaeoecol.* **73**. pp: 25-38.
- Biscaye, P.E. (1965). Mineralogy and sedimentation of Recent deep sea clay in the Atlantic ocean and adjacent seas and oceans. *Geol. Soc. Am. Bull.* **76**. pp: 803-802.
- Biswas, S.K. (1982). Rift basins in western margin of India and their hydrocarbon prospects with special reference to Kutch basin. *Am. Assoc. Petrol. Geol.* **10**. pp: 1497-1513.



- Biswas, S.K. (1987). Regional tectonic framework, structure and evolution of the western Marginal basin of India. *Tectonophysics*. **135**. pp: 307-327.
- Blackburn, T.H. (1983). The microbial nitrogen cycle. *Microbial Geochemistry*. W.E. Krumbein (ed.), Blackwell, Oxford. pp: 63-69.
- Bradley, R. (1985). *Quaternary Palaeoclimatology*. Publ. Allen and Unwin.
- Bryson, R.A. and Swain, A.M. (1981). Holocene variations of monsoon rainfall in Rajasthan. *Quat. Res.* **16**. pp: 135-145.
- Caratini, C., Bentaleb, I., Fontugne, M., Morzadec-Kerfourn, M. T., Pascal, J.P. and Tissot, C. (1994). A less humid climate since ca 3500 yr BP from marine cores off Karwar, western India. *Palaeogeogr., Palaeoclimatol., Palaeoecol.* **109**. pp: 371-384.
- Carver, R.E. (1971). *Procedures in sedimentary petrology*. London. John Wiley.
- Chamyal, L.S. and Merh, S.S. (1992). Sequence stratigraphy of the surface Quaternary deposits in the semi-arid basins of Gujarat. *Man and Environment*. **XVII (1)**. pp: 33-40.
- Chandra, P.K. and Chaudhary, L.R. (1969). Stratigraphy of the Cambay basin. *Bull. O.N.G.C.* **6(2)**. pp: 37-50.
- Chapman, F. (1900). Notes on the consolidated aeolian sands of Kathiawar. *Q.J.G.S.*, London. **5**. pp: 584-588.
- Chappel, J. and Shackleton, N.J. (1986). Oxygen isotopes and sea level. *Nature*. **324**. pp: 137-140.
- Chawla, S., Dhir, R.P. and Singhvi, A.K. (1992). Thermoluminescence chronology of sand profiles in the Thar Desert and their implications. *Quat. Sci. Rev.* **11**. pp: 25-32.
- Craig, H. (1953). The geochemistry of the stable carbon isotopes. *Geochem. Cosmochem. Acta*. **3**. pp: 53.

- Craig, H. (1957). Isotopic standards for carbon and oxygen and correction factors for mass spectrometric analysis of carbon dioxide. *Geochem. Cosmochem. Acta*. **12**. pp: 133-149.
- Cronin, T.M., Szabo, B.J., Ager, T.A., Hazel, J.E. and Owens, J.P. (1981). Quaternary climate and the sea level in the U.S. Atlantic coastal plain. *Science*. **211**. pp: 233-240.
- Debenham, N.C. (1985). Use of UV emissions in TL dating of sediments. *Nucl. Tracks and Rad. Meas.* **10**. pp: 717-724.
- Debenham, N.C. and Walton, D. (1983). TL properties of some wind blown sediments. *PACT*. **9**. pp: 531-538.
- Deines, P. (1980). The isotopic composition of reduced organic carbon. Handbook of Environmental Isotope Geochemistry, Vol. 1. *The Terrestrial Environment A*. Elsevier, Amsterdam. Fritz, P. and Fontes, J. Ch. (eds).
- Demaree, G.R. and Nicolis, C. (1990). Onset of Sahelian drought viewed as a fluctuation induced transition. *Q.J.R. Meteorol. Soc.* **16**. pp: 221-238.
- Denton, G.H. and Karlen, W. (1973). Holocene climatic variations - Their pattern and possible causes. *Q. Res.* **3**. pp: 155-205.
- Desai, V.S. (1975). Studies in radon emanation relevant to thermoluminescent dating. Unpubl. M.Sc. thesis. Oxford Univ.
- Ditlefson, C. (1992) Bleaching of K-feldspars in turbid water suspensions: a comparison of photo- and thermoluminescence signals. *Quat. Sci. Rev.* **11**. pp: 33-38.
- Duller, G.A.T. (1992). Comparison of equivalent doses determined by thermoluminescence and infrared stimulated luminescence for dune sands in New Zealand. *Quat. Sci. Rev.* **11**. pp: 39-43.
- Duller, G.A.T. (1994). Luminescence dating of poorly bleached sediments from Scotland. *Quat. Sci. Rev.* **13**. pp: 521-524.

Fleming, S.J. (1970). Thermoluminescence dating: refinement of quartz inclusion method. *Archaeometry*. **12**. pp: 135-145.

Folk, R.L. (1976). Reddening of desert sands, Simpson desert, Northern Territory, Australia. *Jour. Sed. Petrol.* **46**. pp: 604-615.

Foote, R.B. (1898). *Geology of Baroda State*. Govt. Press, Baroda State pp:194

Forman, S.L. and Ennis, G. (1991). Effect of light intensity and spectra on reduction of thermoluminescence of near shore sediments from Spitsbergen, Svalbard: implications for dating Quaternary waterlain sequences. *Geophys. Res. Lett.* **18**. pp: 1727-1730.

Gemmel, A.M.D. (1985). Zeroing of the thermoluminescence signal of sediments undergoing fluvial transportation: a laboratory experiment. *Nuclear Tracks*. **10**. pp: 695-702.

Ghosh, P.K. (1952). Western Rajputana, its tectonics and minerals, including evaporites. *Bull. Natn. Inst. Sci. India*. **1**. pp: 101-130.

Gillespie, A. and Molnar, P. (1995). Asynchronous maximum advances of mountain and continental glaciers. *Rev. of Geophy.* **33(3)**. pp: 311-364.

Godfrey Smith, D.I., Huntley, D.J. and Chen, W. H. (1988). Optical dating studies of quartz and feldspar sediment extracts. *Quat. Sci. Rev.* **7**. pp:373-380.

Gossens, C. and Berger, A.L (1987). How to recognise an abrupt climatic change. *Abrupt Climatic Change*. W.H. Berger and L.D. Labeyrie (eds.). Reidel, Dordrecht. pp: 31-45.

Goudie, A.S., Allchin, B. and Hedge, K.T.M. (1973). The former extensions of the Great Indian Sand Desert. *Geographical journal*. **139(2)**. pp: 243-257.

Guerin, G. and Valladas, G. (1980). Thermoluminescence dating of volcanic plagioclases. *Nature*. **286**. pp: 697-699.

Gupta, S.K. (1972). Chronology of the raised beaches and inland coral reefs of Saurashtra coast. *Journal of Geology*. **80**. pp: 357-361.

Gupta, S.K. (1973). Stability of the Saurashtra coast during late Quaternary and silting of the Rann of Kutch during Holocene. Unpubl. Ph.D. thesis.

Gupta, S.K. (1975). Silting of Rann of Kutch during Holocene. *Indian Jour. Earth Sci.* **2(2)**. pp: 163-175.

Gupta, S.K. (1976). Quaternary sea-level changes along the Saurashtra coast. *Ecology and archaeology of western India*. D.P. Agrawal and B.M. Pande (eds.). Concept publishing company.

Gupta, S.K. (1991).  $^{230}\text{Th}/^{234}\text{U}$  and  $^{14}\text{C}$  dating of Quaternary carbonate deposits of Saurashtra, India - Comments. *Chem. Geol.* **86**. pp: 179-186.

Gupta, S.K. and Polach, H.A. (1985). *Radiocarbon dating practices at ANU*. Handbook, Radiocarbon Laboratory, Research School of Pacific Studies, ANU, Canberra.

Hashimi, N.H., Nigam, R. and Rajagopalan, G. (1995). Holocene sea level fluctuations on western Indian continental margin: An update. *Geol. Soc. India*. **46**. pp: 157-162.

Hatch, M.D. and Slack, C.R. (1970). Photosynthetic  $\text{CO}_2$  fixation pathway. *Annu. Rev. Plant. Physiol.* **21**. pp: 141-162.

Hedges, J.I., Clark, W.A., Quay, P.D., Richey, J.E., Devol, A.H. and U.D.E.M. Santos. (1986). Compositions and fluxes of particulate organic matter in the Amazon river. *Limnol. Oceanogr.* **31**. pp: 717-738.

Huntley, D.J. (1985a). A note on temperature dependence of anomalous fading. *Ancient TL*. **3**. pp: 20-21.

Huntley, D.J., Godfrey-Smith, D.I. and Thewalt, M.L.W. (1985). Optical dating of sediments. *Nature*. **313**. pp: 105-107.

Islam, Md. B. and Merh, S.S. (1988). Tidal currents and sediments in the Gulf of Khambat. *Procs. Natn Sem. on Recent Quat. Studies in India*. 11-13 Feb. 1988. pp: 79-91.

- Jerlov, N.G. (1976). *Marine optics*. Elsevier Scientific, New York. pp: 231.
- Jones, P.D., Raper, S.C.B., Bradley, R.S., Diaz, H.F., Kelly, P.M. and Wigley, T.M.L. (1986). Northern hemisphere surface air temperature variation: 1851-1984. *J. Clim. Appl. Meteorol.* **25**. pp: 161-179.
- Keeling, C.D. (1961). The concentrations and isotopic abundances of carbon dioxide in rural and marine air. *Geochem. Cosmochem. Acta.* **24**. pp: 277-298.
- Kluge, M. and Ting, I. (1978). *Crassulacean acid metabolism*. Springer-Verlag, New York.
- Kortschak, H.P., Hart, C.F. and Burr, G.O. (1965). Carbon dioxide fixation in sugarcane leaves. *Plant Physiol.* **40**. pp: 209-213.
- Krishnamurthy, R.V., Bhattacharya, S.K. and Kusumger, S. (1986). Palaeoclimatic changes deduced from  $^{13}\text{C}/^{12}\text{C}$  and C/N ratios of Karewa lake sediments, India. *Nature*. **323**. pp: 150-152.
- Krynine, P.D. (1949). The origin of red beds. *Trans. New York Acad. Sciences*, **Sr. II**. pp: 60-68.
- Ku, T.L., Kimmel, M.A., Eason, W.H. and O'Neil, T.J. (1974). Eustatic sea level 120,000 years ago on O'ahu, Hawaii. *Science*. **183**. pp: 959-962.
- Kubeina, W.L. (1963). Palaeosols as indicators of palaeoclimate. *Arid Zone Res.*, UNESCO, Paris. **20**. pp: 207-209.
- Lee, C. and Olson, B.L. (1984). Dissolved, exchangeable and bound aliphatic amines in marine sediments: initial results. *Org. Geochem.* **6**. pp: 259-263.
- Li, J.J. (1990). The patterns of environmental evolution in northwestern China since Late Pleistocene. *Quat. Sci.* **3**. pp: 197-203.
- Mathur, L.P., Rao, K.L.N. and Chaube, A.N. (1968). Tectonic framework of Cambay basin, India. *Bull. O.N.G.C.* **V(1)**. pp: 7-28.

- Matsumoto, E. (1991). Studies on the past global changes (PAGES) with special reference to the Asian region. *Procs. Asian Workshop*. New Delhi.
- Maurya, D.M., Chamyal, L.S. and Merh, S.S. (1995). Tectonic evolution of the central Gujarat plain, western India. *Current Sci.* **69**(7). pp: 610-613.
- Maybeck, M. (1982). Carbon, nitrogen and phosphorus transport by world rivers. *Am. J. Sci.* **282**. pp: 401-450.
- Mejdahl, V. (1985). Thermoluminescence dating of partially bleached sediments. *Nucl. Tracks and Rad. Meas.* **10**. pp: 711-715.
- Mejdahl, V and Winther-Nielson, M. (1983). TL dating based on feldspar inclusions. *PACT*. **6**. pp: 426-437.
- Merh, S.S. (1992). Quaternary sea level changes along Indian coast. *Proc. Indian Natn. Sci. Acad.* **58**. pp: 461-472.
- Merh, S.S. (1995). *Geology of Gujarat*. Publ. Geological Soc. of India.
- Merh, S.S. and Chamyal, L.S. (1993). The Quaternary sediments in Gujarat. *Current Science*. **64**. pp 823-827.
- Nakai, N. and Koyama, M. (1987). Reconstruction of palaeoenvironment from view points of inorganic constituents, C/N ratio and carbon isotopic ratio in the 1400m long core taken from lake Biwa. In *History of Lake Biwa*. Horie, S. (ed).
- Oana, S. and Deevey, E.S. (1960). Carbon-13 in lake waters and its possible bearing on palaeoclimatology. *Am. Jour. Sci.* **258A**. pp: 253-272.
- O'Leary, M.H. (1981). Carbon isotope fractionation in plants. *Phytochemistry*. **20**. pp: 553-567.
- O'Leary, M.H. (1988). Carbon isotopes in photosynthesis. *Bioscience*. **38**. pp: 328-336.
- Osmond, C.B. (1978). Crassulacean acid metabolism: a curiosity in context. *Annu. Rev. Plant. Physiol.* **29**. pp: 379-414.

- Pant, R.K. and Chamyal, L.S. (1990). Quaternary sedimentation pattern and terrain evolution in the Mahi river basin, Gujarat, India. *Proc. Indian. Natn. Sci. Acad.* **56A(6)**. pp: 501-511.
- Pant, R.K. and Juyal, N. (1993). Late Quaternary coastal instability and sea level changes: new evidences from Saurashtra coast, western India. *Z. Geomorph N.F.* **37**. pp: 29-40.
- Park, R. and Epstein, S. (1960). Carbon isotope fractionation during photosynthesis. *Geochem. Cosmochem. Acta.* **21**. pp: 110
- Parthasarathy, B., Sontake, N.A., Monot, A.A. and Kothawale, D.R. (1986). Droughts/floods in the summer monsoon season over different meteorological subdivisions of India for the period 1871-1984. *J. Climatol.* **7**. pp: 57-70.
- Pascoe, E.H. (1964). *A manual of geology of India and Burma.* **3**. Govt. of India press.
- Patel, M.P. and Desai, S.J. (1988). Environmental significance of fossil sand dunes of North Gujarat. *Procs. Natn. Sem Recent Quat Studies in India.* 11-13 Feb. 1988. pp: 139-147.
- Patel, M.P. and Bhatt, N. (1995). Evidence of palaeoclimatic changes in miliolite rocks of Saurashtra, western India. *J. Geol. Soc. India.* **45**. pp: 191-200.
- Pye, K. (1983). *Red Beds in Chemical Sediments and Geomorphology.* Goudie, A.S. and Pye, K. (eds.) Academic Press, London. pp: 227-264.
- Rao, K.K., Jayalakshmy, K.V. and Kutty, M.K. (1991). Ecology and distribution of recent planktonic foraminifera in eastern part of the Arabian sea. *Ind. Jour. Marine Sci.* **20**. pp: 25-35.
- Rao, M.S. (1996). Studies on physical basis of luminescence geochronology and its applications . Unpubl. Ph.D. Thesis. Nagpur University. pp: 136.
- Rao, V.P. (1991). Clay mineral distribution in the continental shelf and slope off Saurashtra, west coast of India. *Indian. Jour. of Marine Sciences.* **20**. pp: 1-6.

- Rao, V.P. and Rao, B.R. (1995). Provenance and distribution of clay minerals in the sediments of the western continental shelf and slope of India. *Continental Shelf Res.* **15(14)**. pp: 1757-1771.
- Raup, D.M. and Stanley, S.M. (1985). *Principles of Paleontology*. CBS publishers and distributors. second edition. pp: 261.
- Reineck, H. -E. and Singh, I.B. (1980). *Depositional Sedimentary Environments*. Publ. Springer Verlag. pp:322.
- Rendall, H.M. and Townsend, P.D. (1988). Thermoluminescence dating of a 10m loess profile in Pakistan. *Quat. Sci. Rev.* **7**. pp: 251-255.
- Sankalia, H.D. (1945). *Investigations into the Pre-Historic archaeology of Gujarat*. Baroda State Press, Baroda. pp: 336.
- Sareen, B.K., Rao, M.S., Tandon, S.K. and Singhvi, A.K. (1992). A tentative chronological framework for the Quaternary deposits of the Sabarmati basin of semi-arid western India using Thermoluminescence. *Abs. Int. Symp. on Evolution of Deserts*. India 11-19 Feb. '92. pp: 177-179.
- Sareen, B.K., Tandon, S.K. and Bhola, A.M. (1993). Slope deviatory alignment, stream network and lineament analysis of the Sabarmati river system- neotectonic activity in the mid to late Quaternary. *Curr. Sci.* **64**. pp: 827-836.
- Scott, M.R. (1968). Thorium and uranium concentration and isotopic ratios in river sediments. *Earth Planet. Sci. Lett.* **4**. pp: 245-252.
- Singh, G., Joshi, R.D. and Singh, A.B. (1972). Stratigraphic and radiocarbon evidence for the age and development of three salt lake deposits in India. *Quat. Res.* **2**. pp: 496-505.
- Singh, G., Wasson, R.J. and Agrawal, D.P. (1990). Vegetational and seasonal climatic changes since the last full glacial in the Thar Desert, northwestern India. *Rev. Palaeobot. Palynol.* **64**. pp: 351-358.
- Singhvi, A.K. and Aitken, M.J. (1978). Americium-241 for alpha irradiations. *Ancient TL.* **3**. pp: 2-9.
- Singhvi, A.K., Sharma, Y.P. and Agrawal, D.P. (1982). Thermoluminescence dating of sand dunes in Rajasthan. *Nature.* **295**. pp: 313-315.



- Singhvi, A.K., Dhir, R.P. and Rajaguru, S.N. (1989). Climatic change in the Indian sub-continent during the Quaternary: some suggestions for research in the nineties. *Mem. Geol. Soc. India*. **16**. pp: 1-4.
- Smith, B.N. and Epstein, S. (1971). Two categories of  $^{13}\text{C}/^{12}\text{C}$  ratios for higher plants. *Plant Physiol.* **47**. pp: 380-384.
- Sood, R.K. (1983). Geomorphology of the Kathiawar peninsula and environs using remote sensing techniques. unpubl. Ph.D thesis.
- Spooner, N.A. (1993). The validity of optical dating based on feldspar. D.Phil Thesis. Oxford.
- Sridhar, V.S. (1995). Sequential stratigraphy and palaeoclimatic studies on the Quaternary deposits of lower Luni and Sabarmati basins of western India. Unpubl. Ph.D thesis, M.S. Univ. Baroda.
- Sridhar, V., Chamyal, L.S. and Merh, S.S. (1994). North Gujarat rivers: Remnants of a super fluvial system. *Jour. Geol. Soc. India*. **44**. pp: 427-434.
- Stuiver, M. (1975). Climate versus changes in  $^{13}\text{C}$  content of the organic component of lake sediments during the late Quaternary. *Quat. Res.* **5**. pp: 251-262.
- Sukeshwala, R.N. (1948). *Geological evolution of Maha-Gujarat*. Monograph 3. Maha Gujarat series. Publ. Gujarat Res. Soc.
- Sukumar, R., Ramesh, R., Pant, R.K. and Rajagopalan, G. (1993). A  $\delta^{13}\text{C}$  record of late Quaternary climate change from tropical peats in southern India. *Nature*. **364**. pp: 703-706.
- Swain, A.M., Kutzbach, J.E. and Hastenrath, S. (1983). Estimates of Holocene precipitation for Rajasthan, India, based on pollen and lake level data. *Quat. Res.* **19**. pp: 1-17.
- Swain, P.H. and Davis, S.M. (1978). *Remote sensing: the quantitative approach*. McGraw Hill, New York.

- Sweeney, R.E., Kalil, E.K. and Kaplan, I.R. (1980). Characterisation of domestic and industrial sewage in southern California coastal sediments using nitrogen, carbon, sulfur and uranium tracers. *Mar. Environ. Res.* **3**. pp: 225-243.
- Talbot, M.R. and Johannessen, T. (1992). A high resolution palaeoclimatic record for the last 27,500 years in tropical West Africa from the carbon and nitrogen isotopic composition of organic matter. *Earth. Planet. Sci. Lett.* **110**. pp: 23-37.
- Tandon, S.K., Sareen, B.K., Someshwar Rao, M. and Singhvi, A.K. (1996). Aggradation history and luminescence chronology of late Quaternary semi-arid sequences of the Sabarmati basin, Gujarat, western India. *Palaeogeogr., Palaeoclimatol., Palaeoecol.* (in press).
- Templer, R.H. (1985). The removal of anomalous fading in zircon. *Nucl. Tracks. Rad. Meas.* **10**. pp: 531-537
- Thornbury, W.D. (1985). *Principles of Geomorphology*. Second Ed. Wiley Eastern Ltd.
- Tieszen, L.L., Senyimba, M.M., Imbamba, S.K. and Troughton, J.H. (1979). The distribution of C<sub>3</sub> and C<sub>4</sub> grasses and carbon isotope discrimination along an altitudinal and moisture gradient in Kenya. *Oecologia*. **37**. pp: 337-350.
- Urey, H.C. (1947). The thermodynamic properties of isotopic substances. *J. Chem. Soc.* pp: 562-581.
- Visocekas, R. (1979). Miscellaneous aspect of artificial TL of calcite: emission spectra, athermal detrapping and anomalous fading. *PACT*. **3**. pp: 258-265.
- Wadia, D.N. (1953). *Geology of India*. Publ. MacMillan and Co.
- Wasson, R.J., Rajaguru, S.N., Misra, V.N., Agrawal, D.P., Dhir, R.P. and Singhvi, A.K. (1983). Geomorphology, late Quaternary stratigraphy and palaeoclimatology of the Thar dune field. *Z. Geomorph. N F.* **45**. pp: 117-151.

- Wasson, R.J., Smith, J.I. and Agrawal, D.P. (1984). Late Quaternary sediments, minerals and inferred geochemical history of Didwana lake, Thar Desert, India. *Palaeogeogr., Palaeoclimatol., Palaeoecol.* **46**. pp: 345-372.
- Wetzel, R.G. (1983). *Limnology*. Saunders, Philadelphia.
- Winstanley, D. (1976). Rainfall trends in Africa, Middle East and India. *Nature*. **243**. pp: 464-465.
- Wintle, A.G. (1973). Anomalous fading of thermoluminescence in mineral samples. *Nature*. **245**. pp: 143-144.
- Wintle, A.G. (1977). Detailed study of minerals exhibiting anomalous fading. *J. Lum.* **15**. pp: 385-393.
- Wintle, A.G. (1985b). Thermoluminescence dating of loess deposits in Normandy. *Ancient TL*. **3**. pp: 11-13.
- Wintle, A.G. (1990). A review of current research on TL dating of loess. *Quat. Sci. Rev.* **9**. pp: 385-397.
- Wintle, A.G., and Huntley, D.J. (1980). Thermoluminescence dating of ocean sediments. *Can. Jour. Earth sciences*. **17**. pp: 348-60.
- Wintle, A.G. and Proszyńska, H. (1983). TL dating of loess in Germany and Poland. *PACT*. **9**. pp: 547-554.
- Yan, Z and Petit-Maire, N. (1994). The last 140 ka in the Afro-Asian arid/semi arid transitional zone. *Palaeogeogr., Palaeoclimatol., Palaeoecol.* **110**. pp: 217-233.
- Yan, Z.W., Ji, J.J. and Ye, D.Z. (1990). Northern hemisphere summer climatic jump during the 1960's, Part 1, rainfall and temperature. *Sci. China B*. **33**. pp: 1092-1102.
- Zeuner, F.E. (1950). *Stone age and Pleistocene chronology in Gujarat*. Deccan College Monograph Series: 6

Zhang, M.L., (1989). Rainfall changes in east China during the recent 100 yrs. *Kexue Tongbao (Sci. Bull)*. **34**. pp: 605-607.

Zimmerman, D.W. (1971). TL dating using fine grains from pottery. *Archaeometry*. **13**. pp: 29-52.